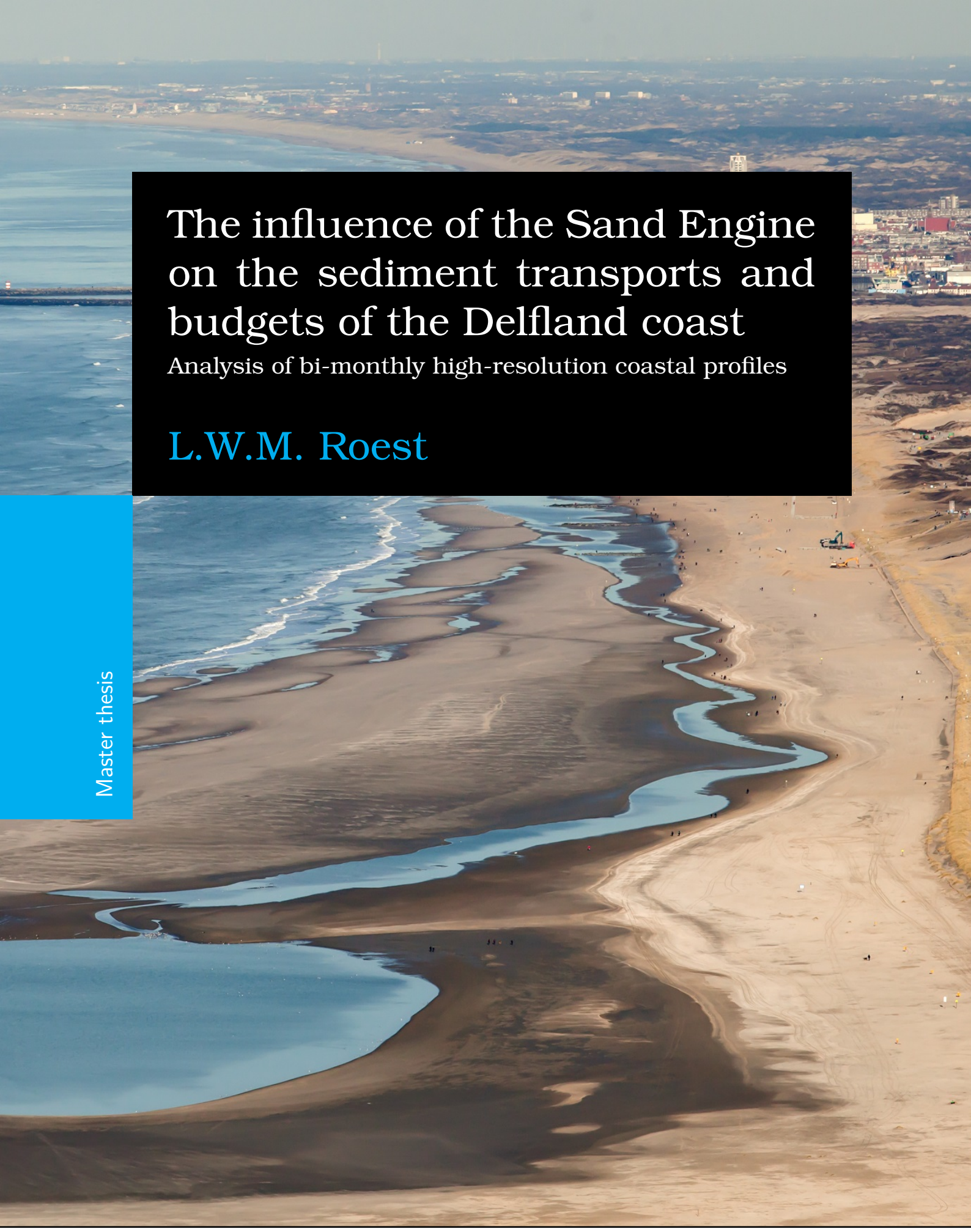

The influence of the Sand Engine on the sediment transports and budgets of the Delfland coast

Analysis of bi-monthly high-resolution coastal profiles

L.W.M. Roest

Master thesis

TU Delft Delft University of Technology

Hydraulic Engineering

Front cover: Aerial photograph of the Sand Engine with Scheveningen in the background. Taken on 16 February 2016, by Rijkswaterstaat/Jurriaan Brobbel, https://www.flickr.com/photos/zandmotor/25106436435/
Back cover: Aerial photograph of the Sand Engine looking to the South. Taken on 16 February 2016, by Rijkswaterstaat/Jurriaan Brobbel, https://www.flickr.com/photos/zandmotor/25080093026/

The influence of the Sand Engine on the sediment transports and budgets of the Delfland coast

Analysis of bi-monthly high-resolution coastal profiles

Master Thesis

For the degree of Master of Science in Civil Engineering
at Delft University of Technology

To be publicly defended on 17th August 2017

L.W.M. Roest

10th August 2017

Graduation committee:

prof.dr.ir. S.G.J. Aarninkhof	Delft University of Technology
dr.ir. S. de Vries	Delft University of Technology
dr.ir. M.A. de Schipper	Delft University of Technology
dr. M.F.S. Tissier	Delft University of Technology

Abstract

The Sand Engine is a new innovation in coastal protection, a mega feeder nourishment. This pilot project was constructed in 2011 along the Delfland coast, which is historically prone to erosion. Since its construction, the Sand Engine is intensively being monitored to track the morphological development.

The objective of this thesis is therefore to assess how the morphology of the Sand Engine is evolving over time and how this evolution contributes to the sediment budgets of the Delfland coast. In this thesis the first five years of morphological evolution of Sand Engine and its surroundings are investigated.

A data analysis is performed on bi-monthly bathymetry measurements, covering the first five years of morphodynamic evolution of the Sand Engine and the surrounding coastal cell. The high temporal and spatial resolution both in alongshore and cross-shore direction provided the opportunity to research in great detail and precision.

Volume changes and sediment transports are successfully derived. Sediments are redistributed in both alongshore and cross-shore direction over the coastal cell. The accretive areas slowly extend alongshore while the erosive part of the Sand Engine remains in the same position. The Sand Engine has a positive net contribution to the sediment budget of 5.8km of coast after 5 years, which is an extension of 3.2km. $4.2 \cdot 10^6 \mathrm{m}^3$ of the initially nourished volume of $17.5 \cdot 10^6 \mathrm{m}^3$, has been redistributed after 5 years, see Figure 1.

A Gaussian curve is fitted to several iso-lines of constant altitude to describe the plan-form adjustment of the Sand Engine at different altitudes. The Gaussian parameters are useful in accurately describing the spatio-temporal behaviour. Yet large differences in adjustment rates are found over the altitude. The decrease in cross-shore extent is fastest around 0m+NAP, and decreases to near zero at -8m+NAP.

Cross-shore profile behaviour is investigated by inspection of the temporal evolution of characteristic cross-sections in accretive and erosive locations along the Sand Engine. Erosive and accretive profiles behave considerably different. The profiles are adjusting rapidly and bed-level activity varies considerably over the altitude, with a maximum morphological activity in the intertidal zone, rapidly decreasing with increasing depth.

The results show that the Sand Engine spreads alongshore and feeds the adjacent coastal sections in the five years after construction. A mega feeder nourishment is therefore capable

of supplying sediments to the adjacent coast. The first year morphodynamic response was much stronger than in any subsequent year. The current results therefore give an improved view on the long-term development of the Sand Engine.

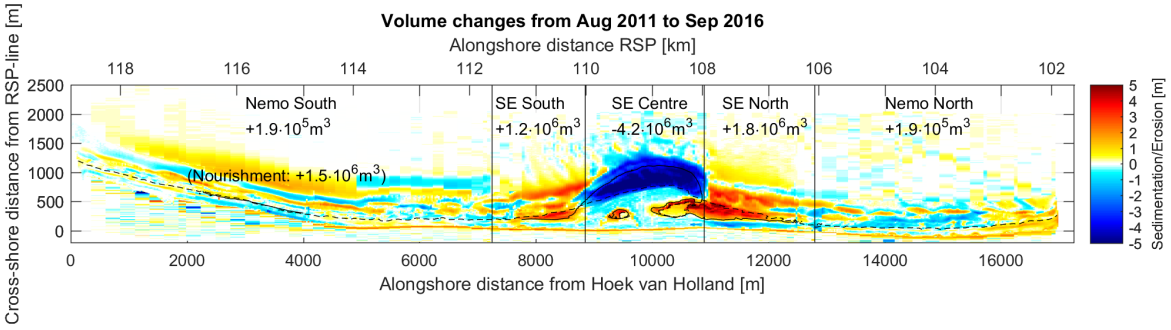

Figure 1: Volume changes in the Delfland coastal cell from August 2011 (Nemo: February 2012) to September 2016. The net volume change over the whole survey area is $-0.8{\cdot}10^6 m^3$. (Excluding nourishment.) Coulours indicate bed-level change, dashed lines indicate the 0m+NAP depth contour.

Samenvatting

De Zandmotor is een nieuwe innovatieve manier voor kustbescherming, een zogenaamde mega suppletie. Dit proefproject is aangelegd in 2011 langs de Delflandse kust. Sinds de aanleg wordt de Zandmotor intensief bemeten om zo de morfologische ontwikkelingen in kaart te kunnen brengen.

Het doel van deze MSc-thesis is om vast te leggen hoe de morfologie van de Zandmotor zich ontwikkeld door de tijd en hoe deze ontwikkeling bijdraagt aan de sediment budgetten van het omliggende kustvak. In dit onderzoek worden de morfologische veranderingen beschreven van de Zandmotor en zijn omgeving in de eerste vijf jaar na aanleg.

Er is een data-analyse uitgevoerd op basis van vijf jaar aan tweemaandelijkse metingen van de bodemligging. Deze metingen bevatten de morfologische veranderingen van de gehele Delflandse kust. De hoge resolutie van deze metingen in tijd en plaats, zowel kustlangs als kustdwars, bieden de gelegenheid voor onderzoek met grote precisie en oog voor detail.

Volumeveranderingen en sedimenttransporten zijn succesvol afgeleid uit de beschikbare data. Het sediment wordt zowel in kustlangse als kustdwarse richting over het kustvak verspreid. De aanzandende gebieden aan weerszijden van de Zandmotor groeien langzaam in kustlangse richting, terwijl het erosieve gebied op zijn plaats blijft. Na vijf jaar heeft de Zandmotor een positieve netto bijdrage geleverd aan 5.8km kust, ofwel een uitbreiding van 3.2km. Van het initieel gesuppleerd volume van $17.5 \cdot 10^6 \mathrm{m}^3$ is inmiddels $4.2 \cdot 10^6 \mathrm{m}^3$ herverdeeld, zie Figuur 1 op pagina ii.

Een Gausskromme wordt gefit op isolijnen van constante hoogte om de ontwikkeling van het bovenaanzicht van de Zandmotor te beschrijven op verschillende hoogten. De parameters van de kromme zijn in staat om het gedrag in ruimte en tijd nauwkeurig te beschrijven. Over de hoogte zijn er echter grote verschillen in de morfologische ontwikkeling. De afname van de kustdwarse grootte is het sterkst rond 0m+NAP en neemt af naar vrijwel nul rond -8m+NAP.

Het morfologische gedrag van kustprofielen is onderzocht door te kijken naar de ontwikkeling van karakteristieke profielen in zowel aanzandende als erosieve locaties van de Zandmotor. Erosieve en aanzandende kustprofielen tonen een aanzienlijk verschil in morfologisch gedrag. De kustprofielen veranderen snel van vorm en de activiteit van de bodemligging varieert sterk over de hoogte van het kustprofiel. Het piek van deze activiteit ligt in het inter-getijdengebied en neemt sterk af met toenemende diepte.

De resultaten tonen aan dat de Zandmotor zich verspreidt langs de kust en aan weerszijden sediment toevoert in de eerste vijf jaar na oplevering. Een mega suppletie is dus in staat om de omliggende kust te voeden met sediment. De morfologische respons was in het eerste jaar veel sterker dan in opvolgende jaren. De huidige resultaten geven daarom een sterk verbeterd beeld van de langetermijnontwikkeling van de Zandmotor.

Acknowledgements

Hereby I would like to express my gratitude towards my supervisors for their involvement in my thesis. Stefan, thanks for the support and being chair of the committee. Sierd, thank you for your extensive support and your eternal enthusiasm of coastal dynamics and this subject particularly. Matthieu, thank you for your input and more critical view, that was very much appreciated. Marion thank you for the feedback on the writing.

Thanks to all the people from the "afstudeerhok" for the good company during the past year. Marloes, Anaïs and Christel, ;) Anaïs, I greatly appreciate your efforts to read trough my thesis.

Bedankt vrienden, Bolkers, Botteraars, etc. voor het zijn van een fantastisch tijdverdrijf de afgelopen jaren.

Beste papa en mama, bedankt voor jullie steun en de mogelijkheid om mijn studie te volgen en af te ronden!

L.W.M. Roest,
Delft, 10th August 2017

Contents

List of Figures

List of Tables

Nomenclature

α	Cross-shore beach slope [degrees]
$\epsilon_{\mathbf{m}}$	Root mean square error of the planform with respect to a gaussian shape [m]
η	Redistribution efficiency [-]
η_n	Nourishment efficiency [-]
ϕ	Incident wave direction [deg N]
θ	Coastline orientation [degree N]
$\theta_{\mathbf{0}}$	Original coastline orientation [degree N]
accretion	Increase of the bed-level
advance	Seaward displacement of isobaths
alongshore	Parallel to the coast
$\mathbf{c}$	Wave celerity [m/s]
$\mathbf{c_g}$	Wave group celerity [m/s]
coastal profile	Cross-section of the coast, altitude versus distance
cross-shore	Perpendicular to the coast
$\mathbf{E}$	Wave energy [J/m]
erosion	Decrease of the bed-level
$\mathbf{g}$	Gravitational acceleration [m/s^2]
gross volume change	Absolute sum of accretion and erosion
$\mathbf{H_0}$	Deep water wave height [m]
$\mathbf{H_s}$	Significant wave height [m]
$\mathbf{i}$	Alongshore index
$\mathbf{j}$	Cross-shore index
$\mathbf{L_0}$	Deep water wave length [m]
morphology	Shape of the bed, forms and changes therein

net volume change	Difference between accretion and erosion
P	Wave power [W/m]
$\mathbf{P_{ls}}$	Alongshore component of wave energy [J/m]
retreat	Landward displacement of isobaths
$\mathbf{S_x}$	Cross-shore sediment transport [m^3/yr]
$\mathbf{S_y}$	Longshore sediment transport [m^3/yr]
sediment transport	(Quantification of) the displacement of sediments
slope	local inclination of of a cross-shore profile
t	Temporal index
$\mathbf{T_p}$	Wave peak period [s]
$\mathbf{T_s}$	Significant wave period [s]
transect	Shore-normal line over which morphological suveys are measured
u	Flow velocity in x-direction [m/s]
v	Flow velocity in y-direction [m/s]
$\mathbf{w_s}$	Sediment fall velocity [m/s]
x	Alongshore coordinate in m from Hoek van Holland
$\mathbf{x_0}$	Position of the center of mass of the planform [m]
$\mathbf{x_{RD}}$	x-coordinate of the Dutch geodetic system
y	Cross-shore coordinate in m from RSP-line
$\mathbf{y_{max}}$	Maximum cross-shore extent [m]
$\mathbf{y_{RD}}$	y-coordinate of the Dutch geodetic system
z	Vertical coordinate in m+NAP
$\mathbf{z_{NAP}}$	z-coordinate of the Dutch geodetic system

List of Acronyms

ADCP	Acoustic Doppler Current Profiler
BKL	Basis KustLijn (Base Coast Line)
CST	Cross-shore Sediment Transport
GPS	Global Positioning System
HAWI	High-angle wave incidence
JarKus	Jaarlijkse Kustmetingen
KNMI	Koninklijk Nederlands Meteorologisch Instituut
LST	Longshore Sediment Transport
MHW	Mean High Water
MKL	Momentane KustLijn (Instantaneous Coast Line)
MLW	Mean Low Water
MSL	Mean Sea Level
NAP	Normaal Amsterdams Peil
NeMo	Nearshore Monitoring and Modelling: Inter-scale Coastal Behavior
RD	Rijksdriehoekstelsel
RD-NAP	Rijksdriehoek-coordinates with NAP height (ESPG:7415)
RMS	Root Mean Square
RMSE	Root Mean Square Error
RSP	Rijksstrandpalen (State beach poles)
RTK-GPS	Real-time kinematic GPS
RWS	Rijkswaterstaat
SE	Sand Engine
SLR	Sea Level Rise
TKL	te Toetsen KustLijn (Test Coast Line)

Chapter 1

Introduction

The objective of this thesis is to assess how the *Sand Engine*[1] is evolving in time and how this evolution contributes to the sediment budgets of the South-Holland coast. The Sand Engine is a new innovation in coastal protection, a mega feeder nourishment. It consists of an artificial sandy peninsula, located at the coast of South-Holland between Scheveningen and Hoek van Holland.

As for now, three important aspects of the Sand Engine remain unclear. The current knowledge gaps are the influence of the Sand Engine on the surrounding coastal cell, the evolution beyond the first 18 months after construction and the adjustment of cross-shore profiles. These aspects will be addressed in the analyses carried out for this thesis.

This chapter is therefore structured as follows. First, in Section 1-1 the coastal system of Holland will be introduced, as well as the traditional measures against erosion. Section 1-2 describes the Sand Engine and its purpose in the coastal system, followed by a state of the art on the initial morphological development in Section 1-3. In the next Section (1-4), a conceptual model is introduced that links the previous parts together. Finally, the research questions are presented in Section 1-5.

1-1 The coastal system of Holland & nourishment strategies

The Holland coast (see Figure 1-1) is a sandy coast of 118 km long, which stretches from Den Helder in the North to Hoek van Holland in the South. The coast is characterised by a sandy beach-dune system, which is only interrupted by the harbour moles of IJmuiden and Scheveningen. The dune system forms the sea defence for large parts of the Dutch provinces of North- and South-Holland (Van Rijn, 1997). The dunes are essential in the prevention of flooding of the hinterland, which is below Mean Sea Level (MSL), densely populated and has high economic value. Thus the consequences of potential flooding are catastrophic on a national scale. It is therefore that the required safety levels set by the Dutch government are also high (Van Rijn, 1997; Stive et al., 2013; Verkeer & Waterstaat, 1990). According to the

[1]The Sand Engine is called *Zandmotor* in Dutch, but is sometimes also referred to as *Sand Motor*. In this report *Sand Engine* will be used.

new regulations as of 2017, the safety level of the Delfland coast is set to 1/30,000 (Slootjes et al., 2016). Yet, achieving the required safety levels has been a continuous challenge.

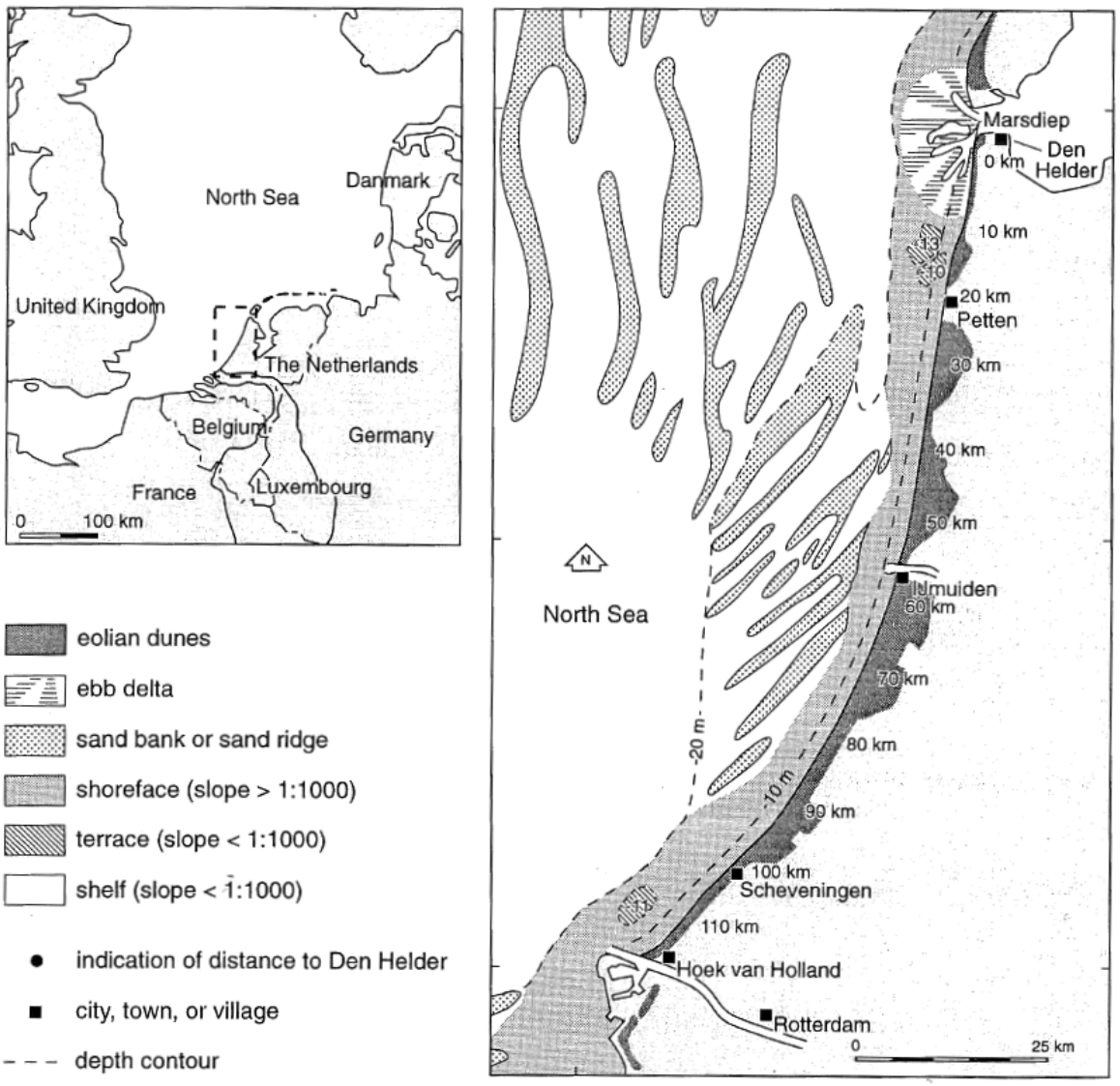

Figure 1-1: Overview of the Holland coast and some important locations. Left panel: Location of the Holland Coast in the Southern North Sea area (Wijnberg, 1995).

The Holland coast has been subject to erosion for centuries. The shoreline has been migrating landward, most dominantly in the Northern and Southern sections at rates of 3 to 5 metres per year (Van Rijn, 1997). The ongoing erosion has lead to a so-called *coastal squeeze*. When the seaward boundary of the sea defence (dunes) is migrating landward, while the landward boundary cannot migrate in the same rate, the sea-defence is getting narrower leading to a decrease of safety. This process of coastal squeeze is most visible near coastal settlements. Due to the landward retreat of the coastline, the villages become more and more exposed to the sea with respect to the adjacent coastal sections, making them more vulnerable to storms and flooding.

The ongoing erosion of the coast was deemed undesirable already in the 19th century and measures were taken against it. The first measures consisted of the construction of shore normal groynes at the beach and intertidal area. These structures were quite successful, in reducing the erosion at the beach and dune foot as recession of the shoreline reduced to approximately 0.5 metre per year. But this was not the case at deeper waters. While the erosion problem shifted to deeper waters, the coastal profiles steepened as the lower shoreface continued to erode (Van Rijn et al., 1995).

From the 1970's new measures against coastal erosion were developed, consisting of the artificial supply of sediments to the coastal system, the so-called beach and dune nourishments. These nourishments were then still limited to immediate mitigation of storm erosion. Also the nourished volumes were generally smaller than nowadays (Hamm et al., 2002; Van Rijn et al., 1995).

A major change in coastal policy emerged with the acceptance of the "Dynamic preservation act" in 1990. No further recession of the coastline was allowed and the coast had to be maintained at its 1990 position (or more seaward) (Verkeer & Waterstaat, 1990; Van Rijn et al., 1995; Stive et al., 2013). This maintenance is performed by frequent nourishments. Annual nourishment volumes were increasing over the years, therefore new strategies for coastal maintenance have to be developed (Hamm et al., 2002; Stive et al., 2013).

Nowadays sand nourishments are a widely accepted measure to increase coastal safety (Stive et al., 2013; Hamm et al., 2002). They form the key to coastal safety in the Netherlands. Different kinds of nourishments have been developed over time, which can be divided in three categories, see Figure 1-2. The first kind is the beach and dune nourishment (see Figure 1-2, upper panel), which takes place on the sub-aerial beach and the dune front. The supplied volumes are relatively small and the costs relatively high due to the use of land-based equipment. Shoreface nourishments (see Figure 1-2, central panel) were developed later and are situated in the shoreface around the outer breaker bar, generally at depths around five metre below MSL. The supplied volume is larger than in beach nourishments. The sediment is meant to be transported onshore due to wave action. Construction costs are lower, as the work can be fully performed by water-based equipment (ships). The latest category is the recently developed mega feeder nourishment (see Figure 1-2, lower panel). It is characterised by a highly concentrated nourished volume of unprecedented scale, with a large cross-shore extent. This nourishment is, as opposed to the other types, meant to be dynamic and to be spread alongshore by hydrodynamic forces. This way it feeds the adjacent coastal sections gradually with sediment. The first pilot project of a mega feeder nourishment is the Sand Engine.

1-2 The Sand Engine

In 2011 the first mega feeder nourishment was installed; a unique and unprecedented project called: the Sand Engine (De Schipper et al., 2016; Stive et al., 2013). This pilot project is meant to gain broad knowledge of the behaviour of a mega nourishment, and the benefits for possible new nourishment strategies at the Dutch coast. Therefore the Sand Engine is intensively being monitored.

The Sand Engine pilot project was initiated to find whether it is possible to provide increased safety by nourishments for longer periods of time. Increasing the nourishment interval time

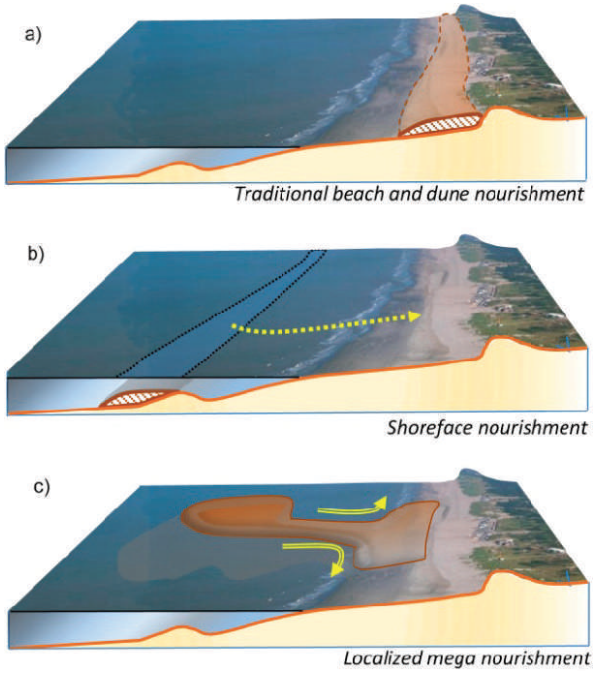

Figure 1-2: Schematic representation of different types of nourishments (Stive et al., 2013). Upper panel: beach and dune nourishment. Central panel: shoreface nourishment. Lower panel: mega feeder nourishment.

would be beneficial for nature and could bring economic scale advantages. Furthermore it was investigated whether it is possible to simultaneously serve other purposes beside coastal safety, by creating additional values (Stive et al., 2013).

The strategy of the mega nourishment is to locally place a large and concentrated volume of sand. This highly concentrated volume has to be redistributed by natural forces, such as waves and wind. Due to this redistribution the effectively reinforced area is much larger than the area where the nourishment is placed initially. Due to the unprecedented size of the Sand Engine, it is also possible to create additional values for nature and recreation. Thus, the advantages of the large spatial scales of a mega nourishment are multiple.

The peninsula is located along the Holland coast between Hoek van Holland and Scheveningen, see Figure 1-3. This area forms the Delfland coastal cell, which is bounded by the harbour moles of the Rotterdam waterway near Hoek van Holland in the South and the harbour moles of Scheveningen (Den Haag) in the North. These harbour moles provide a more or less closed coastal cell, due to the partial blocking of the alongshore sediment transport (Van Rijn, 1995). The coastal cell is characterised by a high but occasionally narrow row of sand dunes. These dunes protect the low-lying hinterland of high economic value from flooding. Before installation of the Sand Engine, the morphology was rather uniform alongshore. The coastal profile is mildly sloping and in general one or two bars could be found (Wijnberg et al., 1995). Estimates of the net alongshore sediment transport in the Delfland coastal cell range from 50000 to 170000m^3/year in Northward direction. These figures are found to depend largely on the wave climate (Van Rijn et al., 1995; Van de Rest, 2004). The Delfland coast has been subject to ongoing erosion and requires large nourishment volumes. It was therefore selected as suitable location for the Sand Engine pilot project.

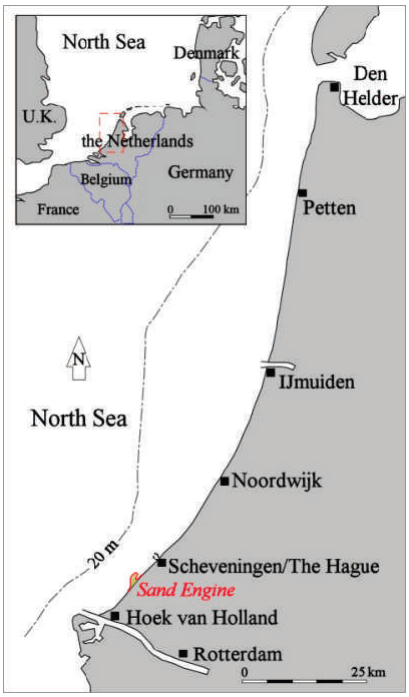

Figure 1-3: Location of the Sand Engine along the Holland coast, the Sand Engine is located between Hoek van Holland and Scheveningen (Den Haag). Inset: Location of the Holland coast in the Southern North Sea area.

The Sand Engine mega nourishment consists of an in-situ volume of 19.5Mm^3 of sand. This sand was applied in the form of a large hook shaped peninsula of 17.5Mm^3 and two alongshore adjacent shoreface nourishments, both circa 1Mm^3 (Stive et al., 2013; De Schipper et al., 2016). Agreement was reached for this design and it was subsequently built (Stive et al., 2013). An aerial photograph of the Sand Engine is shown in Figure 1-4.

The shape of the final design was largely inspired by its potential for the creation of areas for nature and recreational purposes (Stive et al., 2013). The final design consists of a hook shaped peninsula, which is open to the North (see Figure 1-4). The peninsula initially stretched two kilometres alongshore and protrudes almost one kilometre into the sea. Near the base of the peninsula a small sheltered lake is present, surrounded by flood-free areas. This lake attracts many birds and also prevents problems with the groundwater table in the dunes. The area sheltered by the hook of the peninsula, behaves as a lagoon intended to provide a habitat for flatfish, but it also serves kite-surfers and swimmers. The peninsula has an altitude of 3 to 6m+Normaal Amsterdams Peil (NAP), the highest part is found in the centre. These dry parts are therefore flood-free.

1-3 Initial development of the Sand Engine

Due to hydrodynamic and aeolian forces the plan form shape of the Sand Engine has changed considerably. De Schipper et al. (2016) have reported on the initial development of the Sand Engine, based on the first 18 months of observations. In this period, the cross-shore extent of the peninsula has decreased and the alongshore extent has increased already by

Figure 1-4: Aerial photograph of the Sand Engine peninsula just after construction in August 2011, looking to the North (Rijkswaterstaat et al., 2011).

several hundreds of metres. Figure 1-5 shows the first and last survey investigated by De Schipper et al. (2016), in which these observations can be seen. The morphological response was strongest in the first six months after construction, showing large changes in plan-form, essentially smoothing the coastline. The following twelve months have shown less pronounced changes.

The main observations are:

- The middle section of the peninsula erodes and shows shoreline retreat.
- The adjacent sections on both sides accrete and show shoreline advance.
- The alongshore extent of the Sand Engine increases in time.
- The plan-form of the peninsula at MSL becomes nearly symmetrical.
- Morphologic response was strongest in the first six months.
- The majority of losses from the peninsula are found to have accreted in the adjacent coastal sections.

Luijendijk et al., 2017 found that waves and wave energy are found to be the main parameters governing the erosional behaviour of the Sand Engine peninsula in the first year. Tides, surges and wind are found to only play a minor role.

Morphological evolution after the first 18 months, as well as outside of the Sand Engine survey domain have not yet been investigated. It is expected that the processes observed by De Schipper et al. (2016) will continue in the future, which will be further investigated in this thesis.

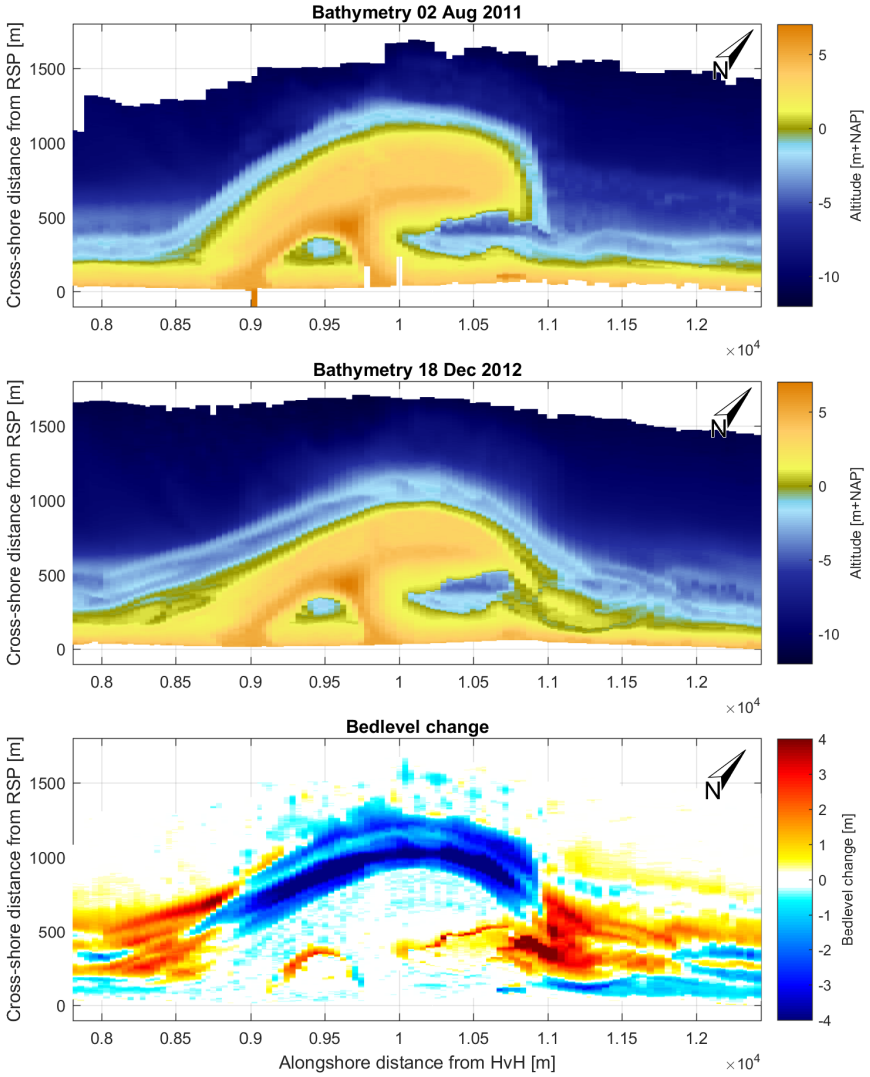

Figure 1-5: Changes in bathymetry of the Sand Engine over the first 18 months. Upper: survey August 2011, middle: survey December 2012, lower: bed-level change over the time interval.

Many of the coastal morphology surveys are measured in transects, such as the Dutch Jaarlijkse Kustmetingen (JarKus) measurements (Knoester, 1990; Minneboo, 1995; Southgate, 2011). Transects are lines which extend into the sea, perpendicular to the coast and have a fixed position in time in case of multiple surveys. Therefore most analyses and studies are also transect based and many parameters have been derived for coastal morphology on a per transect basis, e.g. Knoester (1990), Dean (1991), Wijnberg et al. (1995), De Vries et al. (2015) and De Schipper et al. (2016).

A Coastal profile is a local cross-section (transect) of the coast and shows the altitude with respect to the distance off-shore. Coastal profiles show very dynamic behaviour, the altitude at a certain position may change considerably in time. However these dynamics are bounded in both space and time. It is therefore suggested that a dynamic equilibrium profile exists (Dean, 1991; Ludka et al., 2015). After placement of a nourishment, the cross-shore profile is changed and slopes in the nourished area are generally steeper than before the nourishment. This is especially the case with beach nourishments and is caused by the construction method. The Sand Engine influences the cross-shore profile over an even greater extent in cross-shore direction and very steep slopes were observed after construction (De Zeeuw, 2011–2016; De Schipper et al., 2016).

Due to nourishments, an extra sand volume is added to the coast and the coastal profile is brought out of its dynamic equilibrium state. Observations of nourished beached by a.o. Hoekstra et al. (1996), Grunnet et al. (2005) and Ojeda et al. (2008) suggest that nourished beaches show different morphological behaviour after installation of the nourishment. Not only the cross-shore sediment transports are affected, but also the alongshore sediment transport changes. Nourished beaches also show large initial losses (Verhagen, 1992; De Schipper et al., 2015a). Erosion rates in the first year after installation are considerably higher than before installation of a nourishment, or during the rest of the life time of the nourishment. It is hypothesised that the large initial losses are caused by the steeper (nourished) profiles and the more pronounced wave attack. At the Sand Engine the coastal profiles are extremely far out of their equilibrium and large initial changes are to be expected.

The Sand Engine project is extensively being monitored. Since the project was unprecedented, there were large uncertainties in the behaviour. The goal of the monitoring programme is to study the behaviour and asses the impact of the Sand Engine from different scientific perspectives. Therefore a large multidisciplinary monitoring programme was set-up. Besides morphology, also the geology, biology and hydrology of the Sand Engine and its governance are studied. The ambition is to gain better knowledge in the aforementioned fields by working together. It is expected that using this multi- and inter-disciplinary approach, the different fields of research can profit from each others results.

This thesis involves the morphological behaviour of the Sand Engine and its surroundings, for which the morphology surveys of the Sand Engine are used. The morphology is being measured approximately every two months since August 2011. These altitude measurements include the area between the dune foot and a depth of ten metres below mean sea level. A more thorough description of the morphology surveys can be found in Section 2-1-2. In the next Section (1-4), a conceptual model is presented to frame the morphodynamics.

1-4 Conceptual framework

The morphodynamics of the nearshore area form complex and dynamic system. A lot of different processes play a role in the dynamics of the coast, which also interfere with each other. It is therefore hard to distinguish between the contribution of different processes to the observed changes. The complex morphological behaviour of the coast is caused by the large variation in the spatial and temporal scales of both the forcing and reacting parameters. On the time scale of seconds, sediment is moved with every wave. On the engineering time scale sediment transport is mainly dependent on the average wave climate and tidal currents.

However one major storm of a few hours may have more influence on the morphology than months of low waves.

In order to gain insight in the relations between the governing processes in the complex coastal environment, a conceptual model has been developed which is presented in Figure 1-6.

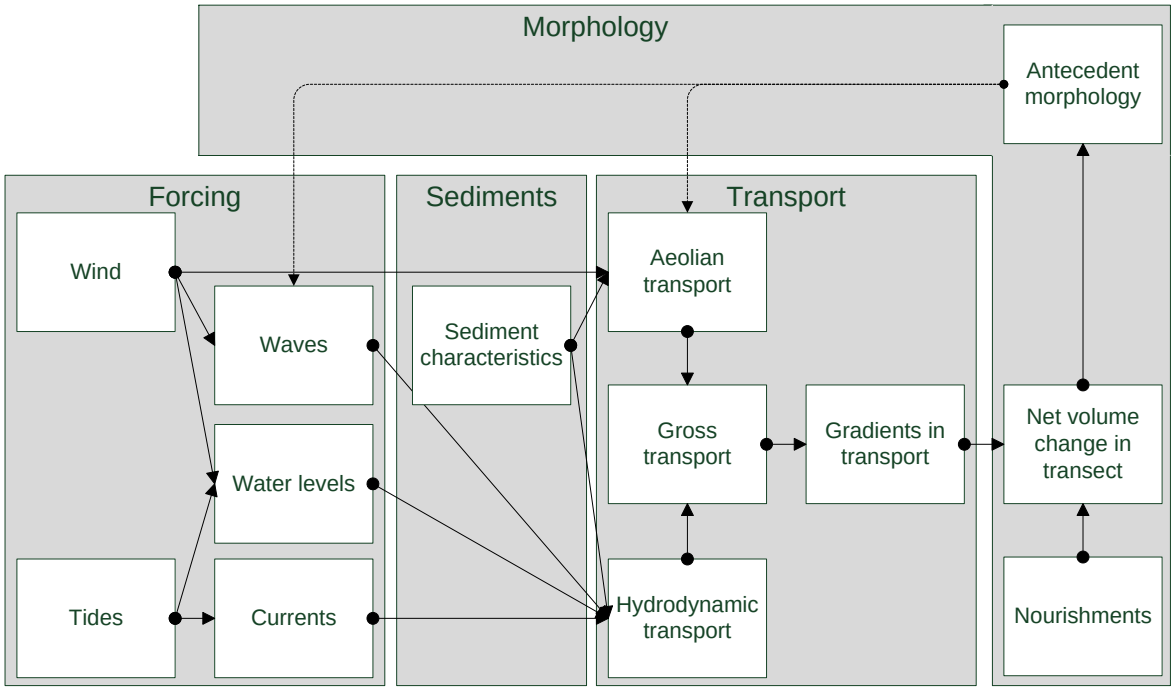

Figure 1-6: Conceptual model for sediment transport and coastal volume changes.

In this framework (see Figure 1-6), the most relevant and large scale processes are presented. The combination of the forcing by both wind and tides causes waves on the free water surface and currents. The combination of wave and current forces causes a transport of sediments in certain locations of the coast. Gradients in gross transport cause time-averaged net bed-level changes. These bed-level changes, adjust the morphology. Now we have arrived in a feedback loop, as the morphology directly influences the local wave forcing. The sediment transport is dependent on the local shear forces, induced by currents and waves. As the morphology changes, so does the forcing.

The process that drives the sediment transport the most depends mainly on the altitude, or the location in the cross-shore profile. At deeper waters the tide dominates the sediment transport, while in the breaker zone the sediment transport is dominated by wind waves. A second sediment transport mechanism is also present. This so-called Aeolian sediment transport is caused by the wind directly. This is the sediment transport mechanism that governs the sediment transport on the supra tidal beach and dunes. Ultimately all forcing is caused by wind and tides, however the more detailed one looks at the coastal system, the more sub-processes one can find which can be related to their respective fluxes.

1-5 Knowledge gaps & research questions

In this section, first the current knowledge gaps will be addressed. Then the research questions are identified. Followed by a few hypotheses which help in answering the presented research questions.

1-5-1 Knowledge gaps

The Sand Engine was the first of its kind, therefore beforehand little was known about the exact behaviour of a mega feeder nourishment. It was unclear what the long term evolution of the Sand Engine would look like. The first 18 months of Sand Engine evolution have been investigated by De Schipper et al. (2016), while the longer term has not. Numerical modelling studies of the morphological behaviour were presented in Stive et al. (2013), Luijendijk et al. (2017) and Arriaga et al. (2017), which show a diffusional behaviour of the peninsula. Some discussion remains on the diffusion rates and volumetric losses, as large differences are found between studies. Recent observations show a decrease in diffusion rate, so that the life time might very well be longer than the initially estimated 20 years in Stive et al. (2013).

Another point of discussion is that the Sand Engine has only been studied inside its initial survey area. Observations have however shown that the Sand Engine has an influence outside this area in alongshore direction. So the alongshore influence of the Sand Engine has not been properly addressed. Parts of the volumetric losses are expected to be deposited in the adjacent coastal sections, but no research on this has yet been performed.

One more aspect that needs some attention is the cross-shore profile. The cross-shore profile slope is expected to have a significant influence on the Longshore Sediment Transport (LST), as stated by De Schipper et al. (2015a) and De Schipper et al. (2016). This hypothesis is based on the correlation between large initial volume losses of nourishments and the (decrease in) steepness of the nourished cross-shore profile. In some empirical formulas for LST, a term including the cross-shore bed-slope is present. For instance the Kamphuis (1991) formula contains such parameter. Also little is known about the adjustment of a coastal profile after nourishment. Since coastal profiles have been observed to significantly change after installation of a nourishment it is meaningful to be able to quantify this process.

Concluding the following knowledge gaps have been identified:

- The long(er) term morphological evolution is yet unknown.
- The Sand Engine has unknown effect on the adjacent coasts.
- Cross-shore profile shape (slope) is expected to have a significant influence on LST, however the actual impact is unknown.

1-5-2 Research Questions

Based on the knowledge gaps identified above, the following research questions have been formulated:

1. What is the contribution of the Sand Engine to the sediment budgets in the Delfland coastal cell in the first five years after construction?

- What are the observed volume changes?
- What are the derived alongshore sediment transports?
- How is the plan-form evolving in time?
- What are the hydrodynamic parameters that govern the observed morphological changes?

2. What is the evolution of nourished cross-shore profile shapes and how can this be characterised?

   - How is the cross-shore profile shape evolving in time?
   - What is the difference in cross-shore profile shape adjustment between cross-shore profiles in accretive and erosive areas?
   - Are nourished cross-shore profiles returning to their pre-nourishment shape?
   - What is the distribution of volume change over the altitude?

1-6 Reader

In Chapter 2 the methods are discussed which are used to answer the research questions. The main method is a data analysis on the data of topographic/bathymetric surveys. In Chapter 3 the main results of the data analysis are presented step by step for each research question. Chapter 4 is dedicated to the discussion, here all assumptions and the accuracy of the results are discussed. Furthermore the results are placed in a broader perspective. Chapter 5 presents the conclusions, as derived from the results and discussion. In the final chapter, chapter 6, some recommendations for further research are presented. In the appendices additional analyses and observations can be found.

Chapter 2

Methods

In this chapter, the different analysis methods performed on the morphology surveys of the Delfland coastal cell will be presented. Before going into the details of the analyses, first a description of the relevant datasets is given in Section 2-1. This will be followed by an explanation of the pre-processing methods in Section 2-2, the coordinate systems (Section 2-3) and the different derived quantities from the data in Section 2-4.

A data analysis is performed on the morphology surveys in the Delfland coastal cell. The used morphology surveys consist of the datasets of four different monitoring programmes: Sand Engine, Nearshore Monitoring and Modelling: Inter-scale Coastal Behavior (NeMo), Vlugtenburg and JarKus. These datasets will be described in more detail in the following sections.

The analysis approach is quite fundamental, starting from raw (quality controlled) data to extensive post-processing and deriving the desired quantities for answering the research questions. The fundamental and structured approach allows to analyse variability in the morphology both time and space. The fixed reference grid allows for easy access to the data and extension with new routines and data when desired. Furthermore, specifically for this Thesis, data originally spanning multiple separate datasets is now combined and made uniformly accessible. This process is represented schematically in Figure 2-1 and will be further discussed and explained in the following sections.

2-1 Data description

Morphology surveys with high spatial and temporal resolution are available for the Delfland coastal cell. These data are present in two datasets, which are part of two different measuring programmes: *Sand Engine* and *NeMo*. Both datasets however are very similar. They are both measured using the same techniques and by the same company, moreover they are measured as much as possible simultaneously. Combined, the Sand Engine and NeMo surveys cover the whole Delfland coastal cell. The Vlugtenburg surveys cover a part of the Nemo area (in a complementary time frame), and the JarKus surveys cover the whole Dutch coast. From the latter only the part covering the Delfland coast is used. More information on the different surveys is shown in the following paragraphs.

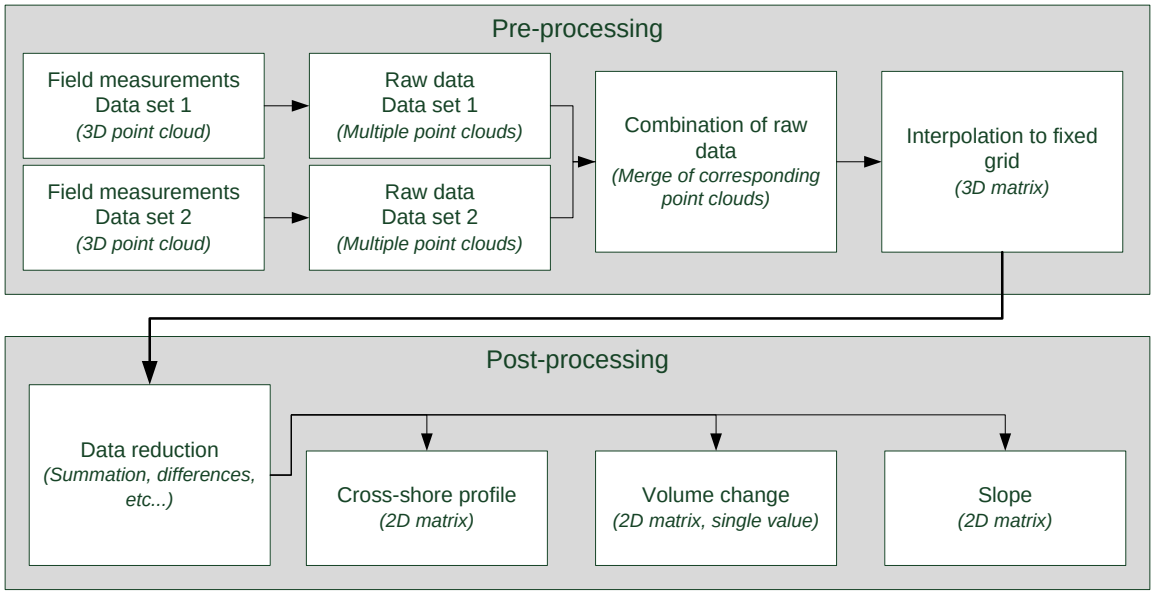

Figure 2-1: Block-scheme of the data processing.

In order to obtain the best insights in the morphology, and to assess the assumptions and boundary conditions it is necessary to cover the largest area possible. Therefore all available datasets covering the Delfland coastal cell are used. The spatial and temporal properties of the surveys will be described shortly.

2-1-1 Survey area

The Delfland coastal cell is bounded by the harbour of Scheveningen in the North-East and the Rotterdam Waterway (Hoek van Holland) in the South-West, stretching approximately 17.2km alongshore. The breakwaters form a hard boundary to the otherwise sandy Delfland coastal cell. In cross-shore direction the survey area is bounded by the dune foot on the landward side, either by a sharp increase in slope or a fence. On the sea side the boundary is set to the approximate position of the -5 or -10m+NAP depth contour for Nemo and Sand Engine surveys respectively (De Zeeuw, 2011–2016).

The morphology measurements of the Sand Engine cover the initial area of the Sand Engine peninsula and the adjacent coast over one kilometre to the North and South. In the cross-shore the measurements range from the dune foot to the approximate -10m+NAP depth, circa 2.5km off-shore. This area is indicated blue in Figure 2-2. The rest of the Delfland coast is covered by the NeMo-surveys, indicated by the yellow area in Figure 2-2. These surveys range from the dune foot to depths of -5m+NAP. The coarser JarKus surveys cover a larger cross-shore area, namely from the land side of the dunes to depths of circa 12m at 3km off-shore. These are indicated by the red area in Figure 2-2. Last the Vlugtenburg morphology surveys cover a small part of the Delfland coast indicated by the green area in Figure 2-2.

The four different datasets differ in the temporal coverage and resolution. The Sand Engine surveys started in August 2011, with a monthly interval until October 2012 and bi- monthly thereafter. The NeMo surveys took place in February 2012 and were performed bi-monthly

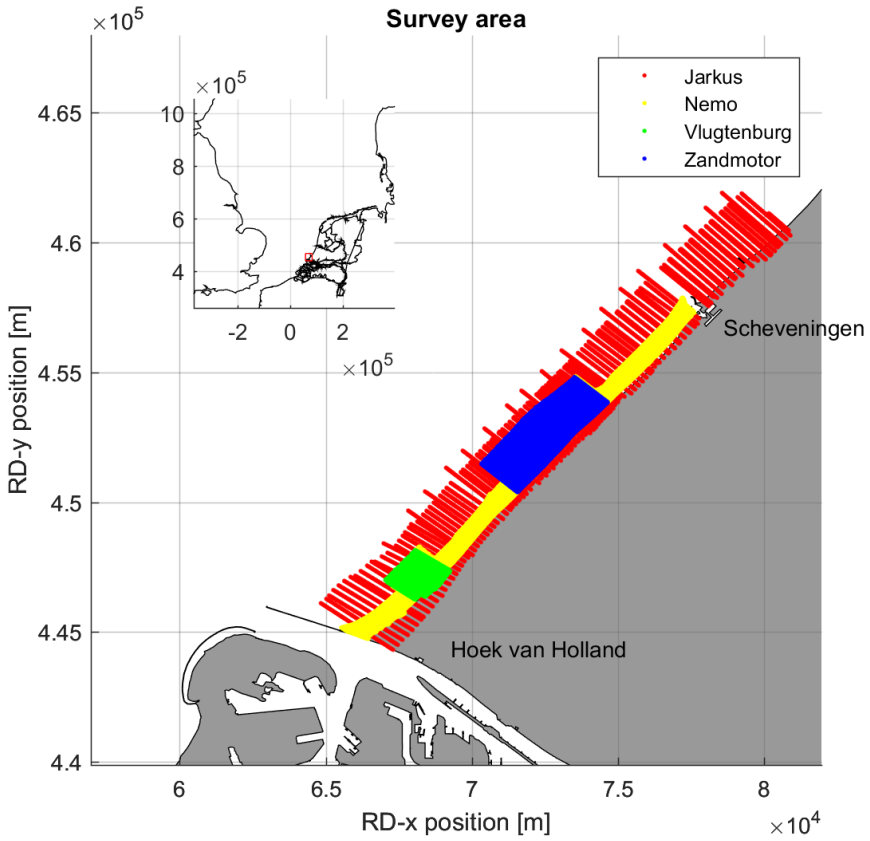

Figure 2-2: Spatial coverage of the different datasets, indicated by colours. JarKus also covers other areas. Inset: Location of the survey area in the Netherlands (red box).

from March 2013 onward. These surveys coincide with a Sand Engine survey. The latest available survey dates from September 2016, for both sets. Figure 2-3 shows an overview of all available morphology surveys in the Delfland coastal cell.

The Vlugtenburg surveys are used for comparison in morphodynamics between the Sand Engine area and the coast outside the direct influence the Sand Engine in the period not covered by the NeMo surveys. These monthly surveys are incorporated in the period from August 2011 to December 2012. JarKus surveys are performed on an annual interval. Surveys are available from 1965 to 2016. Only the surveys from 2012 to 2016 are used. For a complete overview of survey dates, see appendix D.

2-1-2 Measuring methods

During the Nemo and Sand Engine morphology surveys, the altitude of the bed is being measured. This is done on the beach as well as in the shoreface. Measurements are performed using the Real-time kinematic GPS (RTK-GPS) technique, for cm accuracy in positioning. Three types of vehicles are being equipped with Global Positioning System (GPS). The dry

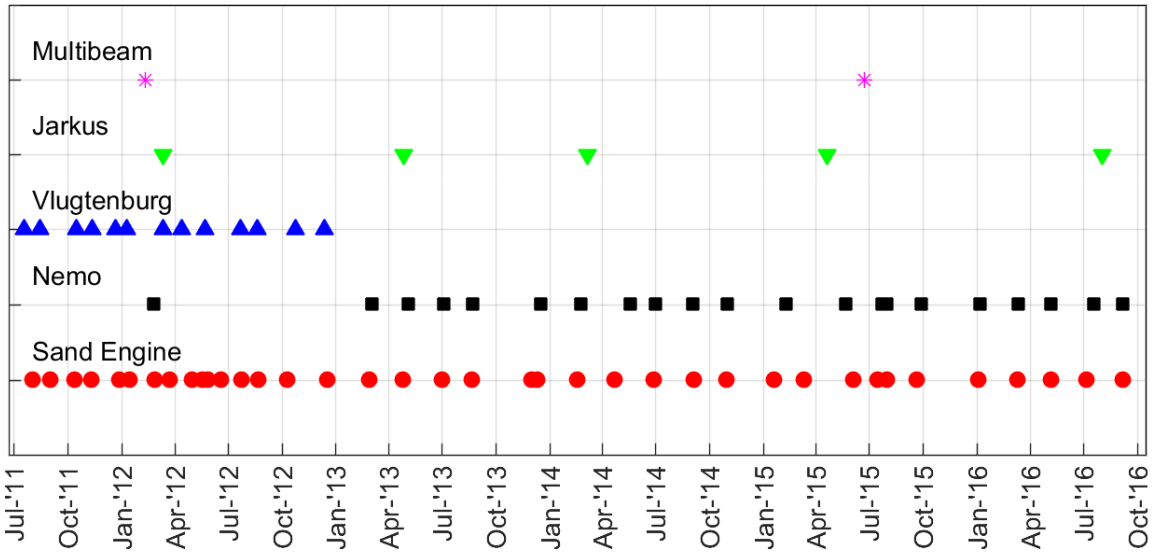

Figure 2-3: Overview of the morphological surveys in the Delfland coastal cell between July 2011 and October 2016.

and intertidal areas are being surveyed with a quad-bike, the wet area with a Jetski and the remaining and difficult to reach parts (pools, steep slopes) by walking with a wheel, see also: De Zeeuw (2011–2016). In Figure 2-4 the equipment is shown.

(a) Jetski **(b)** Quad **(c)** Walking wheel

Figure 2-4: Survey equipment, images: Shore Monitoring and Research (De Zeeuw, 2011–2016)

The surveys are performed along a set of shore-normal lines, the survey grid. These lines find their basis in the JarKus surveys from Rijkswaterstaat (De Zeeuw, 2011–2016). For the Sand Engine and Nemo surveys additional lines have been added in the alongshore direction to increase the alongshore resolution from approximately 250m to 20-40m. Due to the fixed grid, a systematic analysis is easier. Also the surveys of the Sand Engine and Nemo areas are performed in the same time frame as much as possible, to provide a continuous snapshot of the whole coastal cell.

Raw data is being measured as separate points (Equation 2-1) approximately along the lines of the survey grid. However, the points are not exactly on the grid. Therefore the raw data is interpolated in pre-processing. This will be further explained in Section 2-2.

$$z = f(x, y, t) \tag{2-1}$$

Rijkswaterstaat performs an annual coastal survey of the Dutch coast, called JarKus (JAarlijkse KUStmeting) (Minneboo, 1995; Rijkswaterstaat, 2016). These surveys have been performed since 1965. The JarKus surveys give an insight in the historical morphological behaviour of the Delfland coastal cell and can be used to assess the cross-shore fluxes over the boundaries of the Sand Engine/Nemo surveys.

The JarKus measurements are taken in shore normal transects with a 200-250m alongshore spacing, which form a sub-set of the Nemo and Sand Engine transects[1]. Measurements stretch in cross-shore direction from the back of the dune to 3000m from the Rijksstrandpalen (State beach poles) (RSP) line, coinciding with a water depth of approximately 12m below MSL (Rijkswaterstaat, 2016).

Survey data from the Vlugtenburg monitoring programme is included in this thesis for partial coverage of the Nemo-area in the period before the Nemo-surveys were conducted. It also provides the opportunity to compare coastal profile behaviour in and outside the Sand Engine area for an extended amount of time.

For the section between 2.2 and 4km from Hoek van Holland, measurements from the Vlugtenburg survey project are available (De Schipper et al., 2013; De Schipper et al., 2015b). These measurements have been performed from 2009 until the second Nemo survey in march 2013. The alongshore spacing is with 80m coarser than for the Nemo surveys, and transects have a slightly different orientation. A large part of the coarser alongshore resolution is mitigated by re-interpolation from the raw data to the Nemo transects. To confirm whether the interpolation of the Vlugtenburg surveys was of sufficient accuracy a manual inspection has been done between the Vlugtenburg survey of 13 February 2012 and the Nemo survey of 26 February 2012. The interpolated data was in good agreement with the Nemo data. Only near the edges of the Vlugtenburg area incomplete interpolated transects were found, and were therefore discarded.

2-2 Pre-processing

All measurement data is obtained as raw data, which has to be pre-processed for easier and more uniform analysis. Bi-linear interpolation towards cross-shore transects coinciding with the lines used for surveying tends to be the best choice. The pre-processing routine of the raw data consists of four steps:

1. Load raw data (point cloud).
2. Create bi-linear convex hull (triangulation) from all points.
3. Interpolate the convex hull for all points towards all points on the transects.
4. Build matrix with altitudes from all surveys.

[1] Actually, the other way around. SE and NEMO transects were interpolated from JarKus.

The interpolated data is then stored into different matrices for further post-processing.

The raw data consists of a point cloud of 3D-coordinates in RD-NAP coordinate coordinate space. The points have an X- and Y-coordinate in the Dutch Rijksdriehoeksstelsel, with a height with respect to NAP, the Dutch ordinance level. The point cloud is interpolated towards the coordinates of the survey lines. Interpolation is done by first building a convex hull from the raw data and then perform a bi-linear interpolation towards the transect coordinates. No extrapolation is allowed. When both a Sand Engine and Nemo survey are available at a certain time interval, both point clouds are merged and interpolated at once. This is justified because surveys usually take place on the same days and furthermore it avoids boundary effects on the border between the Sand Engine and Nemo areas. The same procedure is followed for Vlugtenburg surveys, when applicable. For a more thorough description of merging coastal surveys, see appendix E.

When mapping the interpolated survey data to a matrix in Matlab, this is done in such way that information of fixed points in the real world, correspond to fixed positions in the matrices. In interpolated form, the data has only three main dimensions: Alongshore position, Cross-shore position and Time (temporal position). The alongshore resolution is 20-40m, the cross-shore resolution is 5m and the temporal resolution is 10-100 days (see also table 2-1). The three main dimensions determine in which ways and dimensions the data can be post-processed initially.

Table 2-1: Resolution of the Survey grid.

Property	Area	Unit	Min	Mean	Max
Alongshore spacing	SE	m	19	37	72
	nemo	m	21	26	30
Cross-shore spacing	All	m	5	5	5
Temporal spacing	SE	days	9	50	100
	nemo	days	9	82	372

The data is organised in such way that all matrices can only have one or more of the main dimensions. Therefore fixed points (or lines) in the real world correspond to fixed indices in matrix space. Furthermore each matrix can hold only one property, for instance altitude, x-position or transect volume. This greatly simplifies post-processing, for instance changing the coordinate system from Rijksdriehoekstelsel (RD) to local axes (or RSP). The matrix space is conceptually drawn in Figure 2-5.

2-3 Coordinate systems

The raw data of the morphological surveys is available in Rijksdriehoek coordinates (RD-NAP). This is the official coordinate system used in the Netherlands. Coordinates are orthogonal with an x-coordinate increasing East and an y-coordinate increasing North. Altitudes are given with respect to NAP. For many purposes it is practical to look alongshore and cross-shore. Therefore a new shore-normal coordinate system has been adopted. These coordinates are based on Rijksdriehoek-coordinates with NAP height (ESPG:7415) (RD-NAP), but shifted and rotated in the horizontal plane to have its origin at the Southernmost transect origin near Hoek van Holland. The coordinates are approximately alongshore and cross-shore

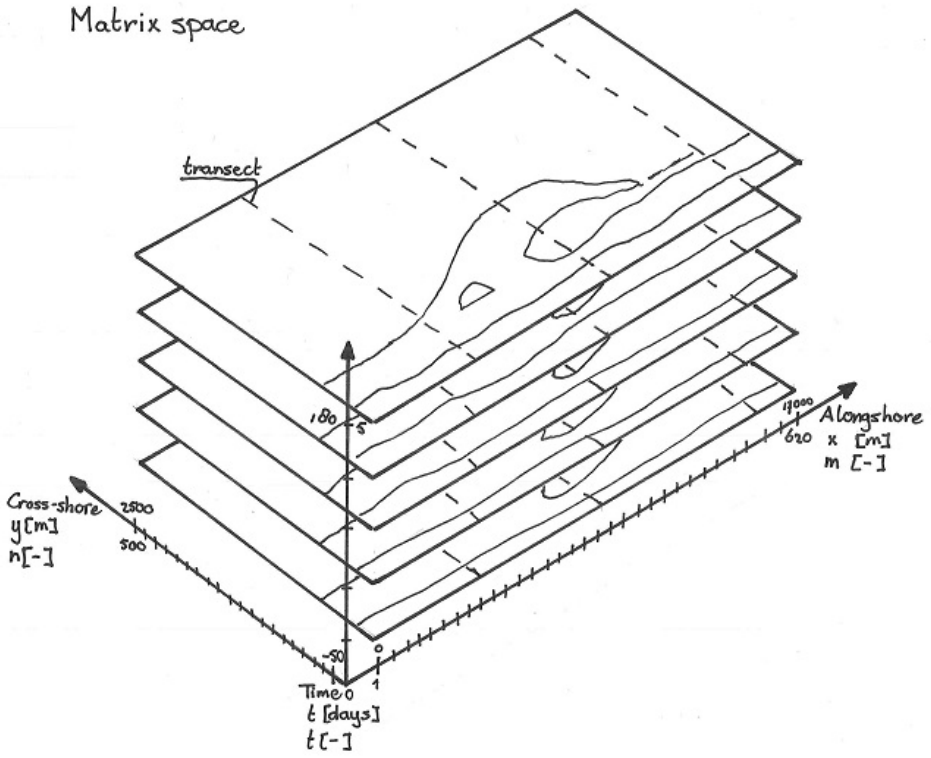

Figure 2-5: Positioning of data in matrix space, here: the altitude matrix.

directed, averaged over the Delfland coastal cell. The alongshore (ls) and cross-shore (cs) coordinates are calculated according to Equation 2-2, altitude coordinates remain NAP based. θ is 311.3 degrees, and the origin is at RD-position (67067,444050). See also appendix G

$$[ls, cs] = \begin{bmatrix} \cos(\theta) & -\sin(\theta) \\ \sin(\theta) & \cos(\theta) \end{bmatrix} \begin{bmatrix} RD_x - RD_{x,origin} \\ RD_y - RD_{y,origin} \end{bmatrix} \tag{2-2}$$

2-4 Data reduction & derivations

Due to the large amount of data, it is important to reduce this data into parameters or properties. After interpolation of the raw data, a 3D-matrix of the altitude at fixed coordinates remains. From this matrix other properties can be derived, either by numerical integration, derivation, taking differences or statistical analysis. These methods will bring the dimension of the data down one or more orders.

Before discussing the more applied methods directly relevant for answering the research questions, first a few general concepts are discussed that are used throughout all analyses.

2-4-1 Cross-shore profiles

In the alongshore direction we find 620 transects (survey lines), of which 125 are in the Sand Engine surveys, the rest in the Nemo-area. It is trivial to create cross-shore profiles

for every transect and every survey. Since every transect corresponds to a column in matrix space for every survey. From the cross-shore profiles it is possible to derive multiple other quantities, such as volumes covered, cross-shore slopes and positions of depth contours. A cross-shore profile is defined as the altitudes on a line extending shore-normal from a point on the RSP-line. An example is shown in Figure 2-6.

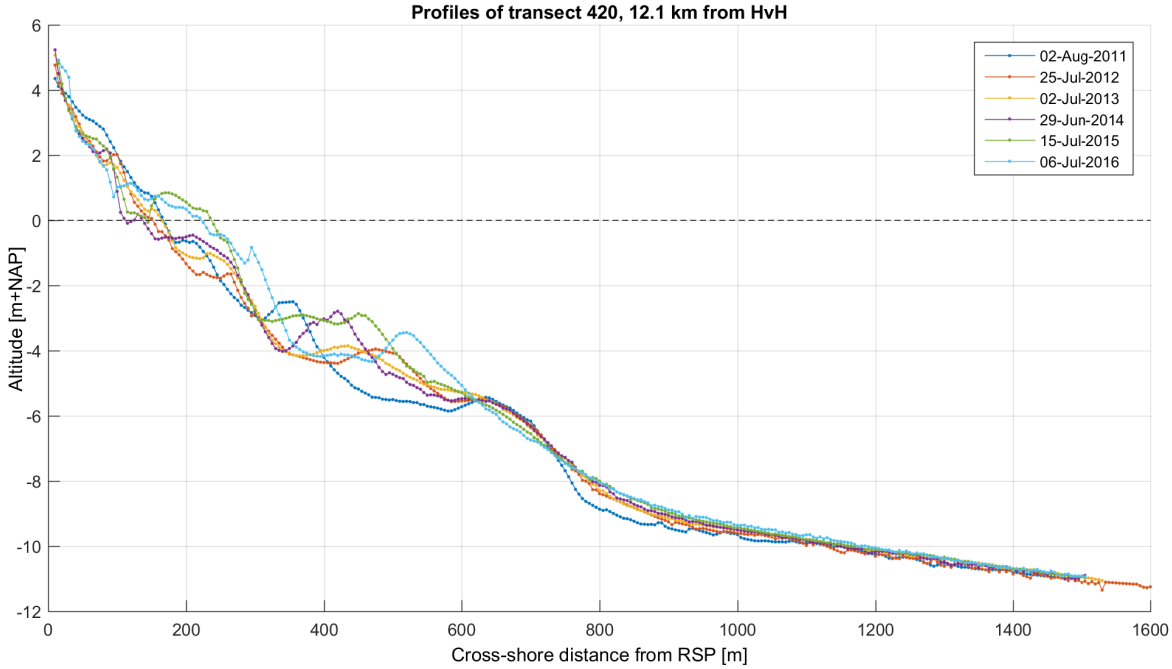

Figure 2-6: Example of a cross-shore profile for multiple surveys in time. Here transect 420 from Hoek van Holland is shown.

2-4-2 Cross-shore slope

Within a transect the cross-shore slope can be determined. This is an important descriptive property in morphological analyses. The cross-shore slope is defined as the slope of the best linear fit trough the points on a single transect bounded by two arbitrary horizontal boundaries (altitudes). An example is given in Figure 2-7. In this figure it is shown that the best-fit slope between -3 and +1m+NAP is equal to -0.015 m/m (or 1:67).

2-4-3 Depth contours and plan-form evolution

A contour or iso-line is the line which connects points with equal altitude. Contour positions are defined as the most seaward intersection of a cross-shore profile with a given altitude. When this is done for every transect a depth contour is obtained.

Based on the positions of depth contours in individual transects the plan-form of the Sand Engine can be tracked. Tracking the Sand Engine plan-form could provide a simple model to describe the morphological behaviour in a few simple parameters. Examples of such parameters are the cross-shore and alongshore extent or the in-situ volume. Time series of such parameters can provide information on the remaining life-time and alongshore spreading.

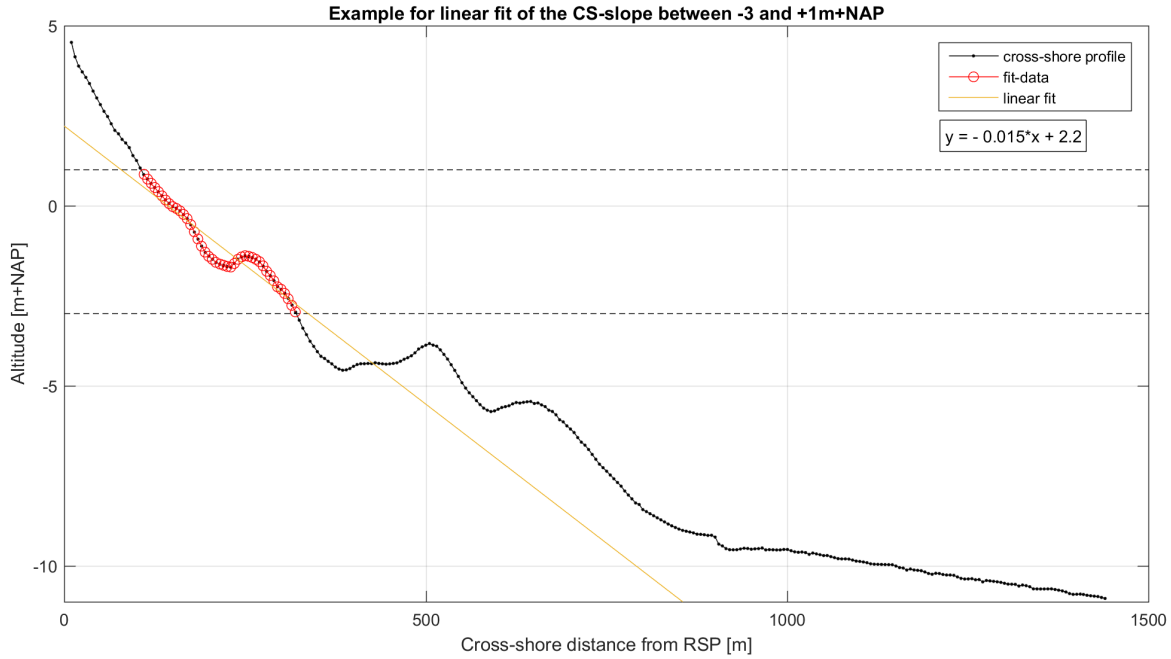

Figure 2-7: Example of the cross-shore slope of a transect. The linear fit is taken through all points between -3 and +1m+NAP.

2-4-4 Volumes

Volumes are defined as the area below a transect bounded by a land- and seaward boundary and an arbitrary vertical reference level. This gives the amount of volume per metre alongshore [m^3/m]. The net volume difference is defined as the difference between volumes of two surveys of the same transect, but limited to the cross-shore distance where both surveys have data on that transect. Hence the volume difference of a transect is the sum of height differences in time multiplied by the distance between points.

The volume of a transect is calculated as in Equation 2-3. Here $V_{j,t}$ is the volume in m^3/m of the transect j at time t, z is the altitude of a point in m+NAP and Δx is the cross-shore spacing between points in m. The volume difference of a transect between subsequent surveys is calculated as in Equation 2-4. Here $\Delta V_{j,t}$ is the net change in volume of transect j from t to t+1 in m^3/m. j is the alongshore index of transects, i is the cross-shore index of measured points and t is the time index of the survey.

$$V_{j,t} = \sum_{i=0}^{m} z_{i,j,t} \cdot \Delta x_{i,j} \tag{2-3}$$

$$\Delta V_{j,t} = \sum_{i=0}^{m} (z_{i,j,t+1} - z_{i,j,t}) \cdot \Delta x \tag{2-4}$$

When calculating volumes, different properties are determined: net volume change, gross volume change, accretion and erosion. In the following list these are defined, and in Figure 2-8 the concepts are visualised.

Accretion The volume difference between surveys where the bed-level has increased.

Erosion The volume difference between surveys where the bed-level has decreased.

Gross volume change The absolute sum of accretion and erosion.

Net volume change The difference between accretion and erosion (can be both positive or negative).

The absolute sum of accretion and erosion is a lower boundary for the gross sediment transport between surveys. It is a measure for the morphological activity in a profile. The difference of accretion and erosion is the net volume change in a transect, the volume that is transported in or out of the transect.

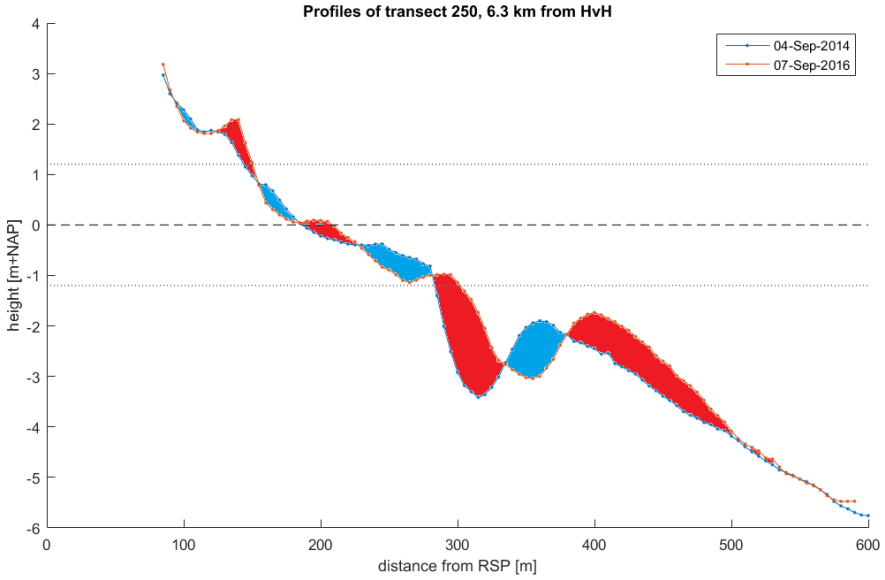

Figure 2-8: Definitions of volume changes; red areas denote accretion, blue areas erosion. Net volume change is the difference (red-blue), gross volume change the summation (red+blue).

To gain insight in the adjustment of coastal profiles, horizontal boundaries are set for the volume calculations. When calculating the volume changes in horizontal slices, a distribution of volume changes over the altitude can be obtained. This addresses the most active parts of the profile and enables to determine progradating and receding areas.

2-5 Research methods

Based on the basic principles and concepts explained above, the specific methods for the different research questions will be presented. They will be ordered according to the research questions.

2-5-1 Sediment budgets & transports

The first research question is: *What is the contribution of the Sand Engine to the sediment budgets in the Delfland coastal cell in the first five years after construction?* Which is then subdivided into three sub-questions. The first one is about the observed volume changes.

The Sand Engine is designed to spread alongshore, thus local erosion is expected in the central part of the peninsula and accretion is expected on both sides alongshore. Calculating the volume changes on a transect basis, for every interval between surveys, areas of accretion and erosion can be tracked in both space and time. When assessing the volume changes of the transects, it becomes clear which parts of the Delfland coastal cell gain sediment, and which parts loose sediment.

Summation of the volume differences in time tells the net change in volume with respect to the initial situation (n-point rate). When integrating the net volume changes per transect over the area (distance alongshore), the net loss of bulk volume out of the survey area can be determined. This is an important parameter quantifying the performance of the Sand Engine. It must be noted that the area over which this volume change is assessed must be much larger than the initial nourished area. In this case, the whole coastal cell is chosen.

The second sub-question is about the (net) sediment transports. These sediment transports can be derived from the volume differences. This is done using the Exner Equation (Exner, 1925), which assumes that a difference in bed level is caused by a gradient in sediment transport, see Equation (2-5). This equation has been derived for rivers, however when it is assumed that sediment transport in alongshore direction only takes place between the depth of closure and the dry beach, it is also applicable to alongshore sediment transport.

The following assumptions have been made to apply the Exner equation on the alongshore sediment transport:

- Alongshore sediment transport takes place in a bounded area.
- This area is fully contained by the surveys.
- No sediment is transported over the seaward boundary in cross-shore direction.
- No sediment is transported over the landward boundary in cross-shore direction.
- The alongshore sediment transport at the Hoek van Holland harbour mole is set to zero.
- Changes in porosity are neglected.

The validity of these assumptions will be further discussed in chapter 4. A preliminary check on the validity has been made. Figure 2-9 shows the standard deviation of the altitude in time, which is a measure of bed activity. Bright means high activity, black is no activity. As can be observed in Figure 2-9, the boundaries of the survey area are relatively dark, which implies that the majority of the bed-level activity is contained within the survey area.

The alongshore sediment transport is defined as the summation of net volume differences in alongshore direction. The value of the alongshore sediment transport is known except for an integration constant. Since the actual transport over the alongshore boundaries is unknown, it is assumed to be zero in Hoek van Holland.

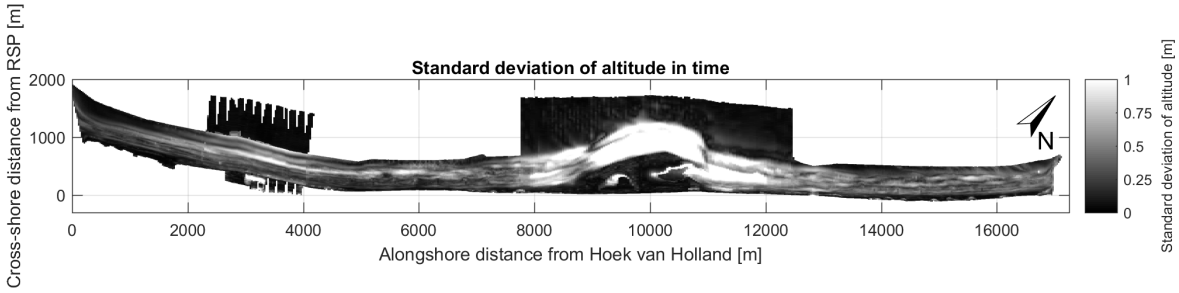

Figure 2-9: Standard deviation of the altitude. Light areas show much activity, dark areas little variation in bed level.

In the Exner (1925) Equation 2-5, a difference in bed-level in time $\left(\frac{\partial \eta}{\partial t}\right)$ is related to a gradient in sediment transport in space $\left(\frac{\partial S}{\partial y}\right)$, including effects of change in porosity. This is a one-dimensional equation, which assumes the bed-level change to be representative for the whole cross-section. Here η is the mean change in bed level, S the sediment transport rate and ϵ_0 the porosity. For the coastal environment this has been reworked to Equation 2-6. With ΔV the change in volume per unit length, and ΔS the change in sediment transport rate.

$$\frac{\partial \eta}{\partial t} = -\frac{1}{\epsilon_0}\frac{\partial S}{\partial y} \tag{2-5}$$

$$\frac{\Delta V}{\Delta t} = -\frac{\Delta S}{\Delta y} \tag{2-6}$$

$$\Delta S = \frac{\Delta V}{\Delta t} \cdot \Delta y \tag{2-7}$$

As the measurements are not continuous, the sediment transport must be derived numerically, as shown in Equation 2-8. In this equation the indices i, j and t denote the matrix index in cross-shore, alongshore and temporal direction. Parameter z is the altitude, x the cross-shore distance, y the alongshore distance and T the numeric time. Since Δx is constant it can be taken out of the summation.

$$S_j = \sum_{j=0}^{m}\left[\frac{\sum_{i=0}^{n} z_{i,j,t+1} - z_{i,j,t} \cdot \Delta x_i}{T_{t+1} - T_t}\Delta y_j\right] \tag{2-8}$$

$$\Delta x_i = x_{i+1} - x_i = 5m \tag{2-9}$$

$$\Delta y_j = \frac{1}{2}\left[(y_j - y_{j-1}) + (y_{j+1} - y_j)\right] \tag{2-10}$$

The third sub question is about the plan-form adjustment of the Sand Engine peninsula. In order to quantify this, several macro-features will be tracked in time, such as the cross-shore extent and the alongshore extent. Two different approached will be used. The first is direct detection of depth contours. The second method involves curve fitting.

To track the plan-form, for every transect the most seaward crossing of a certain depth contour is calculated. The maximum seaward extent of the Sand Engine is the largest distance from the depth contour to the RSP line. The alongshore extent (or footprint) is harder to determine

directly, since the extent of the plan-form decreases from the centre. Efforts have been made to find crossings of the depth-contour positions with pre-construction positions. While this works for the early surveys, an objective position could not be found for later surveys. Alternative methods have been found in tracking volume changes, and curve fitting.

The second method involves curve fitting of the depth contours. Since, from visual inspection, the Sand Engine peninsula appears to evolve into a Gaussian bell shape, depth contour positions can be fitted to this shape. The parameters of the equation then are a measure for the macro features of the peninsula. First the position of the depth contour is determined in alongshore, cross-shore coordinates (ls,cs), then this data is curve fitted to Equation 2-11. In this equation a is the amplitude, b is the mean, c is the standard deviation, and d is the cross-shore off-set. The cross-shore extent from RSP is given by $a + d$, the alongshore extent by approximately $4c$, see also Figure 2-10.

$$y(x) = a \exp\left[\left(\frac{x-b}{c}\right)^2\right] + d \tag{2-11}$$

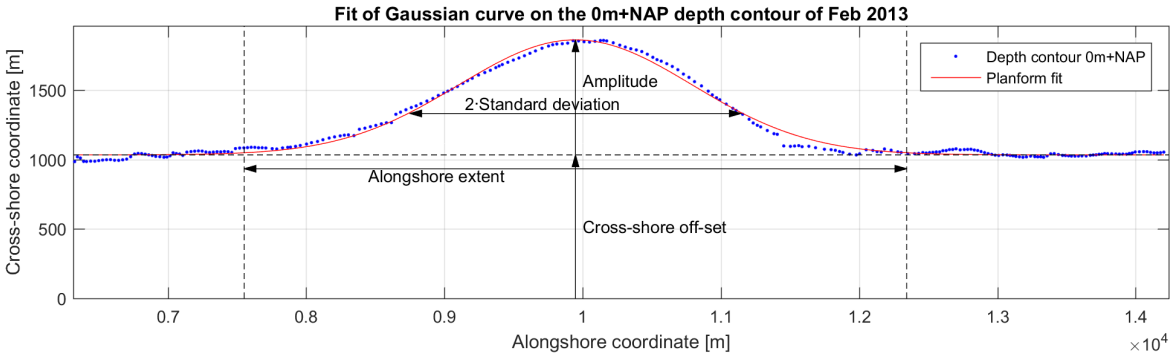

Figure 2-10: Example of a Gaussian fit of a depth contour

From the rate of change of the cross-shore amplitude, the remaining life-time of the Sand Engine can be derived. Provided that there is a clear end-of-life criterion.

2-5-2 Efficiency parameters

Traditionally the efficiency of a nourishment is determined by the ratio of the instantaneous in-situ volume over the nourished volume or hopper volume. Since traditional nourishments are meant to stay in place, this is an attractive parameter. For the Sand Engine however, this is not the case as it is meant to spread beyond its initially nourished area. Therefore two new parameters are introduced: the nourishment efficiency and the redistribution efficiency.

The nourishment efficiency is the ratio of the net volume change and the nourished volume, see Equation 2-12. It is almost the same as the ordinary efficiency, but the volume change is calculated over the whole area which is influenced by the mega nourishment (in the desired timespan). The redistribution efficiency is the ratio of the net volume change over the whole influenced area and the eroded volume from the (central section of the) mega nourishment, see Equation 2-13

$$\eta_n = 1 - \frac{\Delta V_{net}}{V_{nourishment}} \tag{2-12}$$

$$\eta_r = 1 - \frac{\Delta V_{net}}{V_{redistributed}} \tag{2-13}$$

The values of these parameters should be between 0 and 1, where the higher values mean a more efficient process or less net losses from the desired area.

2-5-3 Wave parameters & correlations

The last sub-question is: *What are the hydrodynamic parameters that govern the observed morphological changes?* In order to answer this, correlations will be made between parameters describing the hydrodynamic forcing, and parameters describing the morphodynamic reaction. Therefore time series of wave parameters have been obtained. Wave observations are obtained from the off-shore location Europlatform, approximately 65km WSW from the Sand Engine. Time series of wave height, wave period and wave direction are available throughout time. A second set of wave time-series consists of transformed wave parameters, applied at 10m water depth.

The time series will be reduced to a single value per survey interval, to enable correlations. Different derived parameters will be tested for the highest correlations with observed morphological changes. A few examples are: mean wave height, wave energy and alongshore component of wave energy.

It is expected that the wave energy determines the amount of gross sediment transport, thus high correlations are expected. The (gradient in) net sediment transport is expected to be correlated to the (gradient in) the alongshore component of the wave energy.

Wave energy is calculated according to Equation 2-15. In this equation, P is the wave power per observation, ρ is the density of sea water, g is the gravitational acceleration, H_s the significant wave height, T_s the significant wave period, E is the total wave energy and Δt the interval of observations. The alongshore component of the wave energy is calculated according to Equation 2-16, where ϕ is the wave direction and θ the local coastline orientation.

$$P = Enc = \left(\frac{1}{8}\rho g H_s^2\right)\frac{1}{2}\frac{gT_p}{2\pi} \tag{2-14}$$

$$E = \sum P\Delta t \tag{2-15}$$

$$E_{ls} = \sum P\sin(\theta - \phi)\Delta t \tag{2-16}$$

Correlations between various parameters are performed in two ways: in time and in space (alongshore). Temporal correlations are correlations between time series of two parameters $p1$ and $p2$ for every transect, resulting in circa 620 correlation coefficients, calculated over 22 (Nemo) or 37 (Sand Engine) surveys. Spatial correlations are correlations of parameter $p1$ and $p2$ for every survey (time step), resulting in 22 or 37 correlation coefficients, calculated over circa 620 transects.

Two vectors of properties are linearly correlated against each other. Correlations are performed unsupervised and outliers are not accounted for. The correlations give a Pearson (normal) correlation coefficient. The correlation coefficient is given by Equation 2-20, $\bar{x}$ is the mean value of parameter x and $\tilde{x}$ consists of the residuals. These correlation coefficients show how well the one parameter (y) can be described as a linear function of the other parameter (x), see Equation 2-17. A correlation coefficient of 1 is fully positively linearly correlated, -1 means fully negatively linearly correlated and 0 means uncorrelated.

$$y = f(x) = a \cdot x + b \tag{2-17}$$

$$\tilde{x} = x - \bar{x} \tag{2-18}$$

$$\tilde{y} = y - \bar{y} \tag{2-19}$$

$$r = \frac{\sum \tilde{x} \cdot \tilde{y}}{\sqrt{\sum \tilde{x}^2 \cdot \sum \tilde{y}^2}} \tag{2-20}$$

2-6 Evolution of cross-shore beach profiles

The second research question is *What is the evolution of nourished cross-shore profile shapes and how can this be characterised?* It is split into several sub-questions, which will be assessed separately.

In the vicinity of the Sand Engine, the morphological changes are large. The extent of the peninsula has decreased several hundreds of metres. In order to describe cross-shore profiles which change this much the point of view should be changed. Normally cross-shore profiles are defined with the altitude as dependent variable with respect to the cross-shore distance (see Section 2-4-1), which is rather useless for these analyses. Therefore the cross-shore profile is described a function of the altitude with the cross-shore distance as dependent variable. This alternative approach makes more sense, since the hydrodynamic forcing is more dependent on the altitude than on an arbitrary horizontal position.

First the evolution of cross-shore profiles is qualified. What processes cause the changes in profile shape and what changes are observed. In the intertidal and shoreface zones the hydrodynamic forces of waves and currents will cause sediment transports. The lower in the beach profile, the less the influence of waves becomes. On the sub-aerial beach aeolian transport dominates the sediment transport.

It is expected that differences in profile adjustment exist between accretive and erosive profiles. Already from a physical point of view accretion and erosion are different processes with different net-fluxes. By comparing the profile adjustment of strictly accretive with strictly erosive areas it becomes emergent what the differences and similarities are. Time-series of depth-contour positions and slopes are analysed for this.

Due to the large horizontal displacement of the coastal profiles around the Sand Engine, the characteristics will be related to the altitude instead of a horizontal position. From a fundamental perspective it is also expected that a certain property is linked to an altitude, rather than a horizontal position relative to a cross-shore reference line.

To test whether profiles tend to adjust towards their pre-nourishment state, slopes at equal altitudes will be compared to Jarkus surveys from before 2008. That is before the implementation of the *Weak link programme*[2], in which almost the whole coastal cell was nourished. This large scale coastal reinforcement project started in 2008 and ended in 2010 at the Delfland coast. Shortly thereafter, the Sand Engine was built.

The process of profile adjustment is very complex. Sediment transport processes in both the cross-shore and alongshore direction cause the cross-shore profile to adjust. Furthermore only gradients in transport capacity cause a change in volume, or redistribution over the vertical. Lastly these processes are influenced by feedback from both antecedent morphology and instantaneous wave climate. See the conceptual model, Figure 1-6.

[2]Programma Zwakke Schakels, locatie Delflandse Kust.

Chapter 3

Results

In this chapter the results of the data-analysis are presented. This chapter is structured by the research questions, which will be addressed one by one. The results are supported by figures, which illustrate the results and give the reader better understanding of the presented results. In the first section the results contribution of the Sand Engine to the Delfland coastal cell is presented. This is further quantified by calculating volume changes and sediment transports. Section 3-2 presents the correlations between the hydrodynamic forcing and morphological response. And in Section 3-3 the results of the analysis of cross-shore profile adjustment are presented.

3-1 The contribution of the Sand Engine to the Delfland coastal cell

The first research question is: *What is the contribution of the Sand Engine to the sediment budgets in the Delfland coastal cell in the first five years after construction?* This question is divided into sub-questions which will be addressed separately.

In this chapter certain qualitative areas will be referred to. An overview of these areas is presented in figure 3-1, which shows the altitude of February 2013, colours indicate the altitude with respect to NAP. Hoek van Holland and the Rotterdam waterway are at 0km, Scheveningen harbour is at 17.2km.

3-1-1 Observed volume changes in the Delfland coastal cell

The Sand Engine is meant to *feed* the adjacent coast, therefore the sand has to spread in alongshore direction. When assessing the volume changes of the transects, it becomes clear which parts of the Delfland coastal cell gain sediment, and which parts loose sediment. Volume changes in the Delfland Coastal cell are dominated by the Sand Engine. In the area around the peninsula, from 7500 to 12500m alongshore (see Figure 3-2), a very clear signal is present in the volumetric changes. The peninsula has an erosive middle part, with accretive flanks. The rest of the coastal cell shows only minor volume changes.

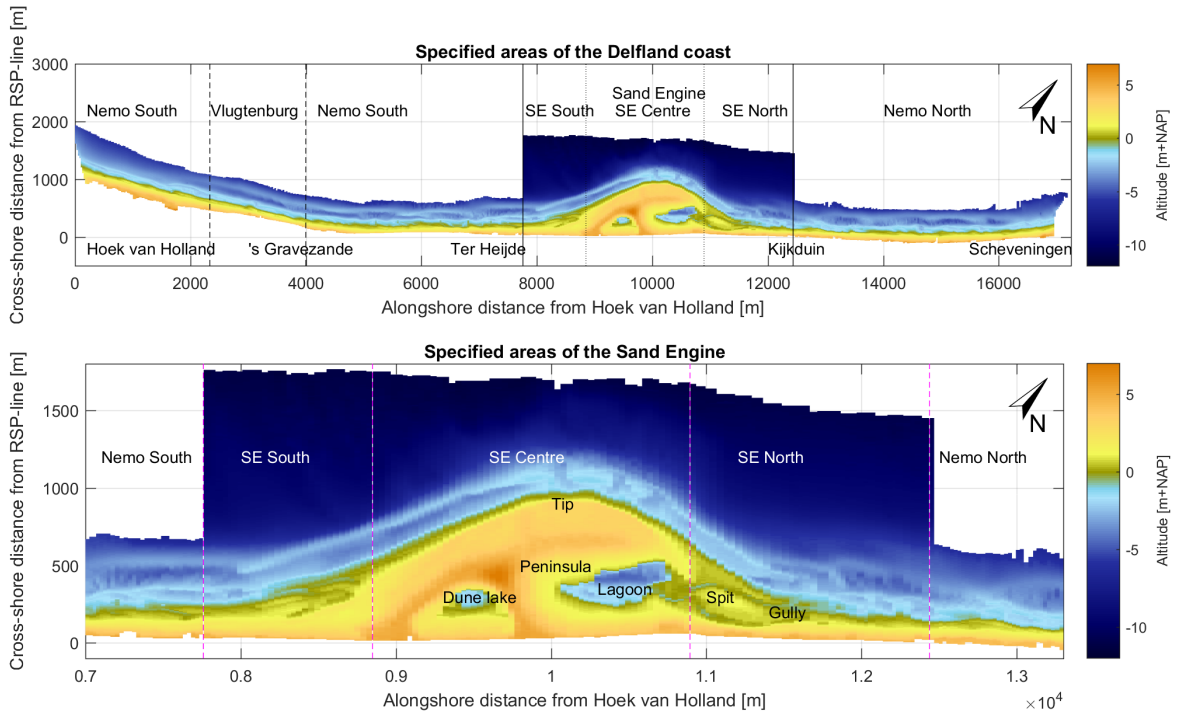

Figure 3-1: Specified areas used for referring in this report. Areas are indicated on the bathymetry of February 2013. Top panel: specified areas of the whole Delfland coastal cell. Bottom panel: specified areas around the Sand Engine peninsula.

The net volume changes from August 2011 (February 2012, Nemo area) to September 2016 in the Delfland coastal cell are shown in Figure 3-2. Net erosion at the Sand Engine peninsula locally peaks at $3000\text{m}^3/\text{m}_{\text{alongshore}}$ and the maximum accretion is found to be $1600\text{m}^3/\text{m}_{\text{alongshore}}$ for both flanks. In the Nemo area the net volume changes are more than one order of magnitude smaller with a magnitude around $110\text{m}^3/\text{m}_{\text{alongshore}}$. Locally this is higher for instance from 2500 to 3000m from Hoek van Holland, but this is caused by a shoreface nourishment in 2013. The area just before Scheveningen harbour (16-17km from Hoek van Holland) also shows a higher volume change.

The temporal behaviour of the net volume change is shown in Figure 3-3. This figure shows a time-stack of cumulative net volume changes in time. The time is on the vertical axis, alongshore position is on the horizontal axis. Every row of colours indicates the cumulative net change in volume since the first survey, for every transect. Warm colours indicate accretion, cold erosion.

The accretive regions on both sides of the initial peninsula slowly grow in alongshore direction, thus the Sand Engine is feeding the adjacent coast. The Northern section has extended 1700±20m and the Southern section 1000±20m, based on a net volume change threshold of $200\text{m}^3/\text{m}$. The Southern accretive area has crossed the boundary of Sand Engine survey area in February 2012 The position of the erosive part of the Sand Engine area varies only little in time. On a yearly time scale the erosive area is bounded between 8800±80m and 10900±80m from Hoek van Holland. Per survey, however, these boundaries are less clear especially in less energetic periods.

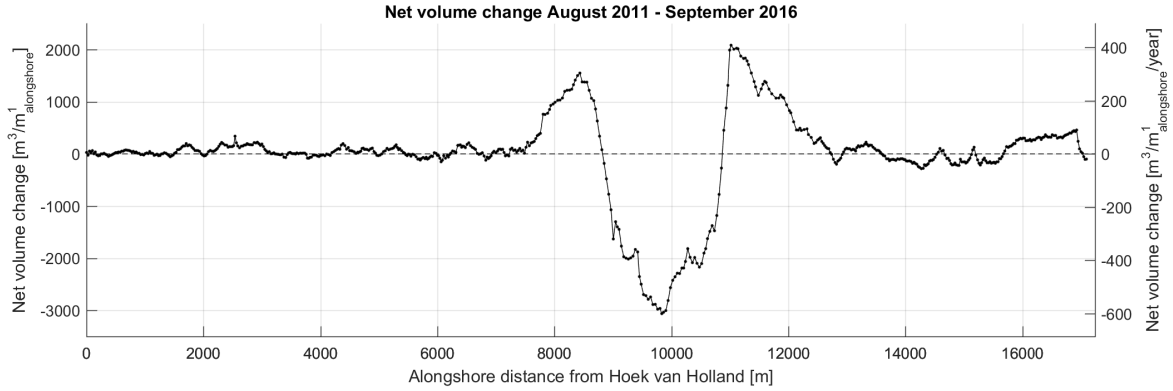

Figure 3-2: Cumulative net volume change [$m^3/m^1_{alongshore}$], from August 2011 (Feb 2012, Nemo) to September 2016.

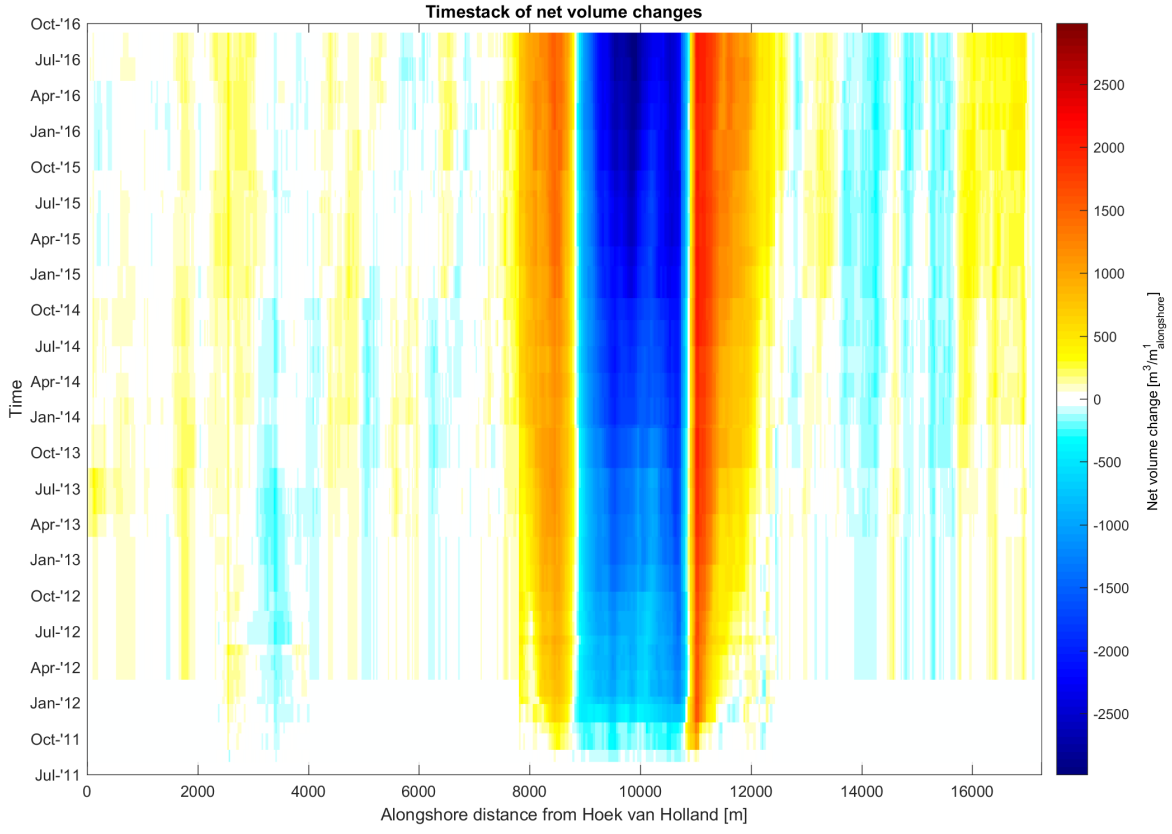

Figure 3-3: Time-stack of cumulative net volume changes per transect [$m^3/m^1_{alongshore}$]. Warm colors indicate accretion, cold colors erosion.

The development of bulk sediment volumes inside balance areas has been tracked in time. The coastal cell has been divided in different areas alongshore, see Figure 3-4. From this development it can be observed that the losses from the central part of the Sand Engine peninsula are largely compensated by gains in the adjacent sections. From the $4.2{\cdot}10^6 m^3$ of erosion from the central peninsula, $3.4{\cdot}10^6 m^3$ has accreted elsewhere. $1.8{\cdot}10^6 m^3$ has accreted in the North, $1.2{\cdot}10^6 m^3$ in the South and $0.38{\cdot}10^6 m^3$ in the Nemo sections. Resulting in a net loss of $0.8{\cdot}10^6 m^3$, all values over 5 years.

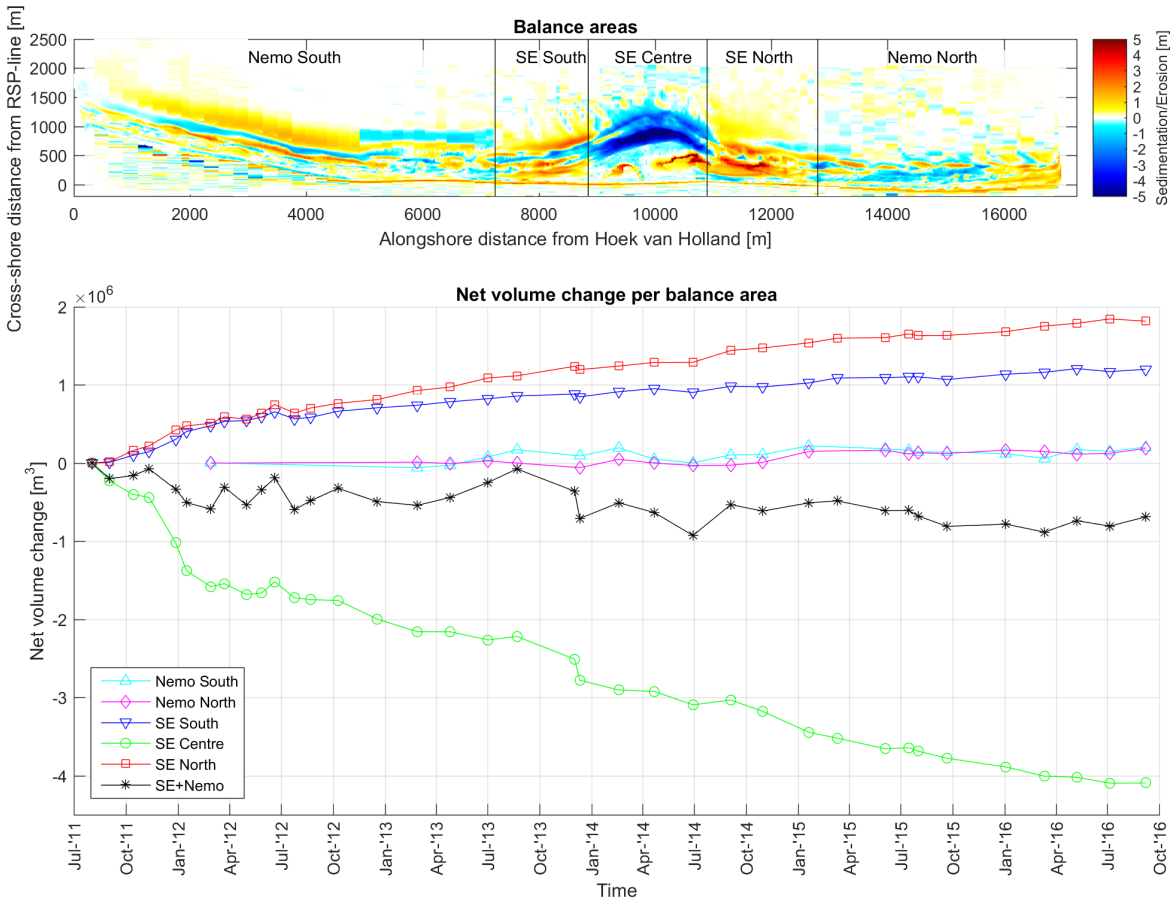

Figure 3-4: Cumulative net volume changes inside the alongshore balance areas, most of the losses from the Sand Engine peninsula are deposited in the adjacent sections. Top panel: Boundaries of the balance areas in the background sedimentation/erosion plot from August 2011 (March 2012) to September 2016. Lower panel: Development of the volume relative to the first survey.

Traditionally the efficiency of a nourishment is described as the ratio of the in-situ bulk-volume after some time and the initially nourished bulk-volume. For mega nourishments such approach does not suffice, since it is meant to spread beyond its initial area. Therefore an alternative parameter is introduced. Two efficiency parameters were introduced in Section 2-5-2, the nourishment efficiency and the redistribution efficiency. The first is like the classic efficiency, only the net volume change over the whole influenced area is taken. The redistribution efficiency describes the how much of the active sediment volume of the mega nourishment is still in the system. High values correspond to low net losses. This number is

defined as 1 minus the net loss of sediment from the survey area ΔV_{net} divided by the amount of redistributed sediment $\Delta V_{redistributed}$, see Equation 3-1. This amounts in a redistribution efficiency of 83% after five years.

$$\eta = 1 - \frac{\Delta V_{net}}{\Delta V_{redistributed}} \tag{3-1}$$

$$0.83 = 1 - \frac{0.8 \cdot 10^6}{4.2 \cdot 10^6} \tag{3-2}$$

3-1-2 Derived alongshore sediment transport

From the observed net volume changes, the alongshore sediment transport has been derived with Equation 2-8. Figure 3-5 shows both the volume changes and alongshore transport in the domain. The upper panel shows the net change of volume from the first to the last survey. Large gradients in alongshore transport are expected along the Sand Engine peninsula. Positive gradients correspond to large gains in volume, negative gradients to losses. The peaks in sediment transport correspond to zero-crossings of the net volume change, where the gradients are largest.

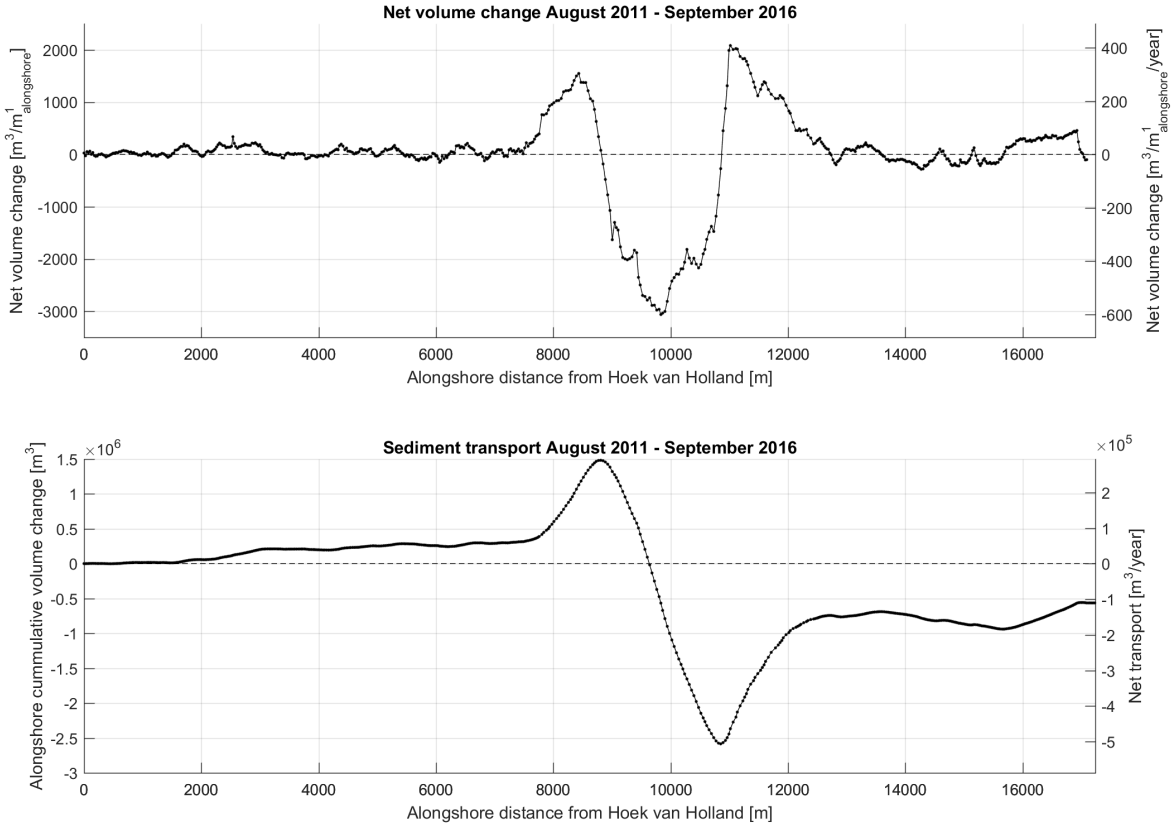

Figure 3-5: Upper panel: cumulative net volume change [m^3/m^1], lower panel: alongshore sediment transport [m^3], Northbound is negative. On the left y-axis the total values are displayed, on the right y-axis the averaged annual value is presented.

The alongshore sediment transport is shown in the lower panel of Figure 3-5. The black line shows the net transport, which has been calculated according to Equation (2-8). The values are with respect to an unknown integration constant, which is set to zero at the Hoek van Holland boundary. Large gradients in the alongshore transport correspond to large volume changes. The peaks in the sediment transport correspond to a zero net volume change. The difference between the initial and final value denotes the loss of sediment over the domain. From this calculation, we may conclude that circa $8{\cdot}10^5 m^3$ of sediment has been lost from the domain. On average there is a gradient in net sediment transport over the coastal cell of $1{\cdot}10^5 m^3$/year, directed to the North. The maximum gradient over the Sand Engine area is $4{\cdot}10^6 m^3$ or on average $8{\cdot}10^5 m^3$/year. A loss from the survey domain is not necessarily equal to a loss from the coastal cell. This will be further discussed in Section 4-1-2.

3-1-3 Observed plan-form changes of the Sand Engine

The bathymetry around the Sand Engine has changed a lot over the past years. The most pronounced changes took place in the first year after construction. It can be observed that the Sand Engine peninsula expands in alongshore direction, while the cross-shore extent reduces. In the Nemo area changes are less spectacular, however there is quite some activity in the sub-tidal bars. In Figure 3-6 the bathymetries of 6 surveys are shown (all around July). Tracking the plan-form changes of the Sand Engine is an efficient way in determining the area of influence of the Sand Engine. It may provide a predictive tool for the remaining life-time.

The cross-shore extent, the most seaward point of the Sand Engine peninsula, has decreased over the years. Furthermore, this point has shifted slightly towards the North. The decrease in cross-shore extent of the peninsula is not uniformly distributed over the altitude. The maximum decrease in cross-shore extent of 340m is found around the 0m+NAP depth contour. Other contours, both below and above, show lower values. The decrease in cross-shore amplitude of the peninsula indicates that the morphological behaviour of the Sand Engine differs over the altitude. The divergence of depth contours in time indicate that the cross-shore slopes must have changed. Since a divergence of depth contours causes a decrease in slope (flattening), a convergence causes steepening of the cross-shore profile. In Figure 3-7 the positions of maximum cross-shore extent of a few depth contours are shown. The +2m and 0m+NAP contours show an equal retreat, while the deeper contours show less retreat. On average the point of maximum extent has shifted 100m alongshore to the North, the peninsula appears to advect slowly to the North, in the direction of net LST. It must be noted that the determination of this alongshore position is quite sensitive, but the trend is clear.

Another approach to assess the plan-form change is curve-fitting of depth contours. These fits are more robust to outliers in the depth contours. Further, more descriptive parameters can be derived. From visual inspection of the bathymetry a Gaussian curve with a cross-shore offset is chosen for the fitting, see Equation 3-3. In this equation a is the amplitude, b is the mean, c is the standard deviation, and d is the off-set. The cross-shore extent from RSP is given by $a + d$, the alongshore extent by approximately $4c$.

$$y(x) = a \exp\left[\left(\frac{x-b}{c}\right)^2\right] + d \tag{3-3}$$

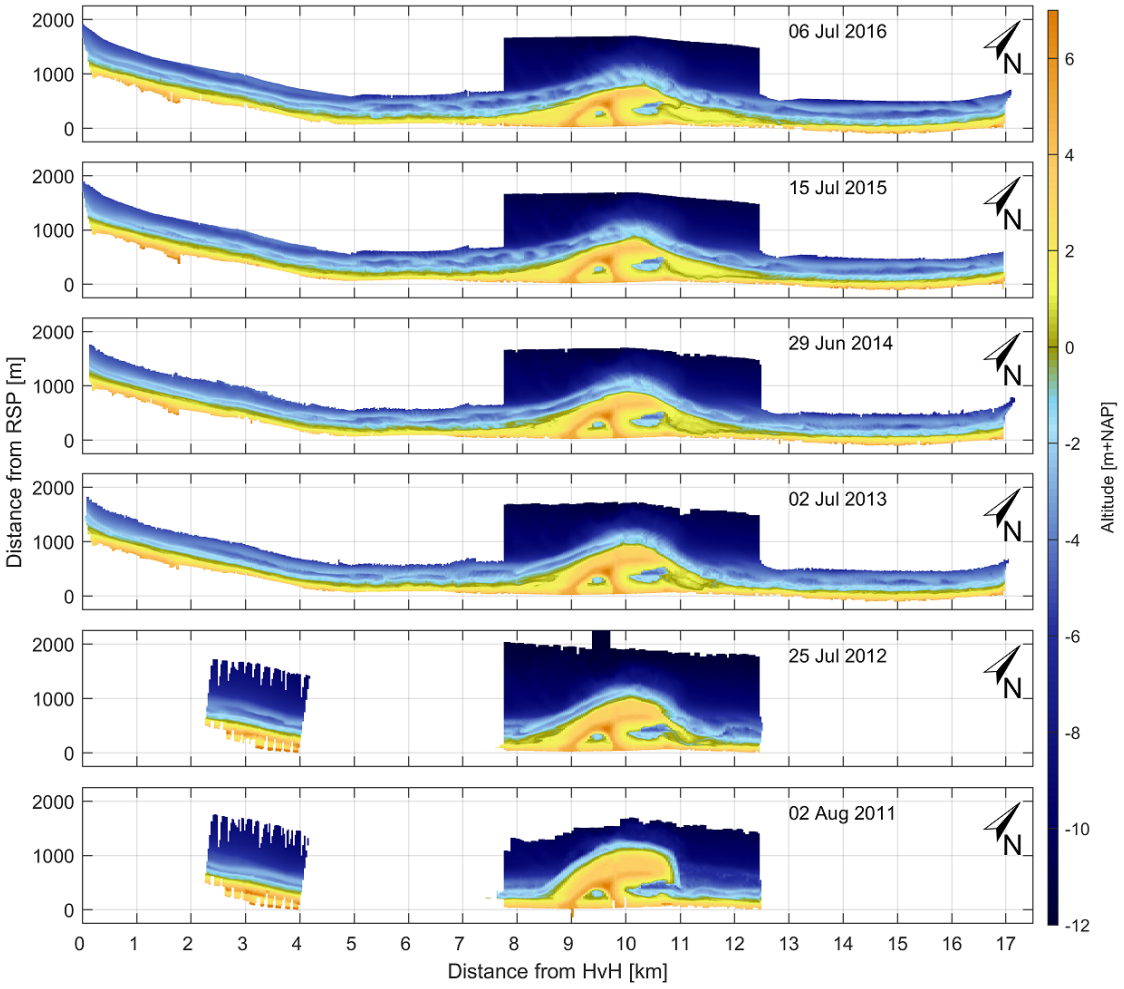

Figure 3-6: Bathymetries of surveys with yearly interval from 2011 (lower panel) to 2016 (upper panel). Over time the plan-form of the Sand Engine has changed considerably.

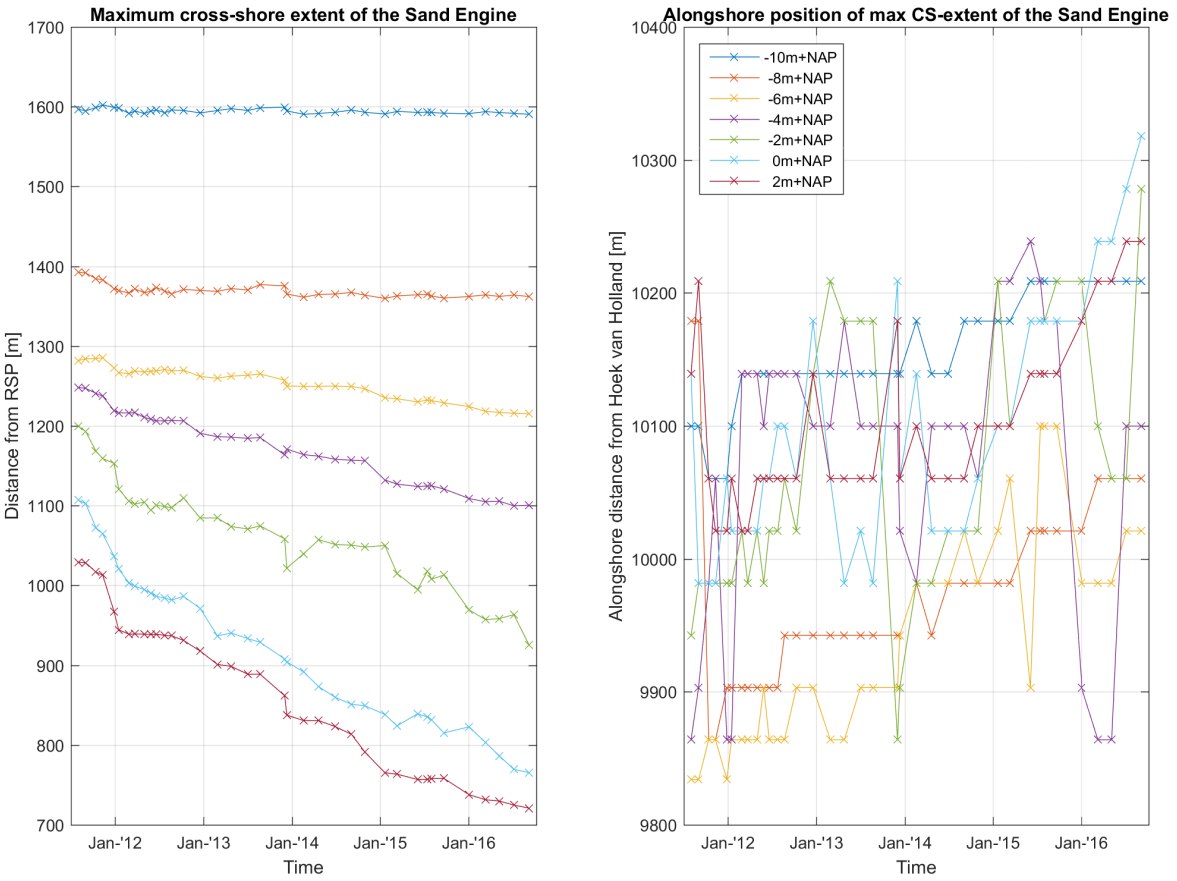

Figure 3-7: Evolution of the cross-shore amplitude of the Sand Engine peninsula, derived directly from depth contours. Left: maximum cross-shore extent of certain depth contours in time, right: alongshore position of maximum extent of these depth contours.

This fitting approach performs very well, with R^2 values of 0.9 and higher, see Figure 3-8. The best fits are obtained for depth contours between -1m+NAP and +1m+NAP. Lower in the profile, the alongshore- and temporal variability of bars slightly influences the results. In the first 8 months the R^2 values rapidly increase, after which they remain fairly constant, the Root Mean Square Error (RMSE) shows the same behaviour. This period coincides with the formation of the spit on the North.

The "real world" parameters of the curve fitting coincide well with the directly obtained parameters especially the cross-shore extent, see figures 3-9 and 3-7. Performance of direct measuring is best during the first eight months after construction, while performance of curve-fitting appears to be best after the first eight months, since the plan-form then resembles a Gaussian shape more.

Due to the large differences in behaviour of the different depth contours, no single representative depth contour can be assigned. Thus description of the over-all morphological behaviour of the Sand Engine peninsula is not possible based on a single depth contour. The cross-shore profile changes shape and not only shifts horizontally. Adjustment of cross-shore profiles is further discussed in Section 3-3.

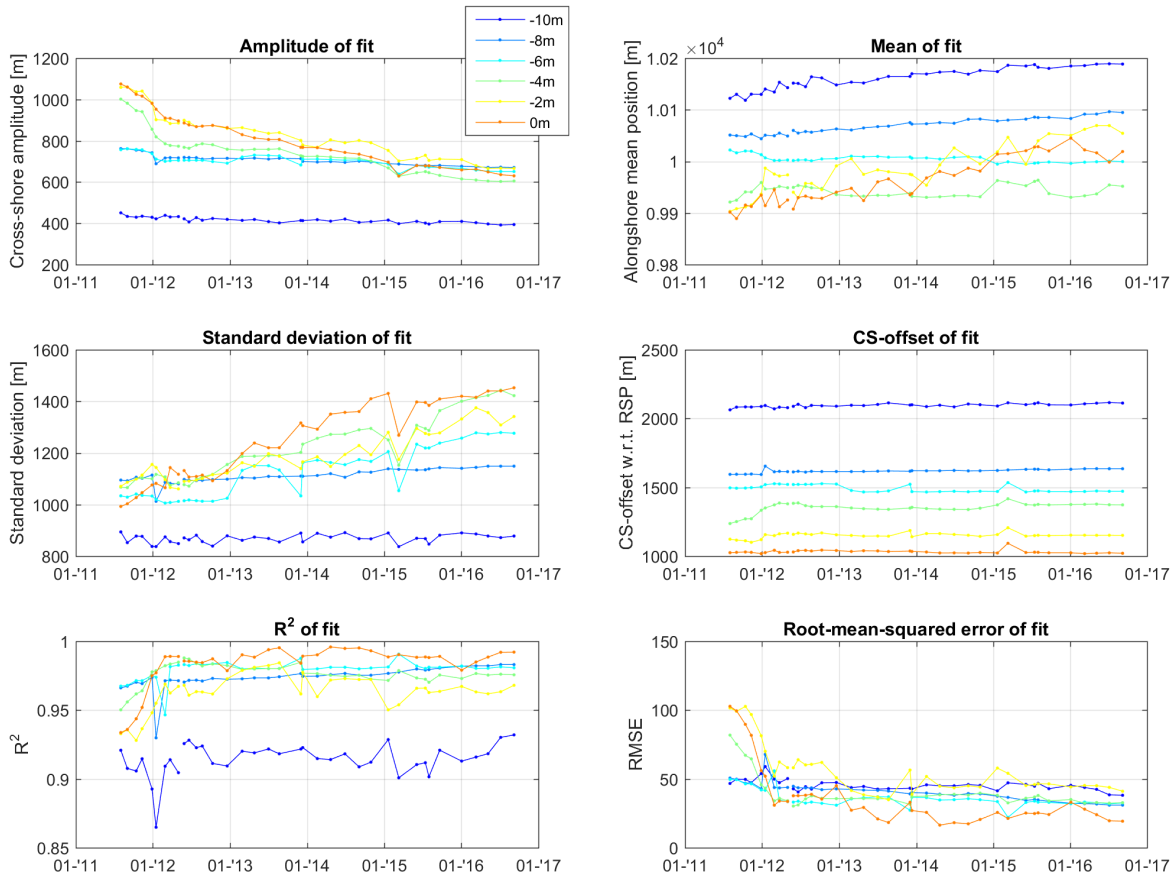

Figure 3-8: Curve fitting parameters of the Sand Engine, for selected depth contours.

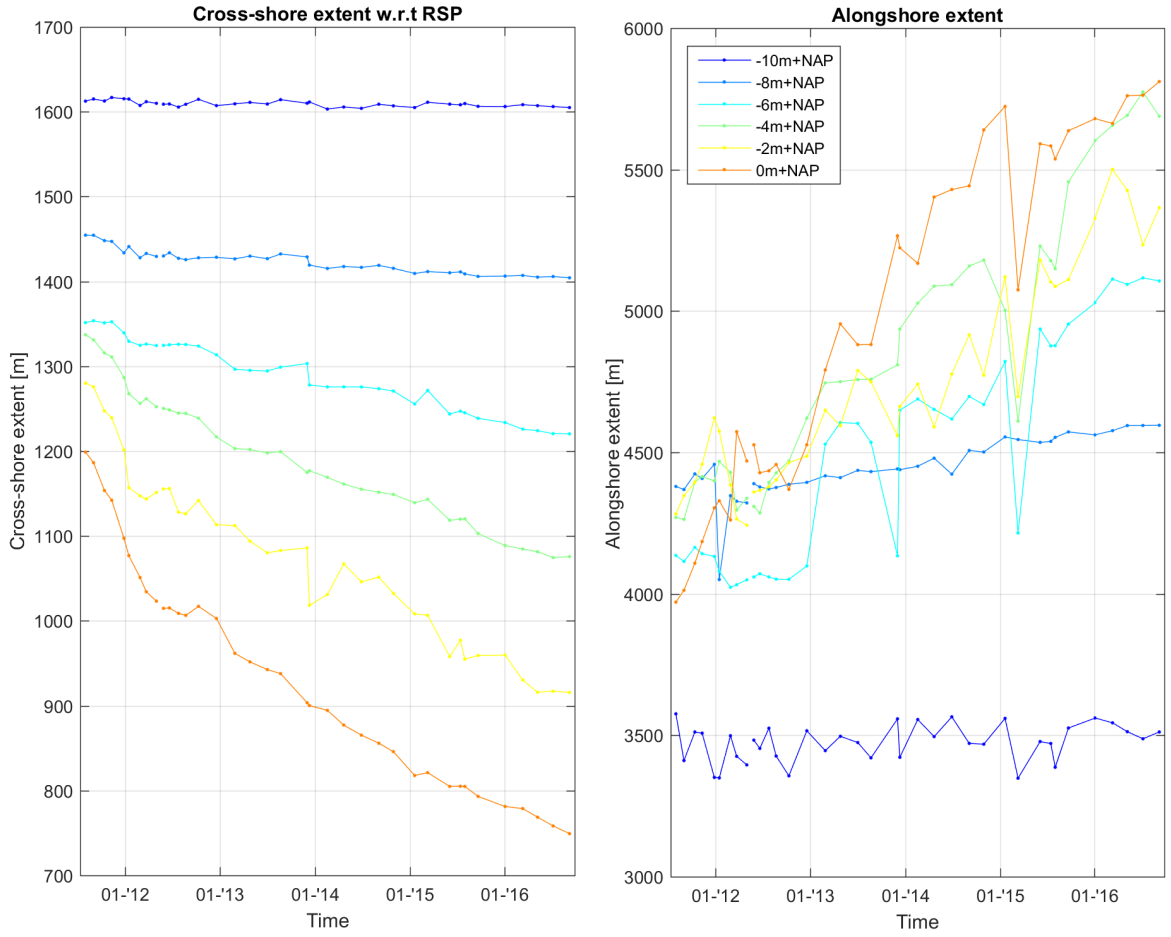

Figure 3-9: Evolution of the of the Sand Engine peninsula, derived directly from curve fitting. Left panel: cross-shore extent (amplitude+off-set) of certain depth contours in time, right panel: alongshore extent of the Sand Engine peninsula.

3-1-4 Summary

Most of the nourished sediments still remain in the survey area, as only $8{\cdot}10^5 m^3$ is lost. The gradient of volume changes over the Sand Engine is $4.2{\cdot}10^6 m^3$, which is a measure of the amount of redistribution. The resulting redistribution efficiency is 83%. There is an average Northbound alongshore sediment transport gradient over the coastal cell of $1.5{\cdot}10^5 m^3$/year. Around the Sand Engine peninsula large gradients in the net alongshore sediment transport are found. The gross gradient in LST over the Sand Engine peninsula is $8{\cdot}10^5 m^3$/year. And the sediment has redistributed over an area of at least 5.8km alongshore.

3-2 Correlations

Several correlations have been made in order to assess the influence of different hydrodynamic parameters on observed morphological changes. The measurement frequency of the morphology (bi-monthly) and wave hydrodynamics (hourly) differ several orders, therefore reduced time-series of wave observations are used. These reduced series are obtained by averaging or summation over the relevant period. One of the most pronounced signals is found in the correlation between wave energy and gross volume change.

The gross volume changes per transect have been correlated against the wave parameters. The correlation appeared to be largest for the relation between the gross volume change and the cumulative wave energy over the intervals between surveys. Correlation coefficients up to 0.95 are obtained (mean is 0.72), see Figure 3-10. In this correlation no distinct signature of the Sand Engine is found. When taking the alongshore component of the cumulative wave energy, a better correlation is exptected than with energy only. This is however not the case, as shown in figure 3-11. The average relative wave angle of incidence did not show significant correlation on itself. This is caused by the long period between surveys, in which the wave climate varies considerably. This variation in the wave direction blurs the wave angle effect. Thus morphodynamic activity is mainly dependent on the wave energy.

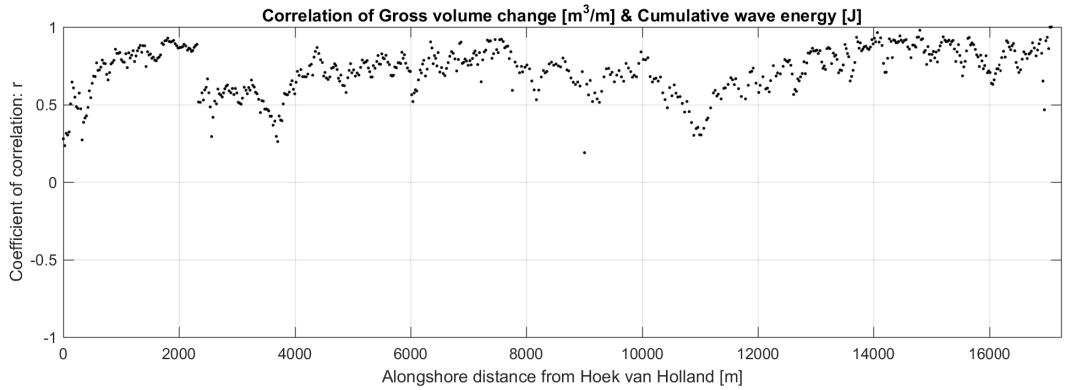

Figure 3-10: Correlation between gross volume change [m^3/m] and cumulative wave energy [J].

The net volume change does not show significant correlations with wave parameters, as shown in figure 3-12, the sign of the correlation coefficient shows wheter a profile is mainly accretive or erosive. The bad correlations may be caused by the way the hydrodynamics force the

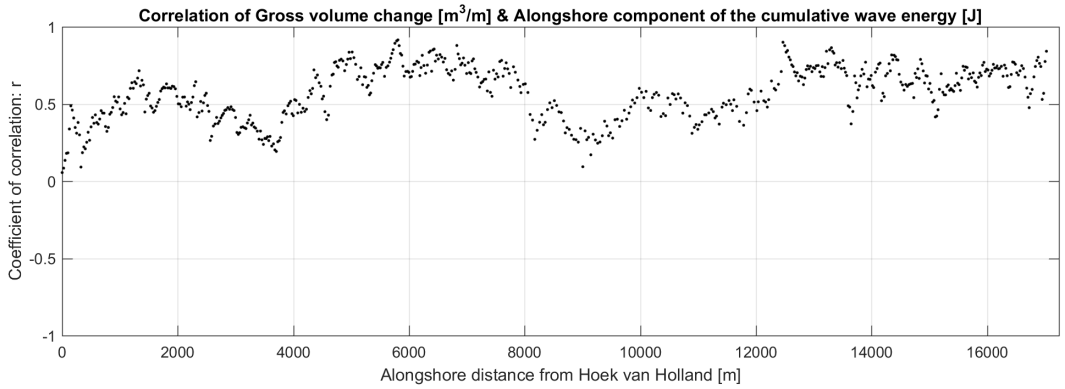

Figure 3-11: Correlation between gross volume change [m^3/m] and the alongshore component of the cumulative wave energy [J].

morphology. Since the hydrodynamic forces cause a sediment transport, but only gradients in this transport cause a net change in volume. Other correlations with net volume change showed even worse results. For more figures of correlations, see Appendix H.

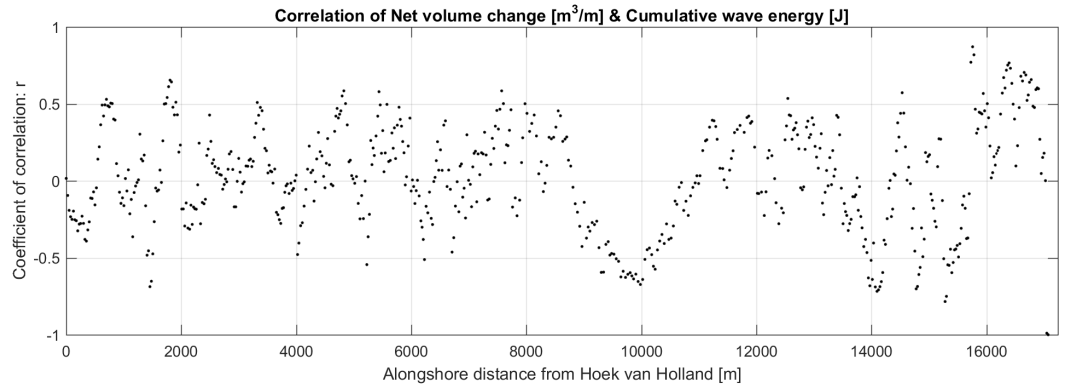

Figure 3-12: Correlation between net volume change [m^3/m] and the cumulative wave energy [J].

3-3 Development of cross-shore profiles shape

The second research question is: *What is the evolution of nourished cross-shore profile shapes and how can this be characterised?* This question is separated into different sub-questions, which will be answered separately. For reference of alongshore positions, see Figure 3-1.

3-3-1 Evolution of post-nourishment cross-shore profiles.

In the Sand Engine area, unprecedented volumes were nourished and large volume changes are observed. After placement of a nourishment, the cross-shore profile is changed and slopes in the nourished area are generally steeper than before the nourishment. The Sand Engine influences the cross-shore profile over a great extent in cross-shore direction and very steep

slopes were observed after construction. As hypothesised it is beneficial to look at accretive and erosive profiles separately.

Over the vertical, different zones can be distinguished in the cross-shore profiles. These zones each have a different behaviour as they are governed by different processes. These zones are discussed below and are shown in figure 3-13.

The sub-aerial zone (> 2m+NAP) is mainly influenced by aeolian processes, since waves do seldom reach these altitudes. Volume changes and bed activity are small.

The wave action zone (< 2m+NAP & > -7m+NAP) is dominated by wave hydrodynamics. The amount of wave energy varies considerably over the altitude. Bed activity is high and the largest volume changes are found here.

The shoreface zone (< -7m+NAP), is governed by tidal and residual currents of non-breaking waves as the action of wind waves has reduced. Bed activity is lower, and time scales involved are longer. But gradual bed level changes are found. During storm events wind waves may still have an influence due to the larger wave heights.

Erosive profiles only, also show a slumping zone (> 2m+NAP). This is the part of the profile which is often not under direct wave attack, as it is too high. However wave attack and sediment transport lower in the profile may cause cliff or beach scarp formation higher in the profile, transporting sediments to lower altitudes. The resulting slopes are very steep.

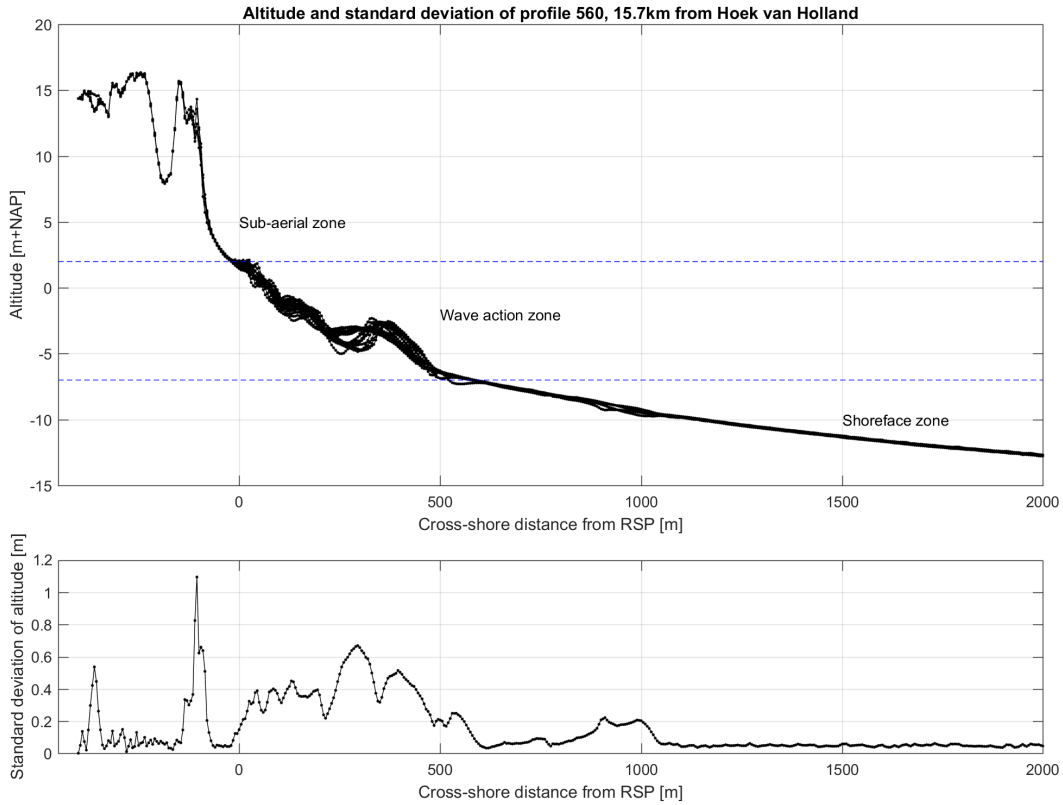

Figure 3-13: Cross-shore profiles of transect 560, the different zones are indicated. In the lower panel the standard deviation of the altitude of the transect is shown.

3-3-2 Typical profile shapes and development for erosive and accretive regimes.

In Figure 3-14 the temporal development of three representative transects is shown. The three transects are situated South, on the tip and North of the initial Sand Engine peninsula respectively. These positions represent areas with a distinct morphological behaviour.

The transect on the left in Figure 3-14 is situated south of the Sand Engine in an accretive area. It took 6 months before the transported sand reached this transect, as can be seen from the sharp increase in volume. After an initial strong net increase in volume, this tapered off to hardly any net volume change after summer 2013. In the profile development the formation of a kind of terrace around 2m+NAP can be observed. It is suggested that this is the upper limit of wave action and also suggests that hydrodynamic processes are dominant in the sediment transport.

The central panels of Figure 3-14 show a profile north of the Sand Engine, which is in an accretive reach, just as the first one. Here the accretion starts earlier than in the southern transect, most likely due to the net sediment transport to the North. The accretive trend decreases much less than in the Southern transect. Also in this profile there is an upper limit in the profile development, albeit a bit lower than 2m+NAP. This is probably caused by the tidal channel to the lagoon of which (a remainder) is in this profile.

The profile on the right of Figure 3-14 is situated around the tip of the Sand Engine peninsula, and is therefore in an erosive area. Clearly the profile is continuously eroding, and some seasonal influence seems visible from the variability in net volume change. The erosion is not limited to a certain altitude and slopes in the active part of the profile above Mean High Water (MHW) are very steep.

The cross-shore slopes of the first and last survey are compared. In figure 3-15 the slopes of the August 2011 and July 2016 surveys are shown, higher values denote steeper slopes. And in figure the change in cross-shore slope from August 2011 to September 2016 is shown. Warm colours indicate steepening, cold colours flattening. Overall accretive profiles tend to steepen in the sub-aqueous reach (0 to -8m+NAP), whereas the erosive profiles tend to flatten over the same vertical reach, see figure 3-16. This is the result of the fact that at the approximate depth of closure, the profile remains in place, while higher in the profile the depth contours shift sea- and landward respectively.

Before execution of the Sand Engine and the Weak Link Programme, coastal profiles are expected to be in dynamic equilibrium, or at least more close than after. Characteristic slopes then were generally milder (0.1 to 1.5 degrees) than after the Sand Engine was just constructed (0.8 to 4.5 degrees), except for the dune front, which was steeper (15 versus 5 degrees). Cross-shore slopes of the latest Sand Engine surveys are generally milder, but are still more steep than pre-nourishment coastal profiles. Yet, it is not possible to objectively conclude that the profiles return to equilibrium.

The cross-shore slope has been compared to the slopes obtained from the Jarkus measurement of 1975, before any nourishment was placed in the vicinity of the Sand Engine. In figure 3-17, both comparisons are shown. Warm colours indicate a steepening of the slope, cold colours a mildening. The middle panel shows the differences just after completion of the Sand Engine in 2011, the lower after five years of wave action in September 2016. In general the slopes

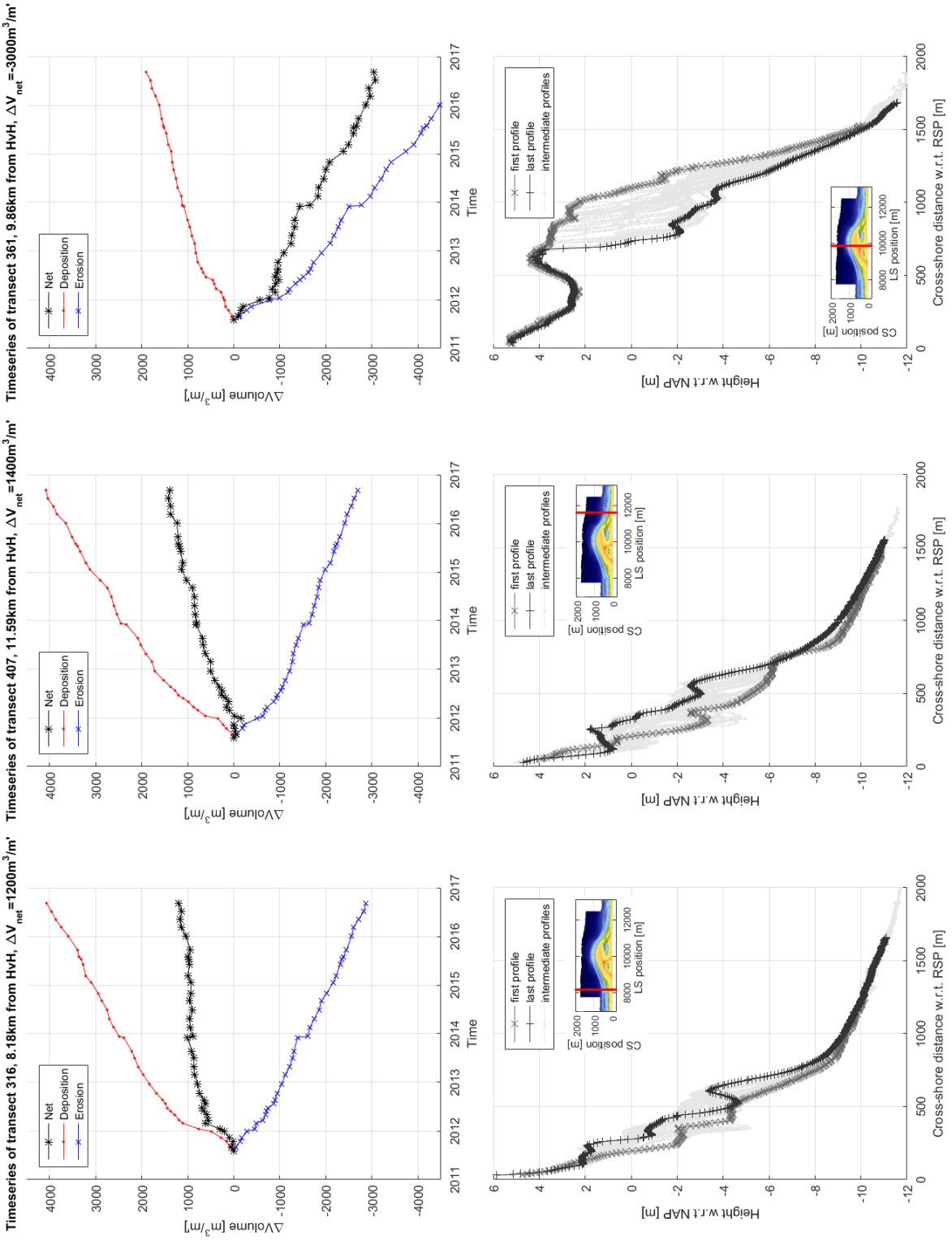

Figure 3-14: Comparision of the morphological development of three representative transects, from left to right: 316, 407 and 361. Left: transect 361, southern accretive area, middle: transect 407, northern accretive area, right: transect 361, erosive area.

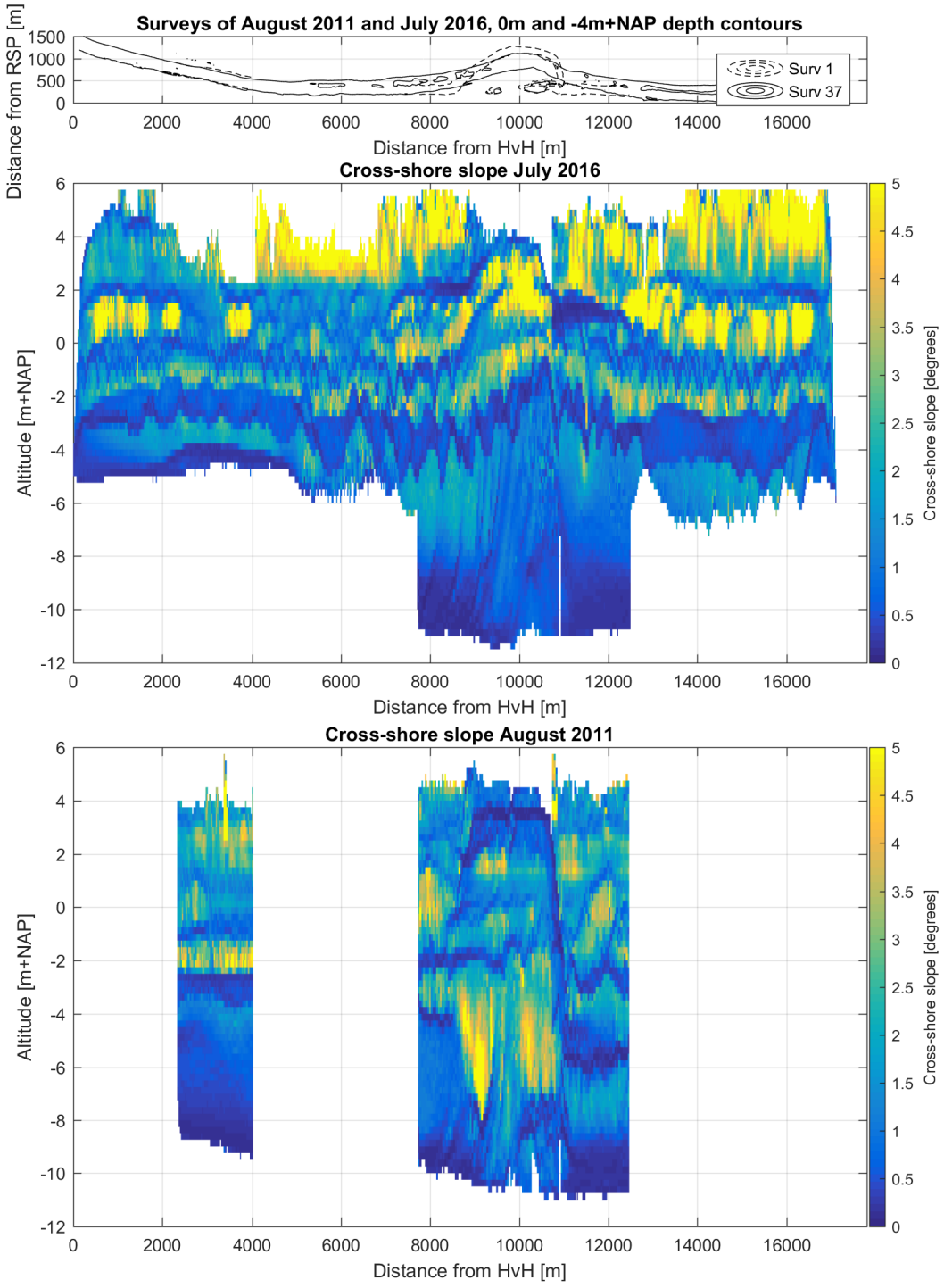

Figure 3-15: Cross-shore slope of the Delfland coast in July 2016 (middle panel) and August 2011 (lower panel). Angles are positive downward, higher values denote steeper slopes. The top panel indicates the positions of the 0m and -4m+NAP depth contours for both surveys.

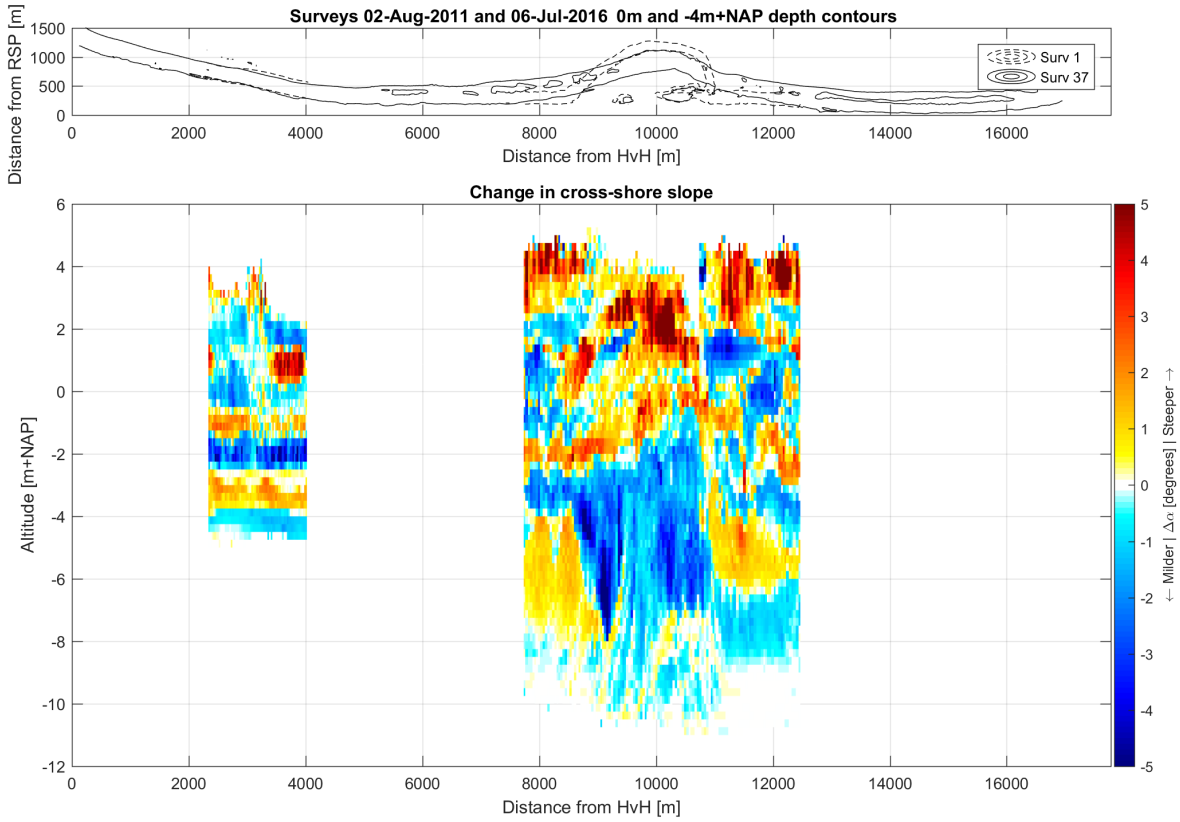

Figure 3-16: Change in cross-shore slope from August 2011 to July 2016. Top panel: 0m and -4m+NAP depth contours from Aug 2011 and July 2016. Bottom panel: red areas show an increase in slope in degrees (steeper), blue areas a decrease (milder). Erosive areas steepen in the intertidal range and milden below, in accretive areas the opposite happens. In all cases the dune front steepens.

of 1975 are milder, and the average difference was larger just after completion of the Sand Engine. The exception is the dune front, which was much steeper in 1975.

3-3-3 Coastal progradation/recession

A robust method for the determination of the position of the coastline, or more general depth contours, was introduced in Section 2-4-4. Calculating the volume changes in thin horizontal layers, determines the change of the depth contour in the horizontal plane. Projecting this parameter onto the vertical alongshore plane, it can be determined where the coast has progradated or retreated. By scaling with the altitude of a layer, the volume change becomes equal to the horizontal displacement.

In Figure 3-18, the horizontal displacement is shown. The Sand Engine peninsula shows consistent retreat over the vertical. In the adjacent accretive areas, the areas below 2m+NAP advance, while above this line, these areas show slight set-back. The Southern flank is less elongated in alongshore direction, but has accreted up to 2m+NAP, while the Northern flank only shows accretion up to 1.5m+NAP. This difference is caused by the additional dynamics of the lagoon and tidal channel in the North. Due to the differences in progradation and recession over the altitude, the diffusive behaviour of the Sand Engine cannot be described correctly by only looking at one depth contour. And the apparent plan-form adjustment of the Sand Engine differs considerably over the altitude, as was shown in Section 3-1-3.

In the top right panel of Figure 3-18 the distribution of net volume changes over the altitude is shown. These volumes are integrated alongshore over the coastal cell. Net accretion is observed above 4m+NAP and below -3m+NAP. The intermediate section shows a net erosion. This distribution is entirely dominated by the Sand Engine peninsula. The upper accretive area is (a part of) the dunefront, which is fed by Aeolian processes.

It can be concluded that there is a net sediment transport from higher towards lower altitudes. Note that this is not necessarily an off-shore directed transport due to the curvature of the Sand Engine peninsula.

3-3-4 Summary

Large differences exist in the development of accretive coastal profiles on the one hand and erosive coastal profiles on the other hand. Erosive profile gradually get a milder overall slope, while accretive profiles steepen. In the vertical distinct reaches are defined, which are governed by different forcing. For accretive profiles, nearly all bed-activity is confined in the wave action zone (2m+NAP to -8m+NAP), while erosive profiles also show adjustment above 2m+NAP. In the shoreface zone (< -8m+NAP), only slow increases or decreases of the bed-level are observed.

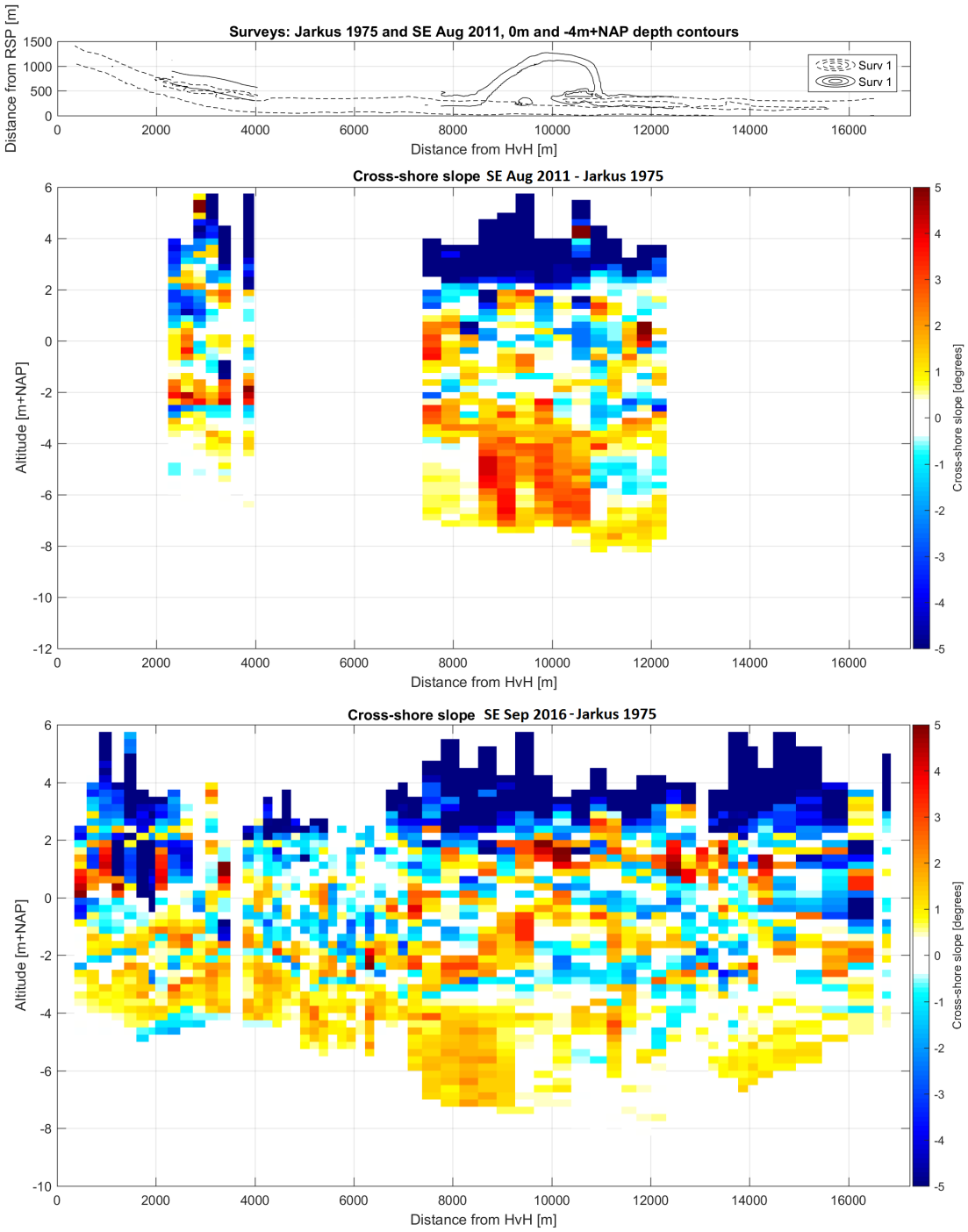

Figure 3-17: Difference in cross-shore slope between Sand Engine surveys and Jarkus of 1975. Central panel: difference just after completion of the Sand Engine, generally differences are large. Bottom panel: differences after 5 years (Sep 2016), the differences in slope have reduced, but in general the slope is still steeper than in 1975. Note: bars create some clutter and sub-aerial slopes are not considered.

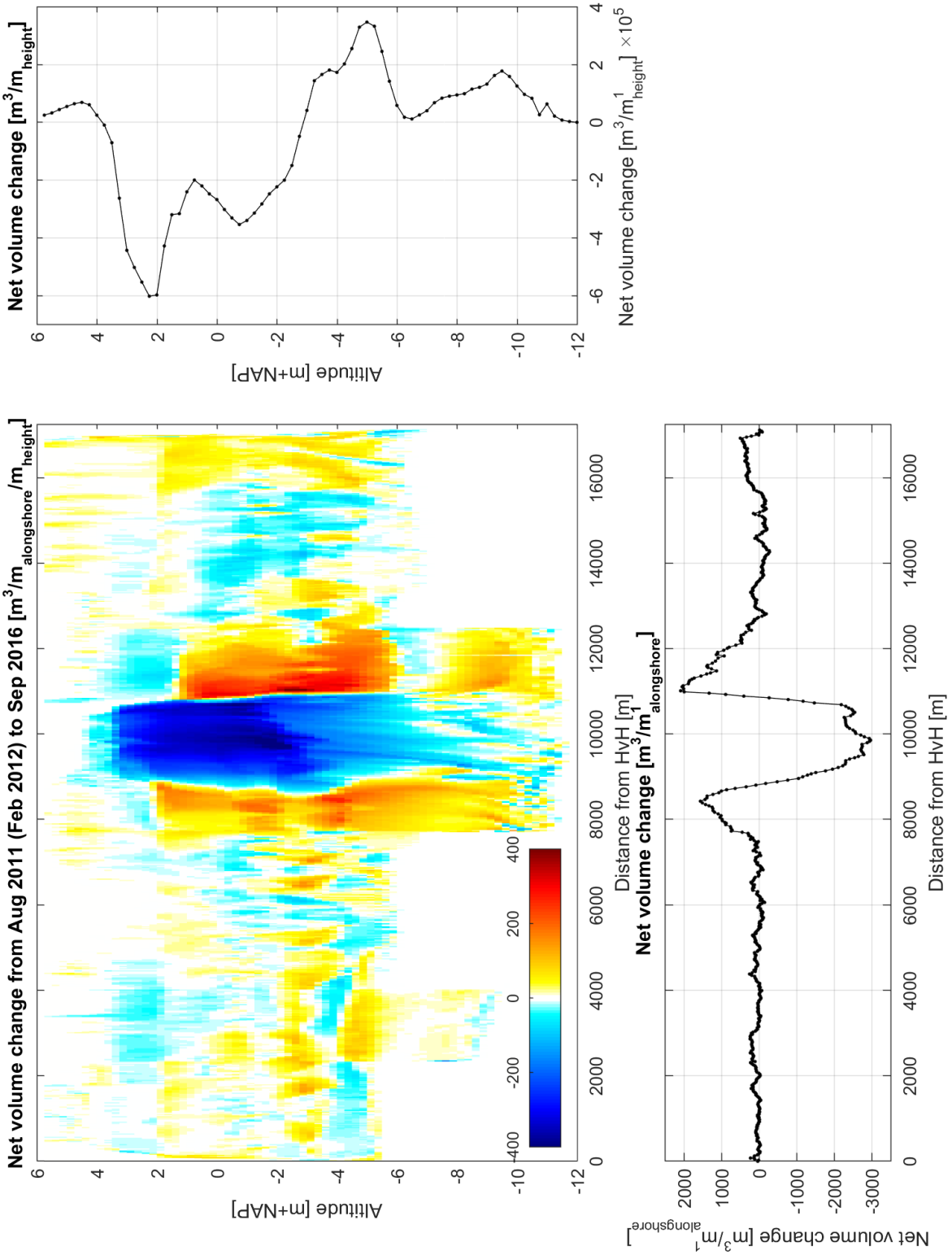

Figure 3-18: Net volume change in the vertical plane, a proxy for coastline displacement. The top left panel shows the net volume change, the top right panel shows the volume change integrated alongshore, and the bottom panel shows the volume change integrated over the altitude.

Chapter 4

Discussion

In this chapter the results of this study are discussed. In the first section, the uncertainties and assumptions are discussed. These assumptions are mandatory for a good analysis, but may influence the results. Here the impact is discussed. In the second part the results are compared with earlier studies and places in a broader perspective.

4-1 Assessment of accuracy, uncertainty and assumptions

4-1-1 Measurement accuracy

According to (Van Son et al., 2009) the measuring techniques used are accurate up to 0.10m. Assuming that the errors in the measurements are random and uncorrelated, the precision of the derived parameters can be assessed. The precision of a single measurement is 0.10m, for the least accurate acquisition method. A transect consists of circa 300 measurements, and the area of 620 transects.

$$\sigma = 0.10m \tag{4-1}$$

$$\sigma_{transect} = \sqrt{n(\Delta x \sigma)^2} = 8.6m^2 \tag{4-2}$$

$$\sigma_{area} = \sqrt{m(\Delta y \sigma_{transect})^2} = 6500m^3 \tag{4-3}$$

An off-set (or bias) in the RTK-GPS measurements may also occur and has a greater impact. Usually these off-sets were already accounted for before the delivery of the raw data. The impact of an 5cm off-set of all measurements in a survey changes the volume by circa 800,000m^3. This is assumed to be the upper limit of the uncertainty due to measurement bias, ans has not been observed in the measurements.

4-1-2 Assessment of cross-shore boundaries on volume changes

The Sand Engine and Nemo surveys do not cover the entire active area of the Delfland coastal cell on a time scale of five years. Therefore the volume changes outside this area are assessed.

The area bounded by the Sand Engine and Nemo surveys is denoted as SE/Nemo-area. This area corresponds to the blue and yellow areas in Figure 2-2.

For most transects the depth of closure is not reached on the 5 year time scale addressed in this thesis. In order to assess the impact of bed-level changes that are offshore of the Sand Engine/Nemo survey area, the JarKus surveys are analysed. These surveys cover the area from the back of the dune to circa 15m water depth, three kilometres off-shore. The period that is assessed is from the first Nemo-survey in March 2012 to July 2016. This corresponds with the period covered by the first Jarkus survey after completion of the Sand Engine to the most recent one. Outside this period, no data is available in these areas. The balance areas are shown in Figure 4-1 and do not overlap.

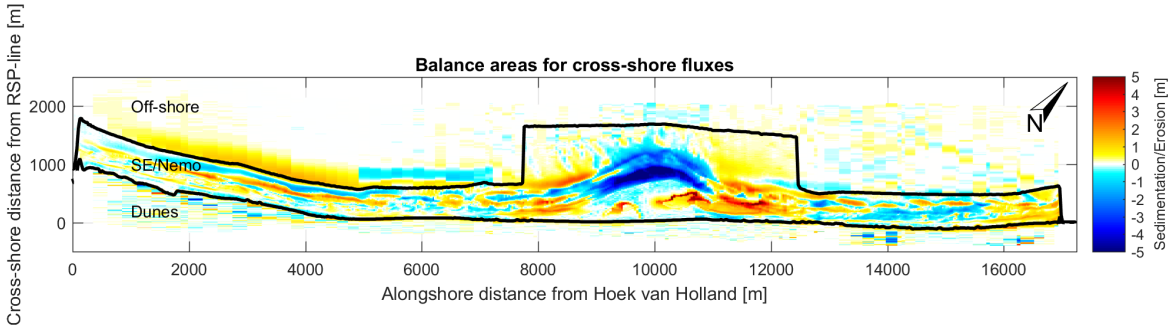

Figure 4-1: Boundaries of the balance areas. Colours give an indication of Sedimentation and Erosion

At the landward side, the SE/Nemo survey area is bounded by the dune foot. Inspection of the altitude measurements near the landward boundary have indicated that sand is deposited at the dune foot. An assessment has been made on the volume changes in the dunes as in indication of the cross-shore transport towards the dunes from the SE/Nemo survey area.

In spring 2013 a shoreface nourishment was placed from km 0.8 to 4.8 with a total volume of 1.5Mm^3. This nourishment originally was just outside the survey area but migrated onshore, therefore creating an input of sediment in this reach of the SE/Nemo survey area.

Volume changes per transect are shown in Figure 4-2. In the area landward of Sand Engine/Nemo survey area net volume changes have a mean magnitude of 37m^3/m, with a standard deviation of 20m^3/m. Over the whole Delfland coastal cell, the dune volume has increased with $580 \cdot 10^3$m^3. Off-shore the influence of the shoreface nourishment is clear, and a net gain of $780 \cdot 10^3$m^3 is found.

The apparent loss of volume in the SE/Nemo survey area can be largely attributed to losses in cross-shore direction. In the assessed period of March 2012 to August 2016, the apparent net loss of volume was $24 \cdot 10^3$m^3. However this number contains a part of the 2013 shoreface nourishment. When excluding the nourished area between km 0.8 and 4.8 from Hoek van Holland, a better assessment of the volume losses in the SE/Nemo area can be obtained. For this part, the net loss in the Sand Engine/Nemo survey area was $464 \cdot 10^3$m^3. In the dunes, $453 \cdot 10^3$m^3 was gained, while off-shore $150 \cdot 10^3$m^3 was lost. This results in a net loss of $161 \cdot 10^3$m^3 in the whole Delfland coastal cell, see table 4-1.

Volume changes not captured by the Nemo surveys are of the same order of magnitude as the

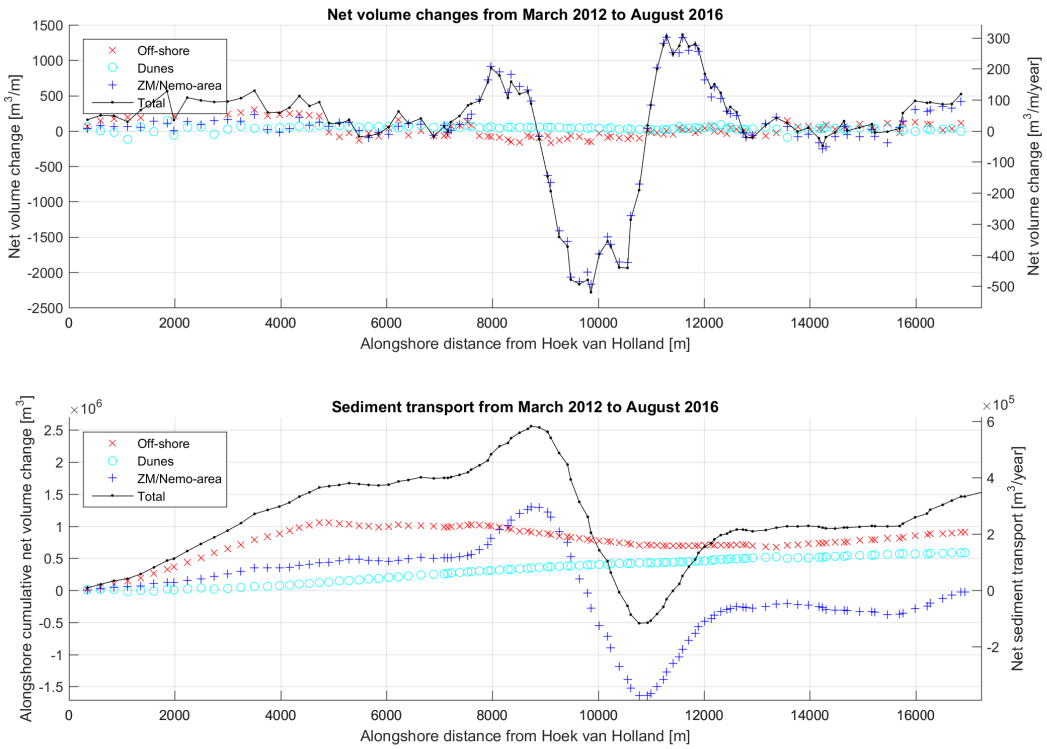

Figure 4-2: Volume changes and transports landward of the Sand Engine/Nemo survey area in the period March 2012 to August 2016. Top: net volume changes, bottom: net sediment transport.

volume changes within the Nemo area. In the Sand Engine survey area, the volume changes inside the survey area are an order of magnitude larger.

The majority of apparent net volume losses from the survey area are compensated by accretion in the dunes and deeper shoreface. Cross-shore transport is responsible for most of the apparent net losses. And considering that there are no further inputs or outputs of sediment, the volumetric losses from March 2012 to August 2016 of the Sand Engine are less than 1% of the initial volume, which is equal to the approximate accuracy. This is in line with Luijendijk et al. (2017), whose modelling studies indicate no net losses from the domain.

Table 4-1: Volume changes in the Delfland coastal cell from March 2012 to August 2016

	ΔV [m^3]			
Area	Dune	Offshore	SE/Nemo	Sum
All	584000	904000	-24000	1464000
Excluding nourishment	453000	-150000	-464000	-161000

4-1-3 Comparison of planform adjustment methods

Direct assessment of plan-form adjustment based on depth contours is very sensitive for measurement errors, since single points can influence the result. A measurement error of 0.10m results in a 10m horizontal shift on a 1/100 slope. It is better to average over a few profiles to reduce the error. This way the accuracy is better than 10m. The alongshore spreading is very hard to determine directly, both due to measurement accuracy and the influence of the cut-off criterion used. A cut-off criterion is necessary to determine the boundary for where the "influence" ends, since it tapers off below measurement accuracy.

The curve-fitting approach presented in section 2-5-1 works better and allows for the determination of multiple variables. The fit of a Gaussian curve through depth contours appears to be a very reliable and robust method for the determination of plan-form change. But care must be taken that the depth contours are described well enough. Especially in the first months after construction the plan-form shape deviates from a Gaussian curve.

For the cross-shore amplitude, the accuracy is comparable with the direct method, while accuracy for the alongshore spreading is superior in the fitting-approach. The accuracy is in the order of 100m alongshore.

4-1-4 Profile adjustment

Methods describing profile adjustment are not readily available and most research describes seasonal variability as opposed to long-term development. Due to the unprecedented scale of the Sand Engine mega-nourishment, the cross-shore profiles are extremely far from what could be considered equilibrium. This provides an unique opportunity to investigate development of coastal profiles to equilibrium.

A radical change of perspective has been proposed, describing the beach profile with respect to the altitude instead of the cross-shore distance. Since profiles are not fixed in horizontal position, but they are more or less fixed in the vertical with respect to their (hydrodynamic) forcing. The new perspective allows for easy comparison of profile parameters (e.g. slopes) at equal altitudes in the profile.

Difficulties arise when describing changes in profile slopes, as the slope generally spans three orders of magnitude either in ratio [m/m] or radians. The distribution of cross-shore slopes over the whole Delfland coast is found to be approximately log-normal. An improvement of the used method of subtracting slopes in degrees would be favourable.

4-2 Results in broader perspective

When possible the results of this study are compared with previous studies. Emergent differences will be discussed.

The volume changes of the balance areas in Section 3-1-1 do coincide with the results presented by De Schipper et al. (2016) for the first 18 months after construction of the Sand Engine. Later surveys have not been previously investigated. The total loss of sediment out of the SE/Nemo survey area has since increased from $5.5{\cdot}10^5 m^3$ to $8.0{\cdot}10^5 m^3$, while the redistribution has grown from $1.5{\cdot}10^6 m^3$ to $4.2{\cdot}10^6 m^3$. Additional analyses of the JarKus surveys

of 2012 to 2016 indicate that the dune volume has increased by $4.5 \cdot 10^5 m^3$. Which explains about half of the net losses. The relatively small amount of net losses are good, as that means that the sediments remain in the coastal cell.

Derivation of the alongshore transport from bathymetry measurements is successful. An average net annual sediment transport of $1 \cdot 10^5 m^3$ in Northern direction was found. But this transport rate varies considerably in time, depending on the wave climate. The number does comply reasonably well with the number of $1.75 \cdot 10^5 m^3$/year in Van Rijn (1997). The peaks in sediment transport around the Sand Engine peninsula are found to be $2.9 \cdot 10^5 m^3$/year in Southern direction and $5.2 \cdot 10^5 m^3$/year in Northern direction on average over 5 years. Which is in reasonable agreement with Luijendijk et al. (2017), who report 1.6 (S) and $5.5 \cdot 10^5 m^3$/year (N) respectively. However the reported background transport of $1.7 \cdot 10^5 m^3$/year to the North reported by both Van Rijn (1997) and Luijendijk et al. (2017) could not be derived in this study.

While De Schipper et al. (2016) have only looked at the plan-form behaviour at the 0m+NAP depth contour, this thesis also addresses other depth contours. From this assessment it became clear that the morphodynamics of the Sand Engine peninsula vary considerably over the altitude. Also the 0m+NAP isobath is not necessarily representative for morphological evolution the Sand Engine as a whole. It was derived that the Sand Engine has a net positive contribution to the sediment budget of the Delfland coast over 5.8km after five years. The actual influence may reach further alongshore but this is not demonstrable because of limited accuracy. Luijendijk et al. (2017) presents an alongshore influence of 6km after two years, using numerical modelling.

The cross-shore amplitude of the Sand Engine has reduced considerably over the first five years. The adjustment rate was considerably higher in the first year than in the subsequent years in which it was fairly constant. At the 0m+NAP depth contour in the first year a set-back rate of 130m/year is found, while the remaining four year show an average rate of 55m/year. The same is observed in the erosion rate of the central section of the peninsula. In the first year $1.5 \cdot 10^6 m^3$ was eroded, mostly in winter. Whereas the subsequent four years are responsible for the remaining loss of $2.7 \cdot 10^6 m^3$ ($0.67 \cdot 10^6 m^3$/year). Both indicators differ a factor 2.2. Thus the fist year or a probably the first storm season is not representative for the long-term development of a mega nourishment. This in agreement with De Schipper et al. (2015a) and Verhagen (1992), who both report larger initial losses for nourished beaches. Both profile adjustment and sediment sorting are said to influence cause this process.

Both sediment sorting and profile adjustment occur at the Sand Engine. Sediment sorting was investigated by Huisman et al. (2014) and Huisman et al. (2016). The overall pattern shows a coarsening of the D_{50} at the eroding section of the peninsula and a fining at the accretive areas North and South. As finer fractions are more easily transported erosion rates were higher in the first year. The coarsening of the top layer may also hamper erosion rates due to plastering effects. Which is in line with the results in this thesis.

Based on the rate of change of volume and the cross-shore extent a prediction could be made of the "life time" of the Sand Engine. The most simple method is an extrapolation of the current rate of change to zero. For example the most seaward point of the 0m+NAP contour shifts landward at an average rate of 55m/year. Given the September 2016 position of 750m+RSP and the pre-nourishment position of 50m, the remaining time is 12.7 year, thus circa 18 years

in total. It must be stressed that a linear trend towards zero is very unlikely and the expected life time is therefore much longer.

As to my knowledge no systematic research has been performed on quantification of the adjustment of cross-shore profiles on nourished beaches. It is however observed by several authors e.g. (De Schipper et al., 2015a),(Elko et al., 2007), that the cross-shore profile of a nourished beach is generally steeper than before nourishment. And also that the initial response of nourished profiles is more pronounced than during the rest of the nourishment life-time.

Chapter 5

Conclusions

Below the conclusions are presented. The conclusions are ordered by their respective research questions. Starting with the first research question in Section 5-1, the second research question is treated in Section 5-2.

5-1 Contribution to the Delfland coastal cell

The first research question is: *What is the contribution of the Sand Engine to the sediment budgets in the Delfland coastal cell in the first five years after construction?* The answers to the sub-questions will be presented each in their own sub-section.

5-1-1 Observed volume changes

Net volume changes in the Delfland coastal cell were successfully derived from a series of altitude measurements over the fist five years after construction of the Sand engine. Sediment is redistributed in both alongshore and cross-shore direction over the coastal cell. The Sand Engine has a net positive contribution to the sediment budget of 5.8km of the Delfland coastal cell after five years.

The observed volume changes have been addressed in several ways. The Sand Engine shows a very clear signal of net volume changes in the Delfland coastal cell. The volume changes at the Sand Engine are an order of magnitude larger than in the rest of the coastal cell. Per transect the maximum observed net erosion is $3000\text{m}^3/\text{m}$ at the centre of the Sand Engine peninsula, the maximum net accretion is found North of the Sand Engine and peaks at $2000\text{m}^3/\text{m}$. Net volume changes in the rest of the Delfland coastal cell are in the order of $\pm 100\text{m}^3/\text{m}$. Both accretive and erosive areas exist.

The net bulk sediment volume in the area covered by the Sand Engine and NeMo surveys has decreased in the period from August 2011 (March 2012) to September 2016. In this area $0.80 \cdot 10^6\text{m}^3$ has been transported out of the surveyed domain. However, of this figure at least $0.45 \cdot 10^6\text{m}^3$ has accreted in the dunes in the period from March 2012 to February 2016.

The central part of the Sand Engine peninsula (8.8 to 10.9km from Hoek van Holland) shows a net erosion of $4.1 \cdot 10^6 m^3$, which is largely compensated by accretion in both Northern and Southern direction. The Northern section (10.9 to 12.3km) shows a net accretion of $1.8 \cdot 10^6 m^3$, the Southern section (7.6 to 8.8km) a gain of $1.2 \cdot 10^6 m^3$. A further $0.4 \cdot 10^6 m^3$ has accreted on both sides in the NeMo domain. This renders the efficiency of the Sand Engine 83% after the first five year after construction.

5-1-2 Derived transports

Net sediment transports were successfully derived from a series of altitude measurements, via transect volume changes. Boundary conditions were validated with additional measurements originating from the JarKus programme. The alongshore flux over the Hoek van Holland boundary is near zero. The net cross-shore flux over the landward boundary (dunefoot) is $7.5 \pm 2 m^3/m/year$. On average $35 m^3/m$ in 4.5 years is gained in the dunes. The net cross-shore flux over the seaward boundary shows a less consistent trend, and is around $-1 \pm 3 m^3/m/year$.

The net sediment transport rate over the Delfland coastal cell is on average $0.15 \cdot 10^6 m^3/year$ to the North ($0.80 \cdot 10^6 m^3$ in 5 years). An important transport gradient exist around the Sand Engine area. This gradient has a gross magnitude of $0.80 \cdot 10^6 m^3/year$ ($4.2 \cdot 10^6 m^3$ in 5 years).

From the volume changes and transports it was derived that the Sand Engine has influenced the Delfland coastal cell outside the Sand Engine survey domain in the first year after construction. The transports over the alongshore boundaries of the Sand Engine area in this period cannot be assessed due to lack of data.

5-1-3 Planform changes

The change in plan-form of the Sand Engine is very pronounced. The amplitude or cross-shore extent of the peninsula shows a gradual decrease and the alongshore extent shows a gradual increase. The shape of depth contours of the Sand Engine can accurately be described and parametrised by fitting a Gaussian curve. The plan form change can also be used as a proxy for the volumetric adjustment.

The change in plan-form varies significantly over the altitude. The lower in the cross-shore profile (altitude), the slower the depth contours change positions. At 0m+NAP, the maximum cross-shore extent has reduced with 400m, at -4m+NAP the reduction is 150m and at -8m+NAP, only 30m. The reduction of the cross-shore amplitude of the peninsula is also more event driven at lower altitudes (<-4m+NAP).

Some asymmetry exists in the alongshore spreading, which also differs over the altitude. The largest contribution to the asymmetry is the development of the spit (North section), which has no accretion above 1.5m+NAP, but is slightly more elongated on lower altitudes as compared with the Southern accretive area (1600m versus 1200m at 0m+NAP). This is most likely caused by the influence of the lagoon and tidal channel in the spit, which is morphologically very active.

The alongshore extent of the Sand Engine peninsula at 0m+NAP has increased from 2.2km in August 2011 to 5.8km in September 2016. However, already in February 2012 the alongshore extent increased to 3.8km, during plan form adjusted towards a Gaussian shape. The

alongshore extent of the Sand Engine shows an increasing trend, with a tendency towards a decreasing growth rate. It is expected that the Sand Engine will remain present in the coastal profile at lower altitudes (< -8m+NAP), well beyond its projected life time.

5-1-4 Hydrodynamic conditions

Gross volume change and wave energy do correlate well, as more wave activity causes larger bed-activity. The mean correlation coefficient is 0.72. No improvement of the correlation was found for the alongshore component of wave energy. Other hydrodynamic parameters did not perform close to the wave energy. Net volume change has no significant correlation with wave parameters.

5-2 Cross-shore profile shapes

The second research question is: *What is the evolution of nourished cross-shore profile shapes and how can this be characterised?* Parameters of coastal profiles are compared based on altitude. By describing coastal profiles as a function of altitude, rather than cross-shore distance, horizontally shifting profiles can easily be compared.

5-2-1 Evolution of the cross-shore profile

The results show that the cross-shore profile development of accretive and erosive profiles is different. Accretive profiles become more steep over time in the inter and sub-tidal reach. Also the accretion is limited to the height of wave run-up, circa 2m+NAP. In contrast, erosive profiles become milder over time in the inter and sub-tidal reach. Furthermore, the erosion is not limited to the altitude of wave run-up. Scarp or cliff-formation causes erosion on the exposed edge of the Sand Engine, and resulting slopes are very steep.

For both accretive and erosive profiles the rate of bed-level change strongly varies over the altitude. Above the intertidal zone (>2m+NAP) bed-level changes are governed by aeolian transport and are therefore the changes are much lower. From a sharp increase in bed activity at 0m+NAP, the rate of bed-level change gradually diminishes to nearly zero at bed levels lower than -8m+NAP. Thus coastal profiles adjust at different rates on different altitudes, instead of shifting uniformly in the horizontal plane. As a result accretive profiles become steeper while erosive profiles become milder on average.

5-2-2 Adjustment towards pre-nourishment shape

An attempt has been made to determine whether coastal profiles adjust towards their pre-nourishment shape. Due to the large nourished volumes at the Delfland coast and especially the Sand Engine, after construction the sub-aqueous slope of coastal profiles was steeper than it was before. In the five years following completion of the Sand Engine a gradual mildening of the sub-tidal slope is observed in erosive areas. The slope of the dune front steepens as the artificial new dune front was quite mild. No definitive conclusion could be drawn on whether cross-shore profiles adjust towards a pre-nourishment shape or theoretical equilibrium.

5-2-3 Distribution of volume change over the altitude.

Averaged over the whole coastal cell, the areas above 3.5m+NAP (dunefront) show a net increase in volume, just as the areas below -3m+NAP. The area in between shows a net loss of sediment, which is entirely dominated by the Sand Engine peninsula.

Averaged over the whole coastal cell, sediment is transported towards lower altitudes (< -2m+NAP) from the higher altitudes (> 2m+NAP). The Sand Engine is very dominant in this process, mainly due to slumping/cliff-forming on the Sand Engine peninsula. Yet, this is not necessarily an off-shore directed sediment flux, due to the plan-form adjustment of the Sand Engine peninsula.

No sediments are deposited hydrodynamically above 2m+NAP, but due to aeolian transport sediment is transported towards the first dune row. The slumping/cliff-forming mechanism on the Sand Engine peninsula is the main cause of transport of sediments from >2m+NAP towards lower altitudes.

5-3 Summary

- The mega feeder nourishment is a working concept.
- The Sand Engine is feeding adjacent coastal sections over 5.8km with sediment in the first five years after construction.
- The morphologic response was strongest in the first year after construction.
- Results of the development in the first year are not representative for the long term.
- Morphodynamic response of the Sand Engine varies considerably over the altitude.
- Accretive and erosive profiles develop differently.
- There is a net transport of sediments from higher to lower altitudes.
- Sediment redistribution is mainly dependent on the wave energy.

Chapter 6

Recommendations

The morphological surveys of the Sand Engine and Nemo areas provide a very rich dataset, especially when they are combined. The high temporal and spatial resolutions, combined with good accuracy provide a wide range of morphological parameters and features to be investigated. Loads of features are still untouched and could therefore be investigated in further research. Not only in direct relation to the Sand Engine, but also for coastal management in broader perspective.

First of all it would be recommendable to investigate which parameters describe the Sand Engine best. It would be favourable to be able to describe the morphology of the Sand Engine and other mega nourishments in a few single-value parameters. This way future mega-nourishments can be objectively assessed and compared.

Secondly the depth-contour fitting approach appears to be very promising as a simple predictive one-line model for the morphological development of mega-nourishments. When successful, extensive monitoring will not be needed as measurements of coastline positions are sufficient. In most places, coastline positions are the only available measurements, if any at all exist. However it is now known that the morphological adjustment of the Sand Engine differs considerably over the altitude. Efforts should be made to account for this effect and make the model work properly for a single depth contour.

Thirdly an improved method for describing cross-shore profile adjustment is welcome. An assessment should be made on whether nourished profiles adjust towards equilibrium and whether erosion rates could be influenced by the initial nourishment profile.

Not directly related to the Sand Engine project, but very relevant for the coastal safety assessments of the Dutch coast is the accuracy of JarKus measurements. Now a very detailed morphological data set is available for the Delfland coast, with both higher spatial and temporal resolution than JarKus, that data can be tested for seasonal and spatial bias. Does it matter in which month the JarKus surveys are performed for the outcome of the Momentane KustLijn (Instantaneous Coast Line) (MKL) and te Toetsen KustLijn (Test Coast Line) (TKL)? And what are the effects of the asynchronous measurement of the sub-aerial and sub-aqueous areas?

Lastly, on the shoreface (<-6m+NAP) transversal sand ridges have been observed along the Delfland coast (RSP-km 101 to 113). These features with an alongshore length of 50m to 300m

and unknown cross-shore extent, appear to propagate slowly alongshore. Height amplitudes range from 0.2m to 0.6m. Passage of these features through a transect may considerably influence the volume or MKL position. Due to the alongshore length scale, these features are not resolved in JarKus, but they are in the NeMo and Multibeam surveys. More in general, the alongshore features purposely measured in the Sand Engine area have been neglected in most previous studies.

Appendix A

Literature Study

This chapter aims to give an overview of the most relevant processes along the Delfland coast, as well as a more in depth description of the Sand Engine site. This will be based on existing literature. First the most relevant coastal processes will be discussed and in the second part the Sand Engine itself will examined.

A-1 Coastal Processes

Different coastal processes will be discussed, starting with a more general overview, followed by an application to the Delfland coast. First sediment transports will be discussed, alongshore as well as cross-shore. Then bar behaviour will be examined and finally the influence of nourishments is described.

A-1-1 longshore transport

Alongshore sediment transport is the net and gross displacement of sediment parallel to the coast over time, whereas cross-shore sediment transport describes the displacement of sediment normal to the coast. The distinction between these two is artificial, as the same forcing drives the sediment transport in alongshore and cross-shore direction. These forcing processes are waves, (tidal-) currents and wind (Bosboom et al., 2015; Schwartz, 2006). In order to gain more insight in the complex relations between the forcing processes and reacting processes, a distinction is being made between alongshore and cross-shore observations.

In the basis all forces on the coast are exerted by three processes: waves, currents and wind. These processes all have a different influence with respect to the longshore sediment transport and are all related to each other. Wind speed and direction influence the forming of wind waves, creating higher waves with increasing wind speed and longer fetch. Conceptually waves are thought to stir up the sediment from the bottom, whereas tidal and residual current transport the suspended sediment particles.

Obliquely incident waves give rise to longshore transport via radiation stress. Radiation stress is the depth-integrated, wave-averaged flux of momentum due to waves. The gradient of the

shore parallel component of the radiation shear stress of the waves (dS_{yx}/dx) transports sediment in shore parallel direction. An increase in radiation stress gives rise to local erosion, whereas a decrease causes deposition (Bosboom et al., 2015).

The longshore sediment transport is not constant in cross-shore direction and takes place mainly on, and just seaward of, the breaker bars. Since these are the cross-shore positions where most wave breaking takes place. Under the influence of the vertical tide, the actual positions may vary over the tidal cycle (Bayram et al., 2001).

Different formulations exist to predict the longshore sediment transport. The most widely used ones are the CERC (USACE, 1984) and Kamphuis (Kamphuis, 1991) formulations, and the more recent Bayram formula (Bayram et al., 2007). See equations (A-1),(A-3) and (A-4) respectively. The CERC formula originates from the late 1940's and is based on the assumption that sediment is transported by wave generated currents (Bayram et al., 2007; Bosboom et al., 2015). However it is still the most used equation for longshore transport. Kamphuis developed his equation based on physical modelling, it includes wave period, beach slope and sediment diameter.

Bayram et al. proposed a new equation for longshore transport including effects of wind and tidal current, while assuming that suspended load is the main transport mode. It provides to be more reliable than previously developed equations (Bayram et al., 2007). Mil-Homens et al. (2013) re-assesed the three aforementioned longshore transport equations, calibrating them with new coefficients. The modified Kamphuis (1991) formula was shown to be the best, however still wrong by a factor of at least 2 for 42% of the cases assessed.

The CERC (A-1), Kamphuis (A-3) and Bayram (A-4) transport formulations:

$$S = \frac{K}{\rho g\,(s-1)\,(1-p)}\,(Enc)_b \cos(\phi_b)\sin(\phi_b) \tag{A-1}$$

$$I_m = \rho(s-1)(1-p)S \tag{A-2}$$

$$I_m = 2.27 H_{s,b}^2 T_p^{1.5}\,(tan(\alpha_b))^{0.75}\,D^{-0.25}\,(\sin(2\phi_b))^{0.6} \tag{A-3}$$

$$I = \frac{\epsilon (Ec_g)_b \cos(\phi_b)}{w_s} V \tag{A-4}$$

A-1-2 Cross-shore transport

As mentioned in A-1-1, cross-shore sediment transport mainly deals with the redistribution of sediment perpendicular to the local coast orientation. The sediment transport is caused by the combined action of waves, tidal currents and wind. This combination of forces results in a rapidly varying complex forcing pattern, causing constant movement of sediment. On longer time scales, months to years, the cross-shore sediment transport behaves more static. (Schwartz, 2006, p. 252)

Observations of cross-shore transport are often made via changes in bed-level over time, as it is too difficult to measure the sediment transport directly in a reliable way. When no gradients in longshore transport are present and the porosity of the soil remains the same, a change in bed-level can be related to cross-shore sediment transport.

Response time and variability of the cross-shore profile strongly depend on the local water depth. Waves have a decreasing influence on the morphology with increasing depth. The

most active part of the profile is found in the surf zone, whereas the deeper shore face only responds slowly Patterson, 2013. The sub-aerial beach and dunes also are less dynamic, therefore reasonable boundaries can be set around the active part of the cross-shore profile.

The lower boundary of transport (depth of closure) depends on wave action, tidal currents and the bed slope. The cross-shore profile is active on a long range of time scales, varying from seconds to millennia. Of interest for engineering purposes are mainly episodic events of circa one day, seasonal variability and long term trends (decades). The active part of the cross-shore profile can be bounded depending on the desired time scale. On the short-term the active profile is bounded by the dune foot and the water depth of approximately $2H_s$ below MSL. While on the long run boundaries are the dune back and some 10's of metres water depth (Van Rijn, 1997; Bosboom et al., 2015). It is stated by Hinton et al. (2007) that the whole shoreface up to depths over 20m is active, especially on longer timescales. The standard deviation of the change in depth tapers off in off-shore direction to the measurement accuracy, which is set as closure criterion. For timescales greater than 10 years, for various positions along the Holland coast a reopening zone is found on deeper water (Hinton et al., 1998; Hinton et al., 2007).

The cross-shore profile (of a certain location) shows some variability on the short-term, but is bound within a envelope when observed over several years. The profile is said to be in dynamic equilibrium. The exact temporal profile is a result of wave- and current forcing and will therefore continuously adapt to the present forces. Over longer time (from year to year) a mean profile is established which oscillates between boundaries.

In the theoretical case of constant stationary forcing, a stable equilibrium profile will develop. In real cases, however, forcing will be changing constantly and the profile will respond accordingly. Due to the time scales involved in the adaptation of the cross-shore profile, fluctuations of the profile are within an envelope. This is referred to as the dynamic equilibrium (cross-shore) profile. Therefore albeit the profile is constantly adapting, fluctuations generally remain bounded (Bosboom et al., 2015; Dean, 1991).

In the case of extreme loads on the shore, with high waves and a large set-up, the cross shore profile can change significantly within hours. Causing major dune erosion and flattening the slope of the upper shore face. This can be seen as an instantaneous perturbation of the equilibrium, which is then gradually approached again under milder conditions (Bosboom et al., 2015).

Dean (1991) described the equilibrium profile in a simple expression (A-5) where A is a specific shape-parameter related to sediment size distribution. Although useful and widely applied for its simpleness, it does not take into account any bars or other complex features. Holman et al. (2014) and (2016) found a parametric model for equilibrium profiles including sandbars in 1DH and 2DH respectively, based on Ruessink et al. (2003). Which is the state of the art. Bases on a few input parameters, shoreline position, equilibrium beach slope, offshore depth, shelf slope and (smoothed) coastline orientation (Holman et al., 2016). Advocating that their model is of use when insufficient bathymetric data is available, or data is not recent enough. Input parameters could be estimated from satellite imagery and nautical charts, which would not provide enough information for a realistic bathymetry on itself (Holman et al., 2014; Holman et al., 2016).

$$z(y) = Ay^{2/3} \tag{A-5}$$

A-1-3 Bar behaviour

As mentioned in A-1-2, in various places sub-tidal bars are present along the shore. These bars are often very dynamic on the short term and are often observed to migrate off-shore over yearly timescales in a cyclic manner (Wijnberg et al., 1995; Shand et al., 1999).

Bars are undulations in the upper shoreface profile, and are generally formed by wave interactions. The physics behind the formation and migration of bars is not clearly understood. In general bars are found on relatively steep beaches with a high wave height to grain size ratio (H_s/D_{50}). Strong feedback is found between wave breaking and the position and magnitude of the bar and many different hypotheses have been formed to explain bar formation (Schwartz, 2006, pp. 120-127).

Along large parts of the Holland coast a bar-trough system is present. A swash bar (mostly) attached to the beach and one breaker bar is present near Den Helder and south of Scheveningen, whereas two breaker bars are present along the central part of the Holland coast (Van Rijn, 1997). In general breaker bars exhibit a net off-shore migration and every few years, and a new bar is formed on-shore of the previous one (Ruessink et al., 2003). On some parts of the Holland coast there is no net on- or off-shore migration (near Den Helder), while somewhat south off-shore migrating system is found with a bar cycle of 15 years. From IJmuiden to Scheveningen also an off-shore migrating system is found with a periodicity of 4 years. Along the Delfland coast one or two bars are found, but the behaviour shows a less clear trend (Wijnberg et al., 1995). The differences in the length of the bar cycle are partially explained by the steeper fore shore profile along the North Holland coast (Bosboom et al., 2015). For an overview see: A-1.

Barred profiles

Ruessink et al. (2003) compared different sites which show off-shore bar migration to find differences and similarities in bar behaviour and dimensions. The cycle time varied between 1 and 15 years. Whereas most direct dimensional parameters showed no similarity, some dimensionless ones did. Six different locations have been studied; the North- and South Holland coast, Terschelling and Ameland in the Netherlands, U.S. Army Corps of Engineers field research facility in Duck and Hasaki in Japan. The landward boundary has been chosen as the +1m MSL line, as it was fairly constant over time in all locations. The seaward boundary has been chosen as the location where the deviation of the depth became a nearly constant, low value. The remaining deviation could then be largely related to measurement errors and accuracy.

Ruessink et al. (2003) proposes that the beach profile can be described by a mean component which is constant in time and a fluctuating component. The behaviour of the bar is then described as a complex eigenfunction. z_b is the bed level, of which $\bar{z_b}$ is the mean part and $\tilde{z_b}$ the fluctuating part. The bar behaviour ($\tilde{z_{bar}}$) is split into a spatial envelope $S(x)$ and a temporal variation therein $R(t)$. $\theta(x)$ and $\psi(t)$ are the spatial and temporal phase shifts, see equations (A-6)-(A-10).

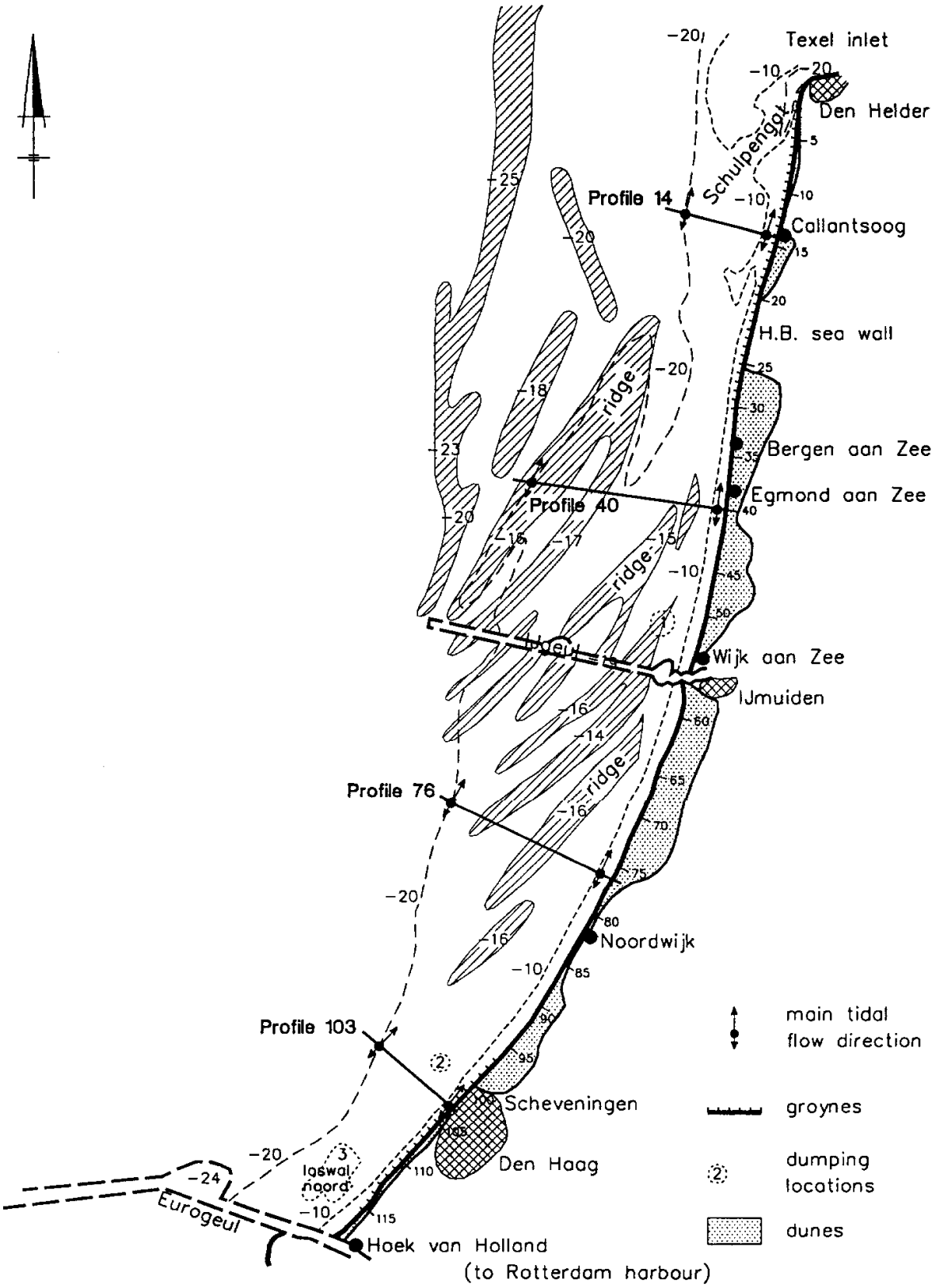

Figure A-1: Overview of the Holland coastal system, Van Rijn (1997).

$$z_b(t,x) = \bar{z}_b(x) + \tilde{z}_b(t,x) \tag{A-6}$$

$$\tilde{z}_b(t,x) = \tilde{z}_{bar}(t,x) + \epsilon(t,x) \tag{A-7}$$

$$\tilde{z}_{bar}(t,x) = S(x)R(t)\cos[\theta(x) - \psi(t)] \tag{A-8}$$

$$\theta(x) = \arctan\left[\frac{\mathfrak{Im}E_1(x)}{\mathfrak{Re}E_1(x)}\right] \tag{A-9}$$

$$\psi(t) = \arctan\left[\frac{\mathfrak{Im}A_1(t)}{\mathfrak{Re}A_1(t)}\right] \tag{A-10}$$

$$S' = \exp\left[\frac{-\{(1-d')^a - b\}^2}{c}\right] \tag{A-11}$$

$$S = \delta + (S_{max} - \delta)\exp\left[\frac{-\left\{\left(1 - \frac{d_0 - d_{sh}}{d_{sea} - d_{sh}}\right)^a - b\right\}^2}{c}\right] \tag{A-12}$$

$$L(\bar{d}) = a\exp(b\bar{d}) \tag{A-13}$$

Based on the equations of Ruessink et al. (2003), Holman et al. (2014) and Holman et al. (2016) found a way to describe and predict cross-shore profiles with the input of only a few parameters, that is without knowing the actual bathymetry. The shape of the bar is presented is dimensionless (A-11) and dimensional (A-12) form (Ruessink et al., 2003; Holman et al., 2014).

Bar-trough systems show considerable longshore uniformity. This uniformity increases exponentially with increasing water depth (A-13), (Ruessink et al., 2003). The shallow bars show more variability alongshore, which explains the offshore increase of the bar length.

Response to nourishments

On the island of Terschelling a shoreface nourishment has been applied between the middle and outer breaker bars, filling the trough in between. This shoreface nourishment has had a major influence on the behaviour of said bars as investigated by Hoekstra et al. (1996) and Grunnet et al. (2005). The shoreface nourishment was designed to act as a feeder berm, supplying sand to the coast, but acted also a breaker berm, thus significantly reducing the onshore wave action. The nourished site was morphologically very active, and within six months the double bar system emerged again. In the mean period strong 3D effects have been observed from oblique rip channels. In general the sediment has been observed moving to the East and onshore.

The rate to which the shore behind the nourishment was accreting was found to be much higher than could be explained by cross-shore redistribution only. Significant gradients in longshore transport existed as well (Hoekstra et al., 1996). These gradients resulted from the shadow effect of additional wave breaking on the nourishment.

Hoekstra et al. (1996) states that wave asymmetry is the governing force for potential onshore sediment transport, by means of an oscillating suspended load flux. However a delicate balance exists between offshore mean fluxes and onshore oscillating fluxes. No significant net onshore

sediment flux can be found, therefore it is not realistic to come up with a reliable sediment balance for the shoreface (Hoekstra et al., 1996).

Grunnet et al. (2005) also investigated the Terschelling shoreface nourishment and observed that off-shore bar migration halted for six to seven years after implementation of the shoreface nourishment, after which the normal offshore migration cycle appeared again (return period approx. twelve years). In the autonomous bar behaviour bar-switching has been observed where a bar (west) connected to one bar shoreward (east). Bar switching has been observed to happen on the outer and middle bar reconnecting to the middle and inner bar respectively. More on bar switching in A-1-3.

While the migration cycle only reappeared after six years, the bar-trough system from prior to the nourishment re-established after only six months, although the middle bar featured 3D morphology with rips instead of being alongshore uniform. The nourishment was also observed to be migrating to the east at a rate of 400m per year, due to gradients in longshore transport.

Subtle changes in the cross-shore distribution of the alongshore sediment transport are held largely responsible for the changes in shoreline retreat to progradation. Due to decreased wave attack, the longshore component of the sediment transport decreases and sediment aggregates (lee-effect) (De Sonneville et al., 2012).

(De Sonneville et al., 2012) identified significant differences between shoreface nourishments along the North-Holland coast. Nourishments connecting to the respective nearest bar tend to have a longer lifetime than non-connecting nourishments. Also the off-shore bar migration is stopped for a longer period of time. Differences in the wave climate were found to be insignificant.

Barswitching

Barswitching is an event where an alongshore uniform bar gets interrupted, realigns and attaches to another bar. Bar switching has been identified by, amongst others, Wijnberg (1995), Hoekstra et al. (1996), Ruessink et al. (2003), Shand et al. (2003) and Grunnet et al. (2005). Two modes of bar switching can be discerned, onshore and static (Shand et al., 2001). In the onshore mode the location of switching migrates onshore and reconnects to one bar nearer to the beach. In the static mode, the location of switching did not migrate. Shand et al. (2001) found that more switching locations more offshore were more likely to migrate onshore. Generally bar switching is associated with strong longshore currents and high alongshore sediment transport rates, as well as high wave energy.

Important differences in time and spatial scales have been identified between the Holland coast and Wanganui beach, New Zealand. Switching episodes along the Holland coast generally took five years to complete, whereas the Wanganui switchings only took several weeks to half a year to complete. Also the alongshore migration acted faster at Wanganui. Shand et al. (2001) suggests that this is due to the larger spatial scales and volumes of the Holland bars. Both on the Holland and Wanganui coast, bar switching was concentrated in certain spots, which suggests that antecedent morphology is important for the onset of barswitching (Shand et al., 2003).

Ruessink et al. (2003) identified that the net offshore bar migration period was not affected at either side of the switching location, but the cycle was severely interrupted at the location of

barswitching itself. Within barswitching areas the bars do not migrate systematically offshore during the switching event (Wijnberg, 1995; Ruessink et al., 2003).

A-1-4 Nourishments

As approximately 75% of the sandy shores world wide are currently eroding (Bird et al., 2015), measures to counteract the erosion have been developed. One of the most recognised measures nowadays is beach nourishment (Bird et al., 2015; Stive et al., 2013; De Schipper et al., 2016). A nourishment is the artificial placement of sediment on the coastal slope. This placement may vary in cross-shore location from the dunes to the lower shoreface. The first nourishments were executed to mitigate the immediate effects of dune erosion after severe storms and were placed at the dunefoot and dry beach. They are generally called beach nourishments. In the 1990's shoreface nourishments have been developed, which are located in the sub-tidal area, usually shoreward of the outer breaker bar.

Nourishments only provide a temporary solution which should be repeated every few years, as the cause of the coastal erosion is not taken care of. When the effects of the previous nourishment have faded, a new one should be performed. Only when the cause of the coastal erosion is not structural, a nourishment might be a finite solution.

Usually nourishments are performed to mitigate the effects of coastal erosion or beach starvation, either for flood protection or recreational purposes. Nourishments appear in a wide range of volumes, spatial extents and objectives (Hamm et al., 2002). An overview of the three main categories of nourishments is given here. The three categories are in order of development: beach-, shoreface- and feeder-nourishment. In Figure A-2 a schematisation of the different types is given. The first developed nourishments were beach and dune nourishments, where sand is placed on the sub-aerial beach or at the dune foot. The first nourishments in Europe were performed in the 1950's, and more structural measures started in the 1970's. Usually the volumes of beach nourishments are small (15.000-50.000 m^3) and the objective was to mitigate incident erosion by storms. When considerable damage was done to the dunes and beach, sand would be supplied to refill the vanished amount. Other objectives, mainly in France and Spain, are to create a wider beach for recreational purposes at (over-)developed coastal areas.

Shoreface nourishments are based on the principle of redistribution of sand by hydrodynamic processes, and are placed in the submerged part of the coastal profile shoreward of the outer breaker bar. Shoreface nourishments were developed since it was easier and cheaper to dump sand at navigable depths rather than on the sub-aerial beach. The lower yield of sand contributing to the coast is accounted for by the reduction in cost per dredged volume. Shoreface nourishments have been applied in the Netherlands since the late 1980's (Hamm et al., 2002). Shoreface nourishments are found to create two distinct processes by which they affect the coastal profile. On the one hand there is the feeder-berm effect and on the other hand there is the lee-side effect. The nourished sand acts as a bar or submerged berm, over which a net onshore sediment transport is present and as such feeds the coast with sediment. The lee-side effect refers to the reduction of wave energy behind the nourished bar, yielding a gradient in alongshore transport. Due to this gradient, sediment will accumulate at and slightly updrift of the nourished site. As such shoreface nourishments prove to be an effective solution against coastal recession (Stive et al., 2013; Grunnet et al., 2005; Hamm et al., 2002; Hoekstra et al., 1996).

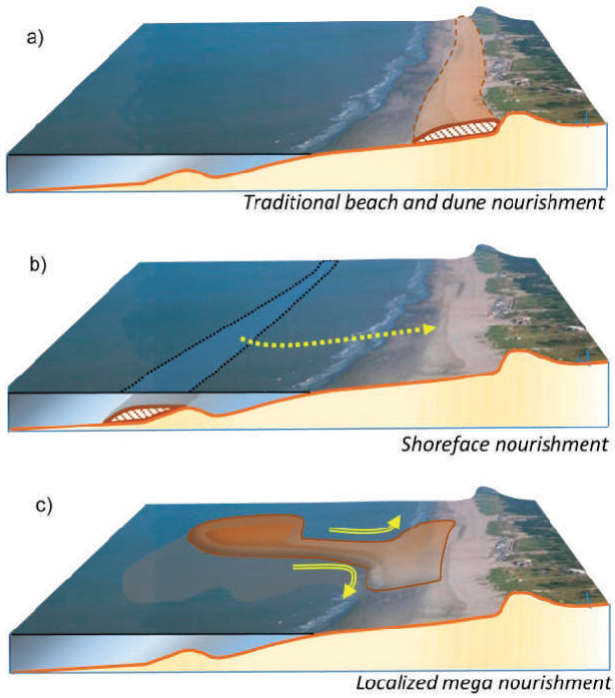

Figure A-2: Different types of nourishments, from top to bottom: beach-, shoreface- and mega nourishment (Stive et al., 2013).

The most recent development is nourishment strategies is the mega-feeder-nourishment (Stive et al., 2013). The objective is to redistribute the nourished volume along the coast, over a stretch much longer than the nourishment itself in a timespan of multiple years to decades. For this to work, the size of the nourishment has to be several orders of magnitude larger than traditional nourishments. The first pilot project, the Sand Engine consists of a nourished volume of 21Mm^3. Due to its enormous size, this redistribution process should last for over 20 years (De Schipper et al., 2016). More on the Sand Engine will be provided in section A-2

One of the main advantages of the mega-nourishment is that sand is supplied to the coast for a long amount of time. Therefore less damage is done to the biological environment on the long run, since interventions occur less frequent. On the short term, the nourished site is just as much disturbed as for traditional nourihsments. Also the cost aspect plays a role, as for these large volumes the price per cubic metre is lower (De Schipper et al., 2016). It is however necessary to have a long term strategy for coastal protection, otherwise the initial costs may prove to be too high of a threshold.

A-2 Sand Engine

In the Netherlands along the Holland coast, a pilot project is initiated to test a new way to protect the coast against erosion and provide additional safety against flooding. This project is called the Sand Engine and consists of a large, concentrated nourishment in the form of a hook-shaped peninsula at the Delfland coast, see Figure A-3 (Stive et al., 2013). It was constructed in 2011 and has been intensively monitored since.

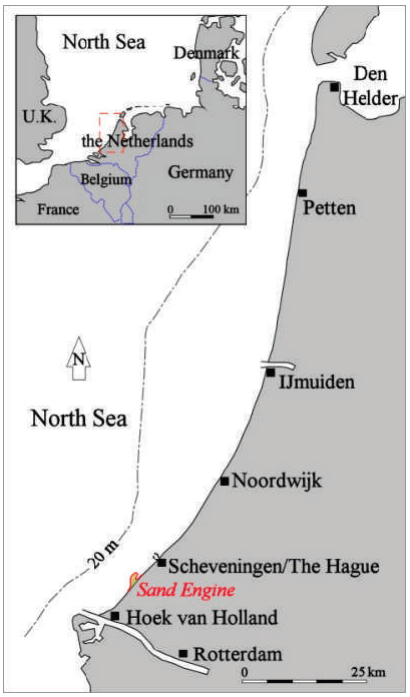

Figure A-3: Location of the Sand Engine along the Delfland coast (Stive et al., 2013).

A-2-1 Shore maintenance

The Delfland coastal section has been eroding at a rate of three to five metres per year from circa 1600 to 1800. Subsequently groynes were built, which reduced the erosion rate to one metre per year. However, the profile steepened because of the groynes and the construction of the Harbour mole at Hook of Holland (Van Rijn, 1997). In the year 1990 it was decided to maintain the coastline seaward of its then position, at all costs (Stive et al., 2013; Van Rijn, 1997). This is done mostly by sand nourishments on the beach, dunes and shoreface. Keeping the Dutch safety levels for flooding high is essential, since the land behind the dunes is below mean sea level. A breach of the Delfland dune section would cause floodings in a major part of the province of South Holland.

Initially nourishments were performed as beach or dune nourishments after storm events, later also shoreface nourishments have been implemented. The Delfland coast has been renourished several times. Volumes have increased to approximately 1.7Mm^3 per year with a total volume of 55Mm^3 since the start of nourishments (De Schipper et al., 2016). Since the lifetime of the executed shoreface nourishments is only three to five years (Hamm et al., 2002), frequent renourishing is required.

In view of the advise of the second Delta Comittee, nourishment volumes should be increased in the future to keep safety levels high. Doing so by only using traditional nourishment methods, would cause a very short return period of renourishing and effectively the whole coast should be nourished. In view of this the Sand Engine was developed, a local mega-nourishment which feeds a long stretch of coast (Stive et al., 2013).

A-2-2 Mega feeder nourishment: the Sand Engine

The Sand Engine pilot project was initiated to find whether it is possible to provide increased safety by nourishments for longer periods of time, so to create less disturbance for marine and benthic life and recreation. Due to its size it was possible to create additional values for recreation and nature alongside its main function of providing coastal safety.

The shape of the final design was largely inspired by the potential for creating areas for nature and recreational purposes (Stive et al., 2013). The final design is a hook shaped peninsula, which is open to the North. Near the base a small sheltered lake is present, surrounded by flood-free areas. The area sheltered by the hook of the peninsula behaves as a lagoon intended to provide a habitat for flatfish. Agreement was reached for this design and it was implemented at the Delfland coastal cell near Kijkduin.

The Sand Engine is expected to provide sediment for the Delfland coastal cell between Scheveningen and Hook of Holland for at least twenty years. The sediment is expected to redistribute along at least ten kilometres (Stive et al., 2013). The redistribution takes place probably more to the North than to the South due to tidal asymmetry and net littoral drift in North direction (De Schipper et al., 2016; Van Rijn, 1997). The hook shaped peninsula is expected to dissipate in cross-shore direction and extend in alongshore direction.

Observations made so far show that the Sand Engine is morphodynamically very active, especially in the first year after construction large changes in planform and bathymetry were observed (De Schipper et al., 2016). However, recent and ongoing observations show that the dissipation process of the Sand Engine slows down over time, and that the expected lifetime might be well over thirty years, instead of twenty[1].

A-2-3 Monitoring scheme

To gain insight into the behaviour of the Sand Engine an extensive monitoring scheme is set-up. The main research is about the morphology, but geographic and biologic research is also performed. Here the morphologic research is explored. The morphology of the Sand Engine is measured approximately bi-monthly, in the first year after completion even every month. The height is measured with RTK-GPS with respect to a fixed base station. On land measurements are mainly performed by quad-vehicle and water-based measurements are done with a jetski. The intermediate domain and small-scale features are surveyed with a wheelbarrow. The surveygrid is based on the Jarkus-transects and is interpolated to obtain a finer alongshore resolution of thirty to forty metres. The most dynamic area, the lagoon and gully, has additional longshore transects with thirty metre spacing and a fan spreading along the NW-section with (approximate) shore-normal transects, see Figure A-4 (De Zeeuw, 2011–2016).

From 2013 onward also morphologic surveys are performed along the rest of the coastal cell between Hook of Holland and Scheveningen. These surveys are executed at the same time as the Sand Engine surveys as much as possible. The survey grid has equal parameters as described for the Sand Engine (30m alongshore spacing, measurements from dunefoot to -8m NAP).

[1]Shown in presentations at the *SandMotor Congress* in Scheveningen d.d. 14-09-2016

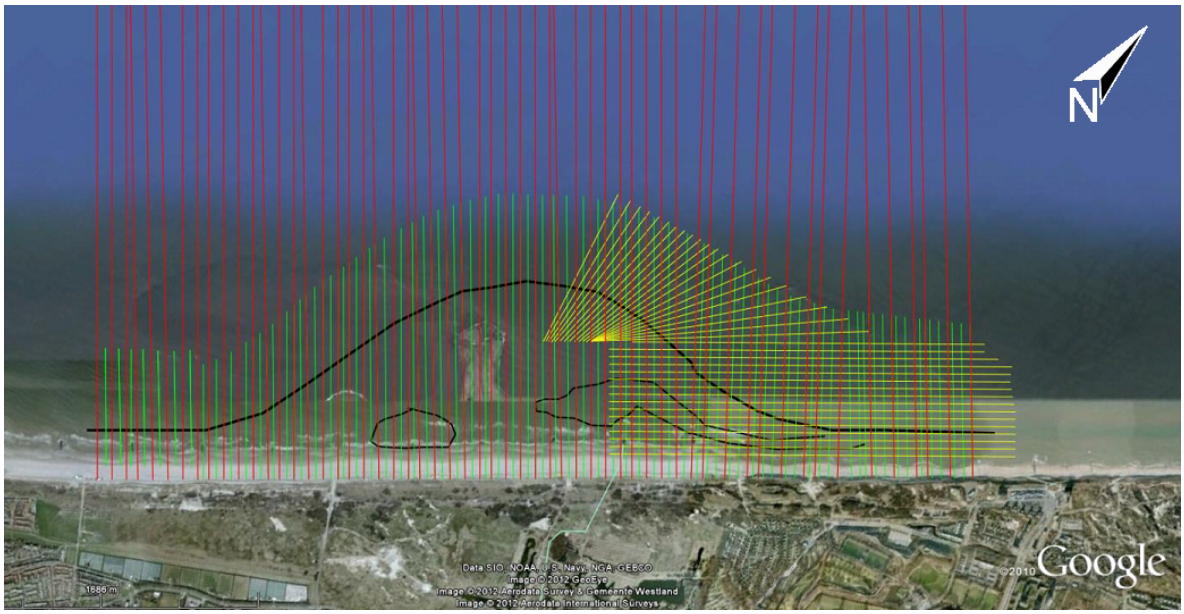

Figure A-4: Surveygrid of the Sand Engine, De Zeeuw, 2011–2016

A-2-4 Observations

Planform

De Schipper et al. (2016) posed a few paramters to describe the planform of the Sand Engine. These include: cross-shore extent (X_{max}), the the centre of mass of the planform (m_1), the alongshore extent w.r.t.t. m_1 (s_l and s_r), the skewness of the plan shape (γ_m) and the root mean square error of a gaussian shape w.r.t.t. plan form (ϵ_m). The planform has been observed to rapidly transform into a gaussian bell shape, which is slightly skewed. At the same time the cross-shore extent of the Sand Engine reduced significantly from 905m to 773m with respect to the pre-nourishment NAP-line. Due to the resemblance with a gaussian shape, the planform has been parametrised as such. Consecutive measurements show a gradual decrease of the root mean square error (RMSE) between the planform and a gaussian function in the first year, after which it became constant. The skewness showed the same behaviour halting at 0.2.

Profiles

The cross-shore profile was very steep directly after construction, with slopes up to 1:38, where pre-nourishment values were around 1:55. This and the blunt artifical shape and a stormy winter caused rapid morphological changes in the first half year after construction. The profile of the intertidal area on the tip of the Sand Engine has changed from steep to more natural 1:60 slope. The most seaward point of the Sand Engine is rapidly shifting towards the shore due to alongshore sediment transport from the tip to the North and South during flood and ebb respectively. The flood-, respectively ebb-currents reach a magnitude of 0.8 and 0.7 metres per second and are mainly shore parallel (Van Rijn, 1997). Scarp formation on the tip of the Sand Engine is often found after storms. The slopes of the peninsula now

show a double convex shape from +3 to -2.5 and -2.5m NAP onward. The upper part of this profile remains very steep.

Alongshore nourishing

The feeding effect of the Sand Engine to the adjacent coastal sections was parametrised by splitting the surveyed area in three parts with boundaries in the initial onset of the Sand Engine to the original shoreline. It was found that most of the eroded sand of the central section was accreted in the Northern and Southern sections. A loss of 1.8Mm^3 was found on the peninsula, and a total gross loss of 0.5Mm^3 was observed. This loss has travelled over the boundaries of the survey area, or are only apparent due to compaction effects (De Schipper et al., 2016).

Lagoon and surroundings

Undoubtedly morphologically the most active part of the Sand Engine is the Northern part where the lagoon is situated. Within five months after construction the lagoon was more or less closed, being only connected to the sea by a tidal gully. The gully itself is especially active and has shown varying lengths from very short (100m) to very long (>2km). Due to elongation of the tidal channel the tidal range inside the lagoon decreased, the channel became shallower and the mean water level higher (De Vries et al., 2015). Near the end of 2015 hardly any tide was present in the lagoon any more, until the breakthrough of a new channel in January 2016. Since the closure of the lagoon two times a new gully has been established due to breakthrough of the spit, providing a shorter channel to the sea and re-establishing the tidal dynamics (De Zeeuw, 2011–2016).

A-3 Selection of MSc-theses on the Sand Engine

In this section a quick overview of different, possibly relevant MSc-theses is given. Focus will be on the discussion and conclusions therein.

A-3-1 Short-term changes in the Zandmotor morphology, (Man, 2012)

Man (2012) looked into the short term changes of the Sand Engine morphology from August 2011 to January 2012, and made hindcast simulations. Qualitatively patterns of sedimentation and erosion could be estimated to a reasonable extent, but quantitatively this was not the case. The model used could not resolve for cross-shore sediment transport and some other important physical processes. Due to the rapid and extreme change in morphology processes controlling the morphology might have changed, especially in the northern part, and therefore a reliable prediction could not be given.

A-3-2 An assessment on hydro- and morphodynamic processes at the sand motor during the Decemberstorm of 2013, (De Kort, 2013)

De Kort (2013) assessed the relevant morphologic processes at the Sand Engine during the Decemberstorm of 2013. Two surveys of the Sand Engine are available just before and just

after the storm of December 5^{th}. It was found that the longshore sediment transport splits into a North and Southbound current around the position of normal wave incidence for the initial bathymetry. This effect faded as the planform diffused to a more smooth form. Sediment transport at the tip of the Sand Engine is found to be circa 2.4 times the net transport of the uniform adjacent coast, and a net southbound sediment transport is present at the southern end of the Sand Engine at a rate of the net northbound transport updrift of the Sand Engine. Although cross-shore sediment transport is not represented in the simulations, and profiles were not well output, over all results were in good agreement with the surveys. One of the recommendations suggests to look into the relation between profile steepness and volume change (due to alongshore transport).

A-3-3 Assessment of the variables influencing sediment transport at the Sand Motor (Kaji, 2013)

(Kaji, 2013) assessed the different morphologic processes influencing the sediment transport at the Sand Engine. Sand bars were found to persist throughout high energy periods, which is ascribed to the amplitude of the features hampering changes. Three dimensional features were more likely to diffuse under relatively low oblique waves than higher normal incident waves. Thus assigning a big role to the offshore wave angle on three dimensionality. The tidal currents were found to play a large role in the longshore sediment flux over the whole submerged profile, effectively determining the gross direction thereof. The contraction of the flow at the tip of the Sand Engine intensifies this effect. At the tip of the Sand Engine median grain size has increased over time, as this part is continuously eroding it is hypothesised that selective erosion is the cause. Which then also (partially) explains the decreasing development rate.

A-3-4 Global Assessment on the Lifetime of Mega Nourishments, (Van Steijn, 2015)

Van Steijn (2015) developed a tool to assess the expected lifetime of a Mega Nourishment. This tool estimates the redistribution of sediment and erosion, based on cross-shore and alongshore sediment transport processes. A few parameters are listed to describe the relative influence on the lifetime of the Mega nourishment. Although the presented parameters can give good insight in the behaviour of a mega nourishment their predictive value might be limited.

Appendix B

Datasets

The following list shows the data used in this thesis, and where to find it. The Jarkus, Nemo, Vlugtenburg and Zandmotor datasets are freely and openly available on the internet.

- Raw data

  Jarkus Not available

  Nemo http://opendap.tudelft.nl/thredds/fileServer/data2/zandmotor/morphology/NeMo/morphology_path_nemo.nc

  Vlugtenburg http://opendap.tudelft.nl/thredds/fileServer/data2/uuid/b798422a-69ec-41be-a394-740aad70df19/Vlugtenburg.nc

  Zandmotor http://opendap.tudelft.nl/thredds/fileServer/data2/zandmotor/morphology/JETSKI/surveypath/jetski_surveypath.nc

- Transects (interpolated data)

  Jarkus http://opendap.tudelft.nl/thredds/fileServer/data2/deltares/rijkswaterstaat/jarkus/profiles/transect.nc

  Nemo http://opendap.tudelft.nl/thredds/fileServer/data2/zandmotor/morphology/NeMo/morphology_transects_nemo.nc

  Vlugtenburg http://opendap.tudelft.nl/thredds/fileServer/data2/uuid/b798422a-69ec-41be-a394-74
  Vlugtenburg.nc

  Zandmotor http://opendap.tudelft.nl/thredds/fileServer/data2/zandmotor/morphology/JETSKI/transects/jetski_transects.nc

The collection of all data concerning the Sand Engine can be found at the 4TU data centre via the following link: https://doi.org/10.4121/collection:zandmotor.

Appendix C

Data Acquisition

The data used in this thesis is acquired by land- and water- based measuring techniques. The exact measuring equipment differs between the different data sets, and is described per set below. The coverage of the different data sets is shown in Figure C-1

C-1 Surveys

During the Nemo and Sand Engine morphology surveys, the altitude of the bed is being measured. This is done on the beach as well as in the shoreface. Measurements are performed using the RTK-GPS technique, for cm accuracy in positioning. Three types of vehicles are being equipped with GPS. The dry and intertidal areas are being surveyed with a quad-bike, the wet area with a Jetski and the remaining and difficult to reach parts (pools, steep slopes) by walking with a wheel, see also: De Zeeuw (2011–2016). In Figure C-2 the equipment is shown.

The Jetski measures the bathymetry in two parts. The shallowest areas of the bathymetry (approximately -3 to 0m+NAP) are surveyed during high tide, while the deeper parts can be measured during the rest of the tidal cycle. During the low tide the land based equipment can measure the intertidal parts of the beach (approximately -1m to 1m+NAP), while the higher parts can be measured during the rest of the tidal cycle. The remaining parts are in difficult to reach places for the Jetski or the quad. For instance because they are in permanently shallow waters or have steep slopes. These areas are measured with the walking wheel (from: De Zeeuw (2011–2016)).

C-1-1 Accuracy

Accuracy of the positioning differs between the different survey methods (vehicles). The Jetski has the lowest accuracy, whereas the quad and wheel have higher accuracy. This is due to the larger amount of degrees of freedom in the Jetski survey system. The vertical accuracy of the Jetski system is in the order of 0.1m (Van Son et al., 2009). For the other systems the accuracy is 0.05m (De Zeeuw, 2011–2016).

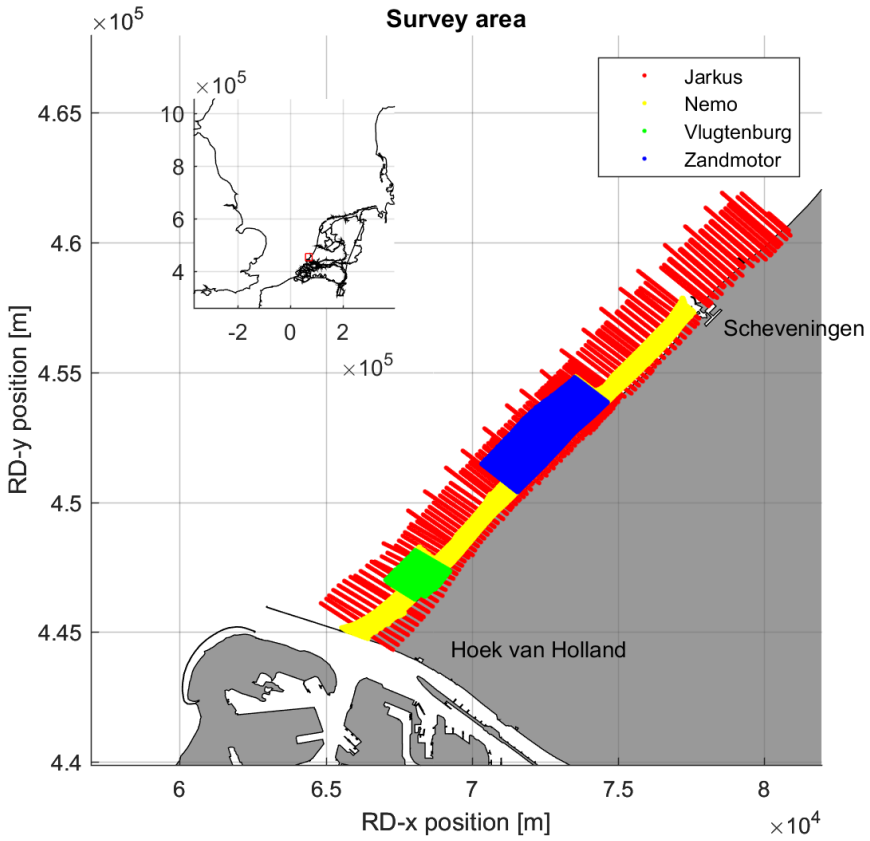

Figure C-1: Location of the survey area in the Netherlands and different domains, inset: red box denotes the survey area.

The surveys of the Sand Engine and Nemo areas are performed in the same time frame as much as possible, to provide a continuous snapshot of the whole coastal cell. At the Sand Engine 38 surveys are available spanning from August 2011 to November 2016, with approximate bi-monthly intervals (monthly during the first year). The Nemo area is covered by 22 surveys, all joint with a Sand Engine survey. The first survey in February 2012 and from then on bi-monthly from March 2013 until November 2016. For a full overview of all surveys, see appendix D.

C-1-2 Survey grid

The surveys are performed along a set of shore-normal lines, the survey grid. These lines find their basis in the JarKus surveys from Rijkswaterstaat, see section C-1-4. For the Sand Engine and Nemo surveys additional lines have been added in the alongshore direction to increase the alongshore resolution from approximately 250m to 20-40m. Due to the fixed grid, it is easy to compare data between surveys. Raw data is being measured as separate points (eqn. C-1) approximately along the lines of the survey grid. However, the points are

(a) Jetski **(b)** Quad **(c)** Walking wheel

Figure C-2: Survey equipment, images: Shore Monitoring and Research (De Zeeuw, 2011–2016)

not exactly on the grid. Therefore the raw data is interpolated in post-processing, see section 2-2.

$$z = f(x, y, t) \tag{C-1}$$

C-1-3 Survey area

The survey area is bounded by the harbour of Scheveningen in the North-East and the Rotterdam Waterway (Hoek van Holland) in the South-West. The breakwaters form a hard boundary to the otherwise sandy Delfland coastal cell, which stretches approximately 17.5km alongshore. In cross-shore direction the survey area is bounded by the dune foot on the landward side, either by a sharp increase in slope or a fence. On the sea side the boundary is set to the approximate position of the -5 or -10m+NAP depth contour for Nemo and Sand Engine surveys respectively (De Zeeuw, 2011–2016).

C-1-4 Jarkus surveys

Rijkswaterstaat performs an annual coastal survey of the Dutch coast, called JarKus (JAarlijkse KUStmeting) (Minneboo, 1995; Rijkswaterstaat, 2016). These surveys have been performed since 1965, and give insight in the historical morphological behaviour of the Delfland coastal cell. The measurements are taken in shore normal transects with a 200-250m alongshore spacing, which form a sub-set of the Nemo and Sand Engine transects[1]. Measurements stretch in cross-shore direction from the back of the dune to 800m from the RSP line, coinciding with a water depth of approximately 8m below MSL.

C-1-5 Vlugtenburg surveys

Survey data from the Vlugtenburg monitoring programme is included in this thesis. These surveys are included for partial coverage of the Nemo-area in the period before the Nemo-surveys were conducted. It also provides the opportunity to compare coastal profile behaviour in and outside the Sand Engine area for an extended amount of time.

[1] Actually, the other way around. SE and NeMo transects were interpolated from JarKus.

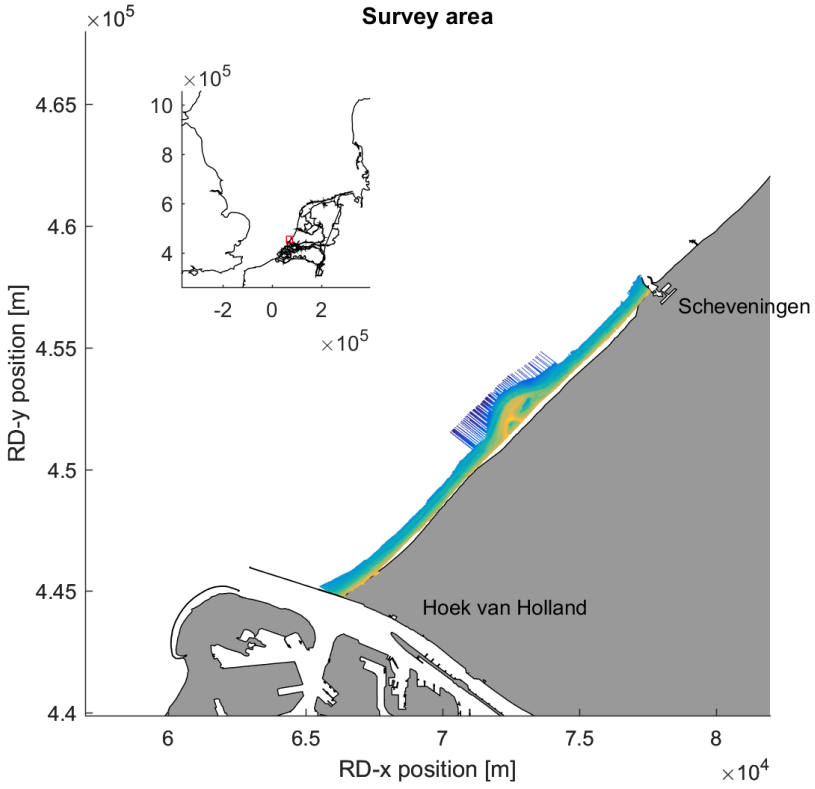

Figure C-3: Survey area of the Sand Engine and Nemo surveys along the Dutch coast.

For the section between 2.2 and 4km from Hoek van Holland, measurements from the Vlugtenburg survey project are available (De Schipper et al., 2013; De Schipper et al., 2015b). These measurements have been performed from 2009 until the second Nemo survey in March 2013. Land based measurements were performed with a GPS-backpack, while water based measurements were performed with the Jetski as mentioned before. The alongshore spacing is with 80m coarser than for the Nemo surveys, and transects have a slightly different orientation. A large part of the coarser alongshore resolution is mitigated by re-interpolation from the raw data to the Nemo transects. To confirm whether the interpolation of the Vlugtenburg surveys was of sufficient accuracy a manual inspection has been done between the Vlugtenburg survey of 13 February 2012 and the Nemo survey of 26 February 2012. The interpolated data was in good agreement with the Nemo data. Only near the edges of the Vlugtenburg area incomplete interpolated transects were found, and were therefore discarded.

Appendix D

Survey days

Overview of the days on which the surveys took place at the Sand Engine and Nemo-area. Numbers in the first column denote the date corresponding with the surveys. Additionally the dates of the Vlugtenburg and Jarkus surveys used in this thesis are shown.

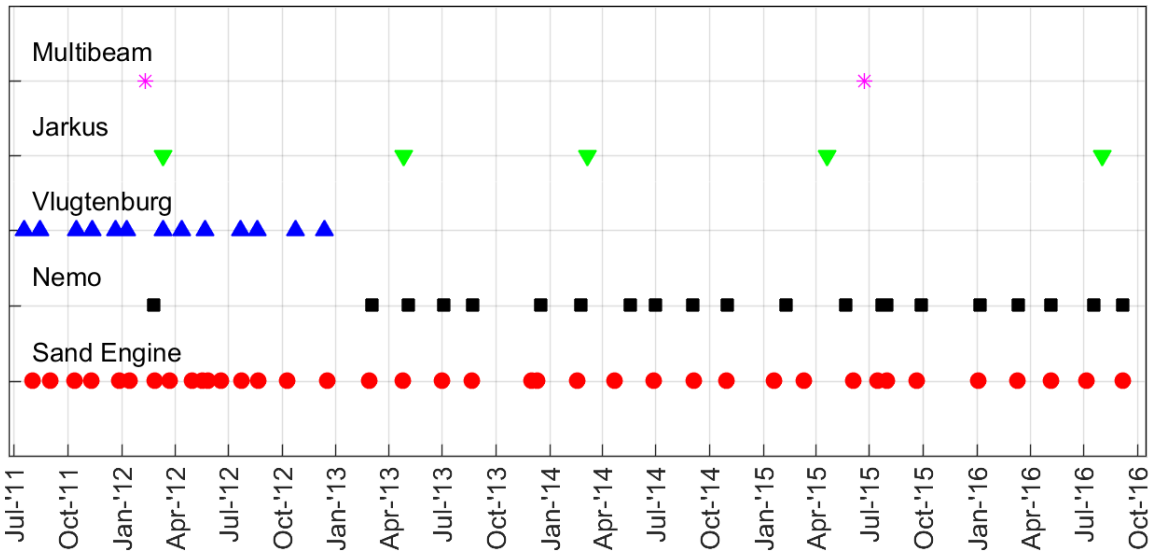

Figure D-1: Overview of Sand Engine and Nemo surveys

Table D-1: Survey days of the Sand Engine

Survey#	Fieldreport#	Survey date	Year	mm_dd					
1	1	2011_08_02	2011	08_01	08_02	08_03			
2	2	2011_09_02	2011	09_01	09_02	09_03			
3	3	2011_10_14	2011	10_13	10_14	10_16			
4	4	2011_11_11	2011	11_10	11_11	11_12			
5	5	2011_12_28	2011	12_26	12_27	12_28	12_31		
6	6	2012_01_16	2012	01_15	01_16	01_17			
7	7	2012_02_28	2012	02_26	02_28	02_29	03_01		
8	8	2012_03_23	2012	03_22	03_23	03_24			
9	9	2012_05_01	2012	04_30	05_01	05_02	05_03		
10	Ingreep spit	2012_05_19	2012	05_19	05_20				
11	10	2012_05_28	2012	05_26	05_27	05_28	05_30		
12	11	2012_06_20	2012	06_19	06_20	06_21			
13	12	2012_07_25	2012	07_24	07_25	07_26	07_27		
14	13	2012_08_22	2012	08_20	08_21	08_22	08_24		
15	14	2012_10_10	2012	10_09	10_10	10_11			
16	15	2012_12_18	2012	12_17	12_18	12_19			
17	16	2013_02_27	2013	02_26	02_27	02_28	03_01		
18	17	2013_04_26	2013	04_25	04_26	04_28			
19	18	2013_07_02	2013	07_01	07_02	07_04			
20	19	2013_08_22	2013	08_20	08_21	08_22	08_26		
21	20	2013_12_02	2013	12_01	12_02	12_03	12_04		
22	21	2013_12_11	2013	12_09	12_10	12_11	12_12	12_13	
23	22	2014_02_18	2014	02_17	02_18	02_19			
24	23	2014_04_22	2014	04_21	04_22	04_23	04_24		
25	24	2014_06_29	2014	06_27	06_28	06_29	06_30	07_01	07_02
26	25	2014_09_04	2014	09_03	09_04	09_05	09_06		
27	26	2014_10_30	2014	10_27	10_28	10_30	10_31	11_01	
28	27	2015_01_20	2015	01_17	01_19	01_20	01_21	01_22	01_24
29	28	2015_03_11	2015	03_09	03_11	03_12			
30	29	2015_06_04	2015	06_03	06_04	06_05			
31	30	2015_07_15	2015	07_15	07_16				
32	31	2015_08_01	2015	07_30	07_31	08_01	08_02	08_04	
33	32	2015_09_21	2015	09_20	09_21	09_22			
34	33	2016_01_03	2016	01_02	01_03	01_04	01_05		
35	34	2016_03_11	2016	03_09	03_10	03_11	03_13	03_14	03_25
36	35	2016_05_07	2016	05_04	05_05	05_07	05_08	05_12	
37	36	2016_07_06	2016	07_04	07_06	07_07			
38	37	2016_09_07	2016	09_05	09_06	09_07	09_09		

Table D-2: Survey days of the Nemo area

Survey#	Fieldreport#	Survey date	Year	mm_dd						
1										
2										
3										
4										
5										
6										
7	1	2012_02_26	2012	02_24	02_25	02_26	02_28	03_01		
8										
9										
10										
11										
12										
13										
14										
15										
16										
17	2	2013_03_04	2013	03_01	03_04	03_05	03_06			
18	3	2013_05_05	2013	05_03	05_05	05_06	05_07			
19	4	2013_07_05	2013	07_05	07_06					
20	5	2013_08_24	2013	08_22	08_23	08_24	08_25	08_26		
21										
22	6	2013_12_17	2013	12_11	12_12	12_13	12_17	12_26	12_28	
23	7	2014_02_24	2014	02_22	02_23	02_24	02_26	02_28		
24	8	2014_05_20	2014	05_16	05_17	05_18	05_20	05_23	05_24	
25	9	2014_07_01	2014	06_28	06_29	06_30	07_01	07_02	07_03	07_04
26	10	2014_09_03	2014	08_31	09_01	09_02	09_03	09_04	09_06	
27	11	2014_11_01	2014	10_30	10_31	11_01	11_04	11_05		
28	12	2015_02_10	2015	02_07	02_10	02_11	02_12	02_13		
29										
30	13	2015_05_23	2015	05_23	05_24					
31	14	2015_07_23	2015	07_22	07_23	07_24				
32	15	2015_08_01	2015	07_30	07_31	08_01	08_02	08_03	08_04	
33	16	2015_09_28	2015	09_26	09_27	09_28	09_29	09_30		
34	17	2016_01_06	2016	01_04	01_05	01_06	01_18	01_19	01_20	
35	18	2016_03_12	2016	03_10	03_11	03_12	03_13	03_14		
36	19	2016_05_07	2016	05_05	05_06	05_07	05_08	05_09		
37	20	2016_07_19	2016	07_18	07_19	07_20				
38	21	2016_09_07	2016	09_06	09_07	09_08	09_09			

Table D-3: Survey days of the Vlugtenburg area

Survey#	Jetski	Walking
29	2011_08_16	2011_08_17
30	2011_09_16	2011_09_18
31	2011_10_16	2011_10_16
32	2011_11_12	2011_11_12
33	2011_12_22	2011_12_22
34	2012_01_10	2012_01_10
35	2012_02_13	2012_02_13
36	2012_03_13	2012_03_12
37	2012_04_13	2012_04_13
38	2012_05_24	2012_05_25
39	2012_07_23	2012_07_24
40	2012_08_20	2012_08_20
41	2012_10_25	2012_10_25
42	2012_12_13	2012_12_13

Table D-4: Survey days of the Jarkus transects

Survey#	Surveydate	Bathymetry start	Bathymetry end	Topography
47	2011_04_25	2011_02_15	2011_06_14	2011_01_27
48	2012_03_14	2012_02_28	2012_03_26	2012_02_20
49	2013_04_27	2013_04_24	2013_05_06	2013_01_14
50	2014_03_07	2014_03_04	2014_03_13	2014_01_18
51	2015_04_20	2015_04_15	2015_04_24	2015_03_08
52	2016_08_04	2016_07_19	2016_08_15	2016_02_15

Appendix E

On the combination of coastal surveys

When multiple datasets covering the same area are available, one might have the wish to combine those. Usually the temporal or spatial extent of one of the datasets is larger, or resolution is better. In order to improve either of those aspect, the surveys may be combined to get better insights.

Here the case of the Delfland coast will be explained, where multiple datasets are available for the coastal morphology. Their properties are presented in table E-1 and Figure E-1.

Table E-1: Properties of the different datasets covering the Delfland coast. Resolutions are averages.

	Δx [m]	Δy [m]	RSP [km]	RSP [km]	Δt [days]	First survey	Current Survey
Jarkus	250	5	101,2	118,5	365	1965	2016
Vlugtenburg	80	5	114,8	116,5	30	aug-09	dec-12
Zandmotor	40	5	106,4	111,1	30-60	aug-11	sep-16
Nemo	25	5	101,8	118,9	60	feb-12	sep-16

E-1 Combining criteria

When two surveys are performed shortly after each other, they may be combined. The combining criterion is the time scale in which significant morphological changes take place, which depends on the wave energy. For storms this may be a day, while for milder conditions two to three weeks is justifiable.

E-2 Combination

The here described data sets are transect based. Data is won in lines (roughly) perpendicular to the (historical) shoreline. When combining different surveys, it is mandatory to use a single

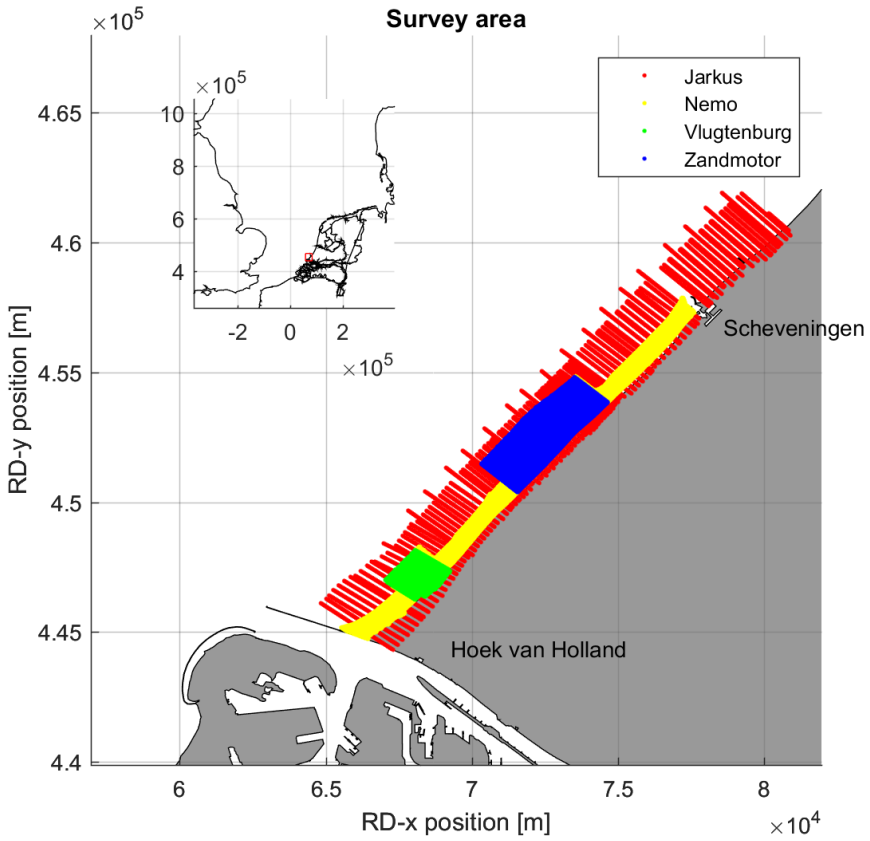

Figure E-1: Location of the survey area in the Netherlands and different domains, inset: red box denotes the survey area.

set of transect for all surveys. Especially when different transect systems exist, it is beneficial to use the raw survey data. That way the point-clouds of the surveys can be merged and a single interpolation surface can be built. This surface can then be queried on the positions of the transects. This approach reduces interpolation errors, due to repeated interpolation and discards any boundary effects that may arise in the overlap between different surveys.

Alternatively, when the transect system is the same, one could superimpose the interpolated data. Starting with the data with the largest coverage to the smallest coverage.

E-3 Example

The Zandmotor and Nemo data sets are complementary to each other, with respect to the spatial coverage. But the temporal coverage differs. A combined set of transects is used, which is a refinement of the Jarkus-transects and is also used by the surveyors. For instance the Zandmotor survey of 28 February 2012, may be combined with the Nemo survey of 26 February to get a coverage of the whole Delfland coastal cell. One might even add the Jarkus survey of 2012, which' topography was measured on 20 February and the bathymetry between

24 February and 26 March. A visual check on a few transects will tell whether the latter is tolerable.

Appendix F

On the problems of alternating transect lengths

In the Sand Engine survey area, only half of the transects is surveyed to 2000m off-shore, the other half is only surveyed to the position of the -5m+NAP contour, see Figure F-1. Several problems may occur from this alternating survey scheme, provided that the depth of closure is situated further off-shore than the length of the shorter transects.

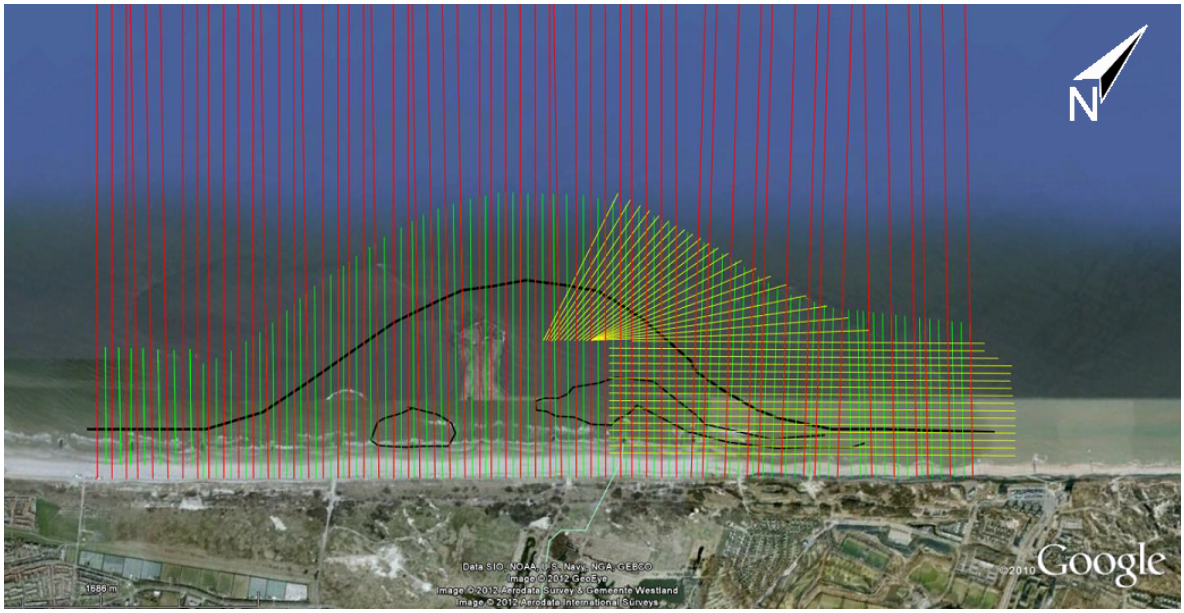

Figure F-1: Transects of the Sand Engine surveys. Transects are alternating long and short. The black line is a schematic representation of the 0m+NAP contour around 2012.

In the Sand Engine surveys, the depth of closure is lower than -5m+NAP, thus the littoral zone is not covered in its entirety by the *short* transects. This could be observed from sedimentation/erosion plots of the area. As a consequence the calculated net volume change in

the *short* transects has a structurally lower magnitude than in the adjacent *long* transects. The (magnitude of the) net volume change of the Sand Engine will therefore be under estimated.

In Figure F-2, the area covered by the Sand Engine surveys is shown. As can be seen in the upper panel, long and short transects alternate. The yellow parts are covered (almost) every survey, while the blue parts are (almost) never covered. Any volume changes in the "blue" parts of the upper panel are not accounted for in the volume analyses. From the lower panel it becomes clear that, indeed bed-level changes do occur in this partly covered area.

Besides under estimation of the net volume change, another discrepancy arises. Due to the larger difference in transect lengths in the both accretive areas (x<9000m and x>11000m)the amount of accretion is *more under estimated* than the amount of erosion in the erosive area (9000m<x<1100m). As a result the *apparent* net loss of volume in the area will be higher than it is in reality. The difference in net volume change is in the order of $300 \cdot 10^5 m^3$.

The solution to this problem is quite simple. Interpolating the bathymetry of the short transects up to the length of the long transects in the initial interpolation script will result in a better estimation of the real net volume changes. Provided that the alongshore variability has a longer length scale than the spacing of two transects (circa 80m). This assumption appears to be good for this area. Any errors resulting from the interpolation are very small with respect to not taking into account the difference in transect length.

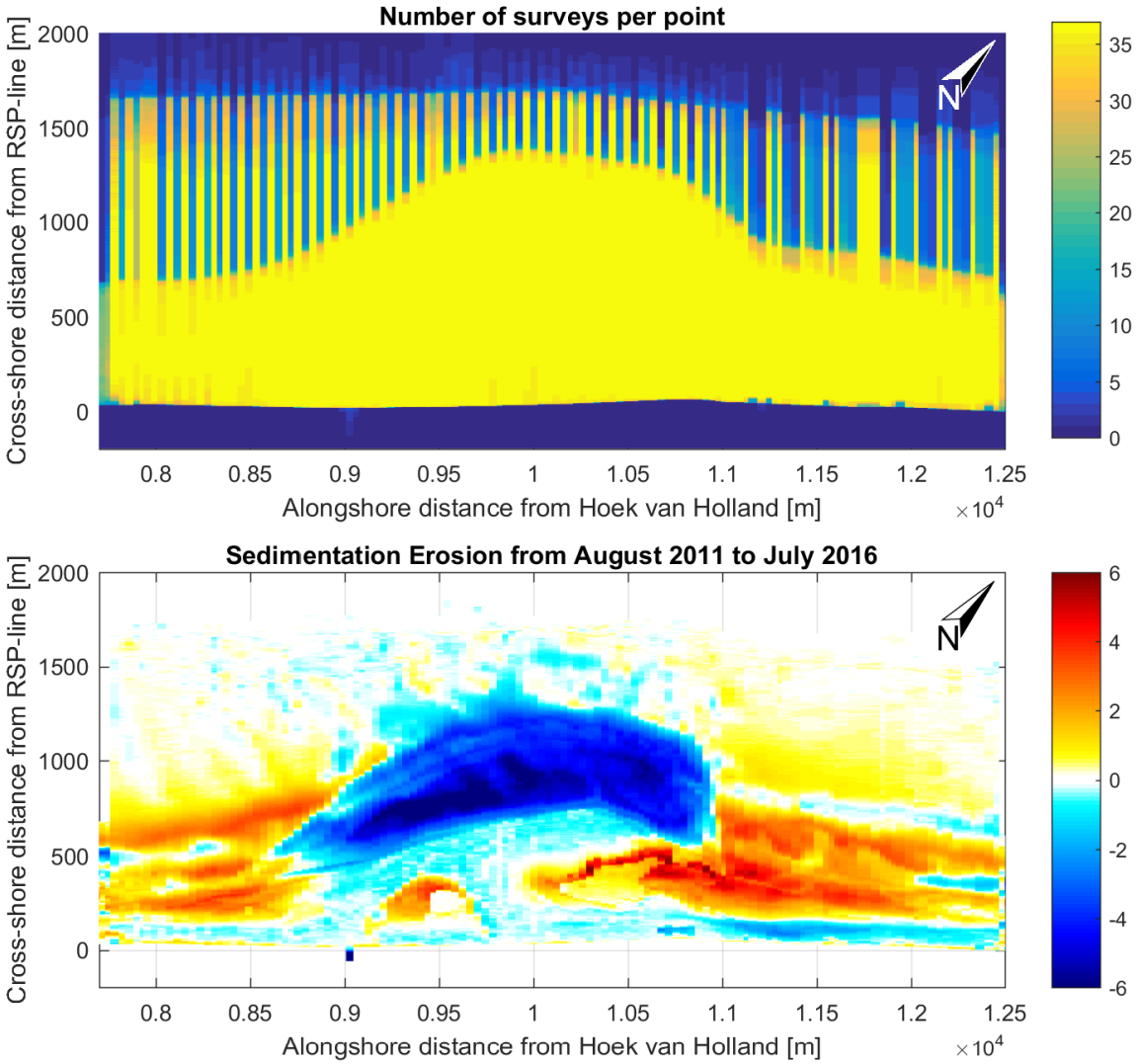

Figure F-2: Long and short transects at the Sand Engine. Upper panel: number of surveys per point, the yellow areas are covered by many surveys. Lower panel: distribution of sedimentation and erosion over the survey area.

Appendix G

Coordinate systems

Three different coordinate systems are used in the processing of the data. Two of which are officially used in the Netherlands. For an overview of the coordinate systems described below, see Figure G-1.

G-1 Rijksdriehoek (RD-NAP)

The Rijksdriehoek (or Amersfoort) coordinates is the official coordinate system used by the Dutch government for land measurements, and extends the Netherlands and part of the Dutch continental shelf. The grid is orthogonal, with a false origin near Paris, and is projected on the Bessel geoid. The altitude coordinates are given with respect to the Dutch ordinance level NAP, which is approximately equal to MSL.

G-2 Rijksstrandpalen (RSP)

The Rijksstrandpalen (State beach poles) system is a non-orthogonal coordinate system based on a base-line indicated by a set of poles on the beach. This line is set out on the whole Dutch coast and follows approximately the high water line at the time of installation. For the Holland coast, numbering starts at Den Helder in the North at 0km and ends in Hoek van Holland at circa 118km. From this alongshore line, lines in (formerly) shore-normal direction extend positive seaward with the origin on the RSP-line. This coordinate system is used in the JarKus programme.

G-3 Shore normal

For practical purposes a shore-normal coordinate system has been adopted for most of the analyses. This coordinate system is based on RD-NAP and is shifted and rotated in the horizontal plane to have its origin at the Southernmost transect origin (Hoek van Holland), and coordinates that are approximately alongshore and cross-shore directed, averaged over the Delfland coastal cell. The alongshore (ls) and cross-shore (cs) coordinates are calculated

according to equation G-1, altitude coordinates remain NAP based. θ is 312 degrees, and the origin is at RD-position (67067,444050).

$$[ls, cs] = \begin{bmatrix} \cos(\theta) & -\sin(\theta) \\ \sin(\theta) & \cos(\theta) \end{bmatrix} \begin{bmatrix} RD_x - RD_{x,origin} \\ RD_y - RD_{y,origin} \end{bmatrix} \tag{G-1}$$

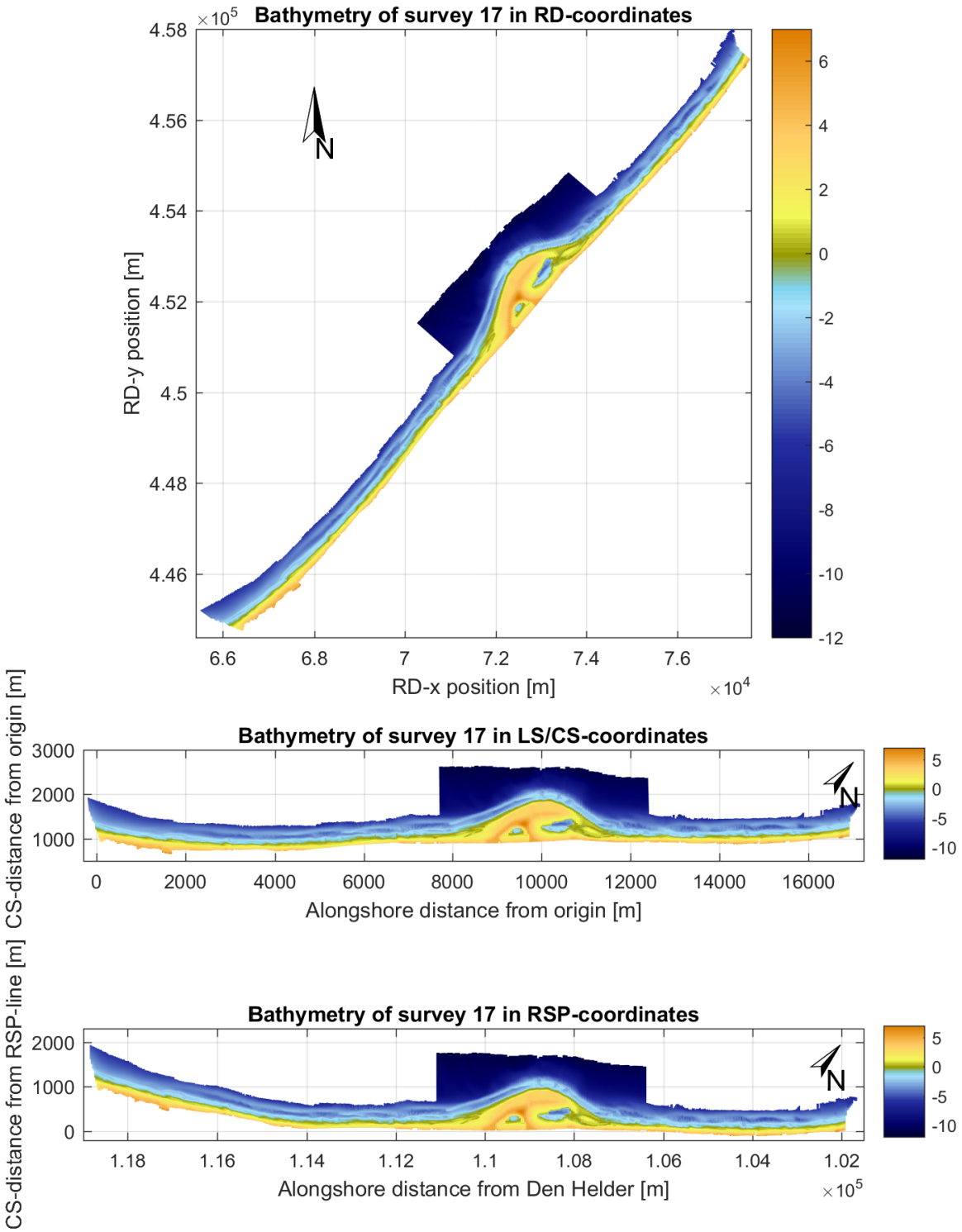

Figure G-1: Bathymetry of survey 17, plotted in different coordinate systems. Top: Rijksdriehoek, centre: local shore normal, bottom: RSP.

Appendix H

Correlations

In this Appendix additional correlations are shown between the hydrodynamics and the morphology. Most correlations are not significant.

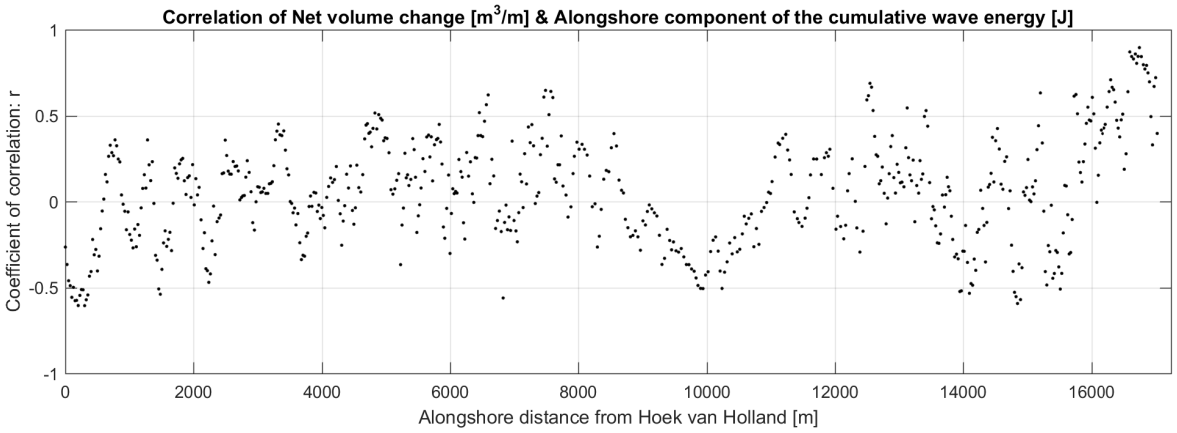

Figure H-1: Correlation of net volume change and the alongshore component of cumulative wave energy.

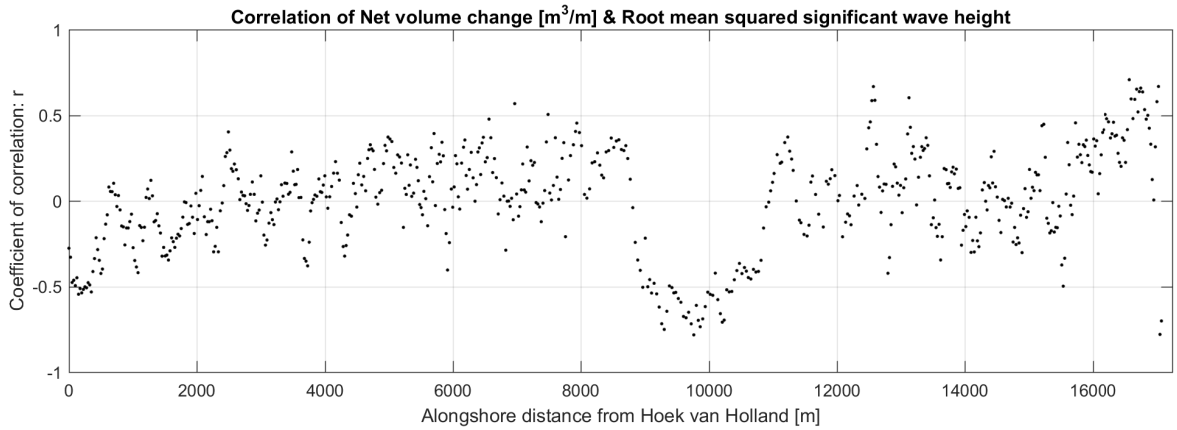

Figure H-2: Correlation of net volume change and average wave steepness.

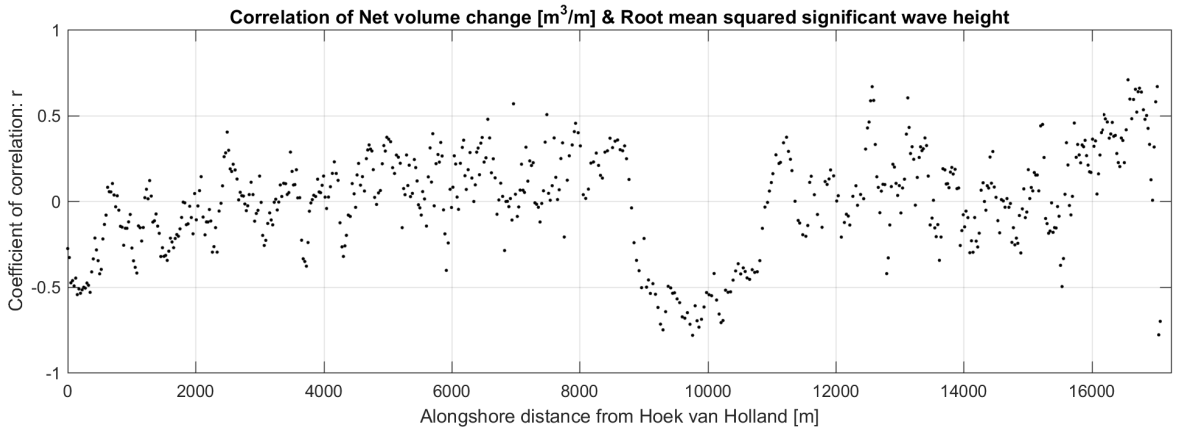

Figure H-3: Correlation of net volume change and root mean square wave height.

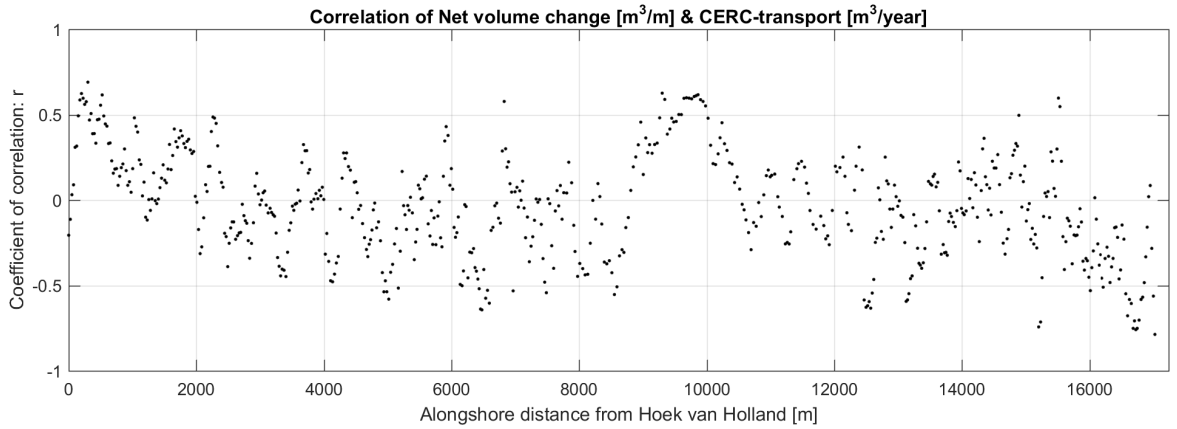

Figure H-4: Correlation of net volume change and LST derived from CERC.

Appendix I

List of Matlab-scripts

The following list contains an overview and short description of all Matlab scripts that were developed for this thesis.

```
%Overview of scripts in the NeMo-suite.
%nemo                          - Master script of the thesis research of Bart ...
    Roest. This script
%nemo_EOF                      - Performs Empirical Orthagonal Function analysis on ...
    the nemo-data.
%nemo_adcp_import              - Import numeric data from a text file as column ...
    vectors.
%nemo_animate_alongshore       - Shows 5 consecutive CS-profiles, cycling through.
%nemo_bar_detector             - Detects locations of local maxima (bars) and ...
    minima (troughs).
%nemo_build_extra_transects    - Defines missing transects near HvH.
%nemo_build_shorenormalgrid    - Creates a RSP-based grid. (0,0)=southern most ...
    transect origin.
%nemo_build_shorenormalgridjarkus - Creates a RSP-based grid. (0,0)=southern most ...
    transect origin.
%nemo_build_slope              - Calculates the average bed slope between two bed ...
    levels;
%nemo_build_surveylines        - Builds the transects for the Delfland coast.
%nemo_closuredepth             - Finds the depth of closure based on the variance ...
    of the altitude.
%nemo_coastline_orientation    - Calculates the orientation of a depth contour
%nemo_combine_jarkus_shore     - Combines Jarkus measurements and Shore surveys.
%nemo_correlate                - Correlates two properties, both scaled and unscaled
%nemo_correlate_profiles       - correlates two profiles, and return paramters.
%nemo_crossref_surveydates     - Import data from text file.
%nemo_depth_contour            - Finds the most seaward cs-index and position of ...
    the desired depth.
%nemo_depth_contour_accurate   - Finds the most seaward position of the desired depth.
%nemo_depth_contour_lc         - Finds the most seaward position of the desired ...
    depth on ls,cs grid.
%nemo_depth_contour_xy         - Finds the most seaward position of the desired ...
    depth on the RD-XY grid.
%nemo_depth_contours_accurate  - Finds most seaward position of depth1 and first ...
    position of depth2 following depth1.
%nemo_get_data_line            - Gets data from surveypath for arbitrary line.
%nemo_get_profile_steepness    - Rough estimate of the nearshore steepness between ...
    heights.
%nemo_get_slope                - Calculates the offshore slope of transects from ...
    altitude matrix.
```

```
26 %nemo_gradients                - calculates the gradient in x and y direction of ...
       the specified coordinate system.
27 %nemo_initize_jarkus           - Returns indices and values of NeMo/ZM transects ...
       for which jarkus data exists.
28 %nemo_interp                   - Interpolates the whole nemo domain to rectangualar ...
       RD meshgrid
29 %nemo_interp_jarkus            - Interpolates Jarkus transects to surveygrid (5m ...
       spacing instead of 10m).
30 %nemo_interpolate_jarkus       - Interpolate the Jarkus measurements to shore
31 %nemo_jarkus                   - Retreives Jarkus data for Jarkus-area from Jarkus ...
       NetCDF.
32 %nemo_jarkus2shoregrid         - Maps Jarkus transects to Shore surveygrid.
33 %nemo_jarkus_interp_cs         - Interpolates Jarkus data in cross-shore direction ...
       to 5m.
34 %nemo_load_adcp                - Loads all raw ADCP-data into a Struct.
35 %nemo_movie2                   - makes a movie based on prepared frames, based on ...
       D.time.
36 %nemo_movie_bathy              - Creates a movie from prepared frames of the bathymetry
37 %nemo_planbound                - Sets limits to axes for the NeMo or SE area.
38 %nemo_plot_adcp_availability   - Plots where ADCP-data is available and indicates ...
       Shore surveys.
39 %nemo_plot_bathymetry          - Plots Jarkus and Shore-based bathymetry per survey.
40 %nemo_plot_csdata              - Plots a stack of the minimum and maximum ...
       CS-position with data.
41 %nemo_plot_depthcontour        - Plots the outer position of a certain depth on a ...
       shore-normal, transect based grid.
42 %nemo_plot_envelope            - Plots the envelope of directional velocities
43 %nemo_plot_jarkbathymetry      - Plots Jarkus-based bathymetry per survey.
44 %nemo_plot_slope               - Plots slopes for several surveys and indication on ...
       bathymetry.
45 %nemo_plot_slope_stack         - Plots a timestack of the slope for individual surveys.
46 %nemo_plot_slope_timestack     - Plots a stack of surveyareas with pointwise cs-slopes.
47 %nemo_plot_stats               - Plots the desired statistical value of the depth ...
       array.
48 %nemo_plot_surveygrid          - plots the survey interpolation grid of the ...
       Delfland Coast.
49 %nemo_plot_transect            - Plots a single defined transect for the given surveys.
50 %nemo_plot_transratio_stack    - Plots a timestack of the transport-ratio
51 %nemo_plot_volume_stack        - Plots a timestack of volume changes per transect ...
       of the whole survey area.
52 %nemo_plot_volume_timeseries   - Plots timeseries of the volumetric development
53 %nemo_plot_volume_transport    - Plots the derivated sediment transport and volume ...
       changes.
54 %nemo_plot_volume_transport_daily - Plots the derivated sediment transport and ...
       volume changes scaled by time.
55 %nemo_plot_volume_transport_total - Plots the derivated sediment transport and ...
       volume changes scaled by time.
56 %nemo_plot_volume_transport_total_daily - Plots the derivated sediment transport and ...
       volume changes scaled by time.
57 %nemo_print2thesis              - Prints figures in pre-defined format to fit nicely ...
       in my MSc-thesis :)
58 %nemo_raw2transects            - Script to convert the .mat files of the Shore ...
       surveys into a NetCDF file
59 %nemo_read_surveytxt           - Convert Shore .txt to .mat-file
60 %nemo_read_txtVlugtenburg      - Read Shore Vlugtenburg-survey txt-files and output ...
       a struct.
61 %nemo_read_txtwalking          - Read Shore Vlugtenburg-survey walking .txt-files ...
       and output a struct.
62 %nemo_slopes                   - Temporary file to calculate all kinds of ...
       profile-steepnesses. Use: NEMO_BUILD_SLOPE.
63 %nemo_stats                    - Calculates various statistics of a (t,x,y)-array ...
       over t.
64 %nemo_tracker                  - Tracks different marco features of the Sand Engine
65 %nemo_transform_surveypath     - Transforms the coordinates of Surveypath to ...
       globally shorenormal.
66 %nemo_vb_txt2mat               - Reads raw data from Vlugtenburg and exports a ...
```

```
        .mat-file.
67  %nemo_volumes                   - Calculates volume changes of transects.
68  %nemo_zm_retreat                - Shows and calculates the cross shore extent of a ...
        certain transect at a certain height.
```

Appendix J

Survey observations 5&6 September 2016

J-1 Introduction

In order to gain insight in the accuracy and possibilities of the data used in this MSc-thesis, I joined the survey team at the Sand Engine on the 5^{th} and 6^{th} of September 2016. My personal observations are presented in this appendix. The work in the field has gained me insights in the way surveys are executed and what is contained in the data, and what is not.

J-2 Measuring techniques

All vehicles are equipped with a Real-time kinematic global positioning system (RTK-GPS), which allows for very accurate positioning in the field, as well as in height. In principle this is accurate up to 1cm. A base station for referencing is placed on a fixed position near the centre of the domain. The RTK-GPS is set-up to log a point at least every half of a second.

Land based measurements are performed during low tide, whereas water based measurements are performed during high tide. Thus ensuring some overlapping between measurements.

J-2-1 Walking

This technique is used on terrain which is not suitable for the quad nor the jetski can go, or to measure small features. When the terrain is too steep, the quad cannot drive. Permanently submerged terrains which are not deep enough for the jetski are also handled by walking. Walking measurements are performed with a RTK-GPS mounted on a pole fixed to a barrow frame to ease the handling and maximise the accuracy.

J-2-2 Quad

Sub-aerial terrain is handled by the quad. The measurements of the quad are slightly less accurate, but are a lot faster than walking.

J-2-3 Jetski

Sub-aqueous terrain is handled by the jetski, which has the least accuracy of the measurement techniques used. However it is the only way to measure bathymetry on deep and shallow water up to a minimum of ca. 60cm.

J-3 Visual observations

J-3-1 Surrounding coast

The beach adjacent to the Sand Engine area is very steep and in some places quite narrow. Beachclub owners are very active in managing the sand around their properties. Bulldozers and shovels are regularly deployed to reshape the beach and duneface. An abundance of sand is dumped elsewhere, whereas shortages are filled from sand further alongshore. This means that the coastal profiles in front of, or directly adjacent to beach clubs are not in equilibrium.

At the flood line a lot of shells are found.

J-3-2 Aeolian transport

Aeolian transport is hindered at some places at the Sand Engine. Predominantly on the high, flood-free part around the lake a lot of shells are present in the sand. The sand around the shells is transported away, after which the shells form a nearly closed top-layer. The sand gets plastered and aeolian transport is diminished.

On low-laying areas around the dune lake a clay-layer is found. This clay layer is present due to infrequent flooding of these parts on which the clay settles and hardens when it gets dry. On places where the clay layer is interrupted shallow erosion holes are present, indicating that no aeolian transport is present in areas covered by clay.

On the south side of the Sand Engine new pioneering dunes are found halfway between the dune foot and the shoreline. Small hills are covered with marram (helmgras), fixing the position.

J-3-3 Scarp

On the North-West side of the Sand engine a scarp is present varying from 0 to 1.5m height. This coincides with the most eroding part.

J-3-4 Quicksand

Quicksand has been found on the south-west side of the dune lake. Walking and driving with the quad was possible without any effects, but the Landrover got stuck till the axles. Liquefaction in a deeper layer is the cause of the quicksand. When (relatively) heavy vehicles drive over the quicksand area, the upper layer forms a wave and dilation cracks appear at the surface.

J-3-5 Dune Lake

The dune lake has unstable and very steep banks at the sea side, and very mild slopes at the dune side. The land round the lake is very flat and only a bit higher than the water level of the lake. The bottom of the lake is covered with water plants and a thin mud/algae layer where the slopes are mild.

J-3-6 Lagoon

The lagoon has steep slopes on the sea sides and relatively mild slopes on the East and South-East sides, with increasing steepness to the South. In the mouth of the tidal gully sedimentations takes place in the lagoon. Due to the mild slopes of the land above the ebb-level of the lagoon extensive intertidal mud-flats are present East of the Laguna.

J-3-7 Tidal gully ("Nieuwe geul")

The new gully connecting the lagoon to the sea flows quite fast and keeps flowing to the sea until the water level of the sea is risen enough with the flood. During low water (at sea) the depth of the gully is approximately 1 to 1.5m near the lagoon and only 10-15cm near the mouth to sea. At approximately 2/3 of the distance to sea the flow becomes super-critical and sediment transport is high. Fast migrating bed forms up to 10cm are observed. More upstream the bed forms are more stable and slightly bigger. Near the lagoon pits are found, being 0.5m deeper than the surrounding bed at 2-3m distance from each other. Slopes in the outer bends are very steep and slightly unstable, the inner bends are more gentle.

J-3-8 Dead arm ("Oude geul")

The old gully, which now has a tidal divide halfway, is very muddy since the flow velocities have become low. Only at high water the gully is entirely flooded.

J-3-9 Beach houses

Around beach houses (strandtenten) plateaux are bulldozered in place to provide a flood free area. This may have some influence on the volume calculations.

Appendix K

Field observations

K-1 Field observations 15 September 2016

Zandmotor congress.

K-2 Field observations 10 December 2016

It was very foggy at sea this day, therefore clear photographs were hard to obtain.

On the peninsula clear aeolian features are present in the lower areas around the lagoon and lake. Shell provide a shelter for the sand and are found on top of towers of cohesive material.

The mouth of the new channel has shifted North. Seaward slopes of the channel are steep (overwash?).

Further no apparent differences from September.

K-3 Field observations 23 March 2017

K-3-1 Beach plateaux

Beach plateaux (strandbanketten) have been constructed for beach clubs and recreational houses. Sand has been dug from the dune foot, as well as the spit and old channel. See Figure K-1.

K-3-2 Lagoon and channels

The lagoon is connected to the sea via the new channel only, the bed of old channel lies very high. The old and new channel now share one flood delta in the lagoon, about 100m from the lagoon they split up. Remainders of the old delta of the new channel are still visible, but severe overwash of sand over the spit has filled up this part of the new channel. The low-water level in the lagoon is much higher than the sea and circa 30cm below high water level in the lagoon.

Small parts of the spit are now above MHW level, so they remain dry.

(a) Beach plateaux for beach houses.

(b) Sand dug from the dune foot.

Figure K-1: Beach plateau and influence on the dune foot.

K-3-3 Outer edge

The outer edge of the peninsula has steep slopes, and breakers are mostly of the plunging type (though not very high). Scarps are mostly faded away, but their signature remains visible. A steep slope separates the dry peninsula (3m+NAP) from the intertidal beach (ca 1.5m+NAP).

K-3-4 Peninsula

The peninsula remains largely paved with shell, except for accretive areas where new dunes are forming. The low parts around the lagoon and lake show layers with clay.

K-4 Field observations 10 April 2017

K-4-1 Northern Area

The spit of the Sand Engine to the North has extended again. The main channel to the lagoon has elongated and migrated to the North. Where previously two completely separate channels existed (new and old), both channels now share the bed for the last 100m to the entrance into the lagoon.

The bank which is enclosed by the two channels has accreted so far that it remains dry with spring tide (circa 1.50m+NAP) and wave run-up. It was clearly visible that this area has been dry for an extended time. This dry island is not connected to the main land, since the depressions of the old channel and the new channel do flood during high tide.

K-4-2 Lagoon

The water level in the lagoon lags with respect to the water level at sea. The dimensions of the tidal channel prevent the lagoon from emptying to a water level lower than ca. -0.2m+NAP.

Water keeps flowing out of the new channel until the water level and wave run-up outside become higher than the lagoon water level.

Since it was spring tide with some wind set-up, water levels were highest of the past month. Large parts of the lagoon area were flooded for the first time in at least 30 days. Flooding of these dry parts occur in a quite remarkable way. Since the sand is very dry it first acts a a sponge, any water flown on top by small waves immediately is drained into the sand, only when the pores are filled the water front advances again. (This is partly caused by the extremely mild slope)

Most surface of the lagoon area is only flooded by a few centimetres (<20cm) and a clear low-water line is present. Below the low-water line, slopes are steep, above they are very mild to horizontal. At the spit, steep aeolian forced slopes are present.

K-4-3 Rip-Runnel systems

On the outer edge of the Sand Engine peninsula rip-runnel systems are present. These systems are located high in the profile and are only active around high water. A bar is present with a distinct crest. The outer slope is steep, and the inner slope is back-sloping mildly. Waves pass this bar by wave run-up (and run-over). This causes a set-up in the runnel, which is emptied by the rip-channel. A block of wood in the runnel was in an apparent circulation with a frequency of 1/minute. Flow velocity in the runnels is high and transport sediment towards the rip. Over the ridge an onshore sediment transport is found. Both one-sided (rip to the south) and two-sided systems are found.

Figure K-2: Rip-runnel system. Waves are flowing over the crest, into the runnel. The water in the runnel flows via the rip-channel to the sea.

Bibliography

Arriaga, Jaime, Jantien Rutten, Francesca Ribas, Albert Falqués and Gerben Ruessink (2017). "Modeling the long-term diffusion and feeding capability of a mega-nourishment". In: *Coastal Engineering* 121, pp. 1–13. ISSN: 0378-3839. DOI: http://dx.doi.org/10.1016/j.coastaleng.2016.11.011. URL: http://www.sciencedirect.com/science/article/pii/S0378383916303659.

Bayram, Atilla, Magnus Larson and Hans Hanson (2007). "A new formula for the total longshore sediment transport rate". In: *Coastal Engineering* 54.9, pp. 700–710. ISSN: 0378-3839. DOI: http://dx.doi.org/10.1016/j.coastaleng.2007.04.001. URL: http://www.sciencedirect.com/science/article/pii/S0378383907000464.

Bayram, Atilla, Magnus Larson, Herman C. Miller and Nicholas C. Kraus (2001). "Cross-shore distribution of longshore sediment transport: comparison between predictive formulas and field measurements". In: *Coastal Engineering* 44.2, pp. 79–99. ISSN: 0378-3839. DOI: http://dx.doi.org/10.1016/S0378-3839(01)00023-0. URL: http://www.sciencedirect.com/science/article/pii/S0378383901000230.

Bird, Eric and Nick Lewis (2015). *Beach renourishment*. Springer.

Bosboom, Judith and Marcel J.F. Stive (2015). *Coastal Dynamics I Lecture Notes CT4305*. Delft Academic Press. ISBN: ISBN 978-90-6562-3720.

De Kort, J.G. (2013). "An assessment on hydro- and morphodynamic proceses at the sand motor during the Decemberstorm of 2013". MA thesis. Delft University of Technology. URL: http://resolver.tudelft.nl/uuid:e1642ed8-697e-40a2-a0e9-c155c35925b6.

De Schipper, M. A., S. De Vries, B. G. Ruessink, R. C. De Zeeuw, J. Rutten, C. Van Gelder-Maas and M. J. F. Stive (2016). "Initial spreading of a mega feeder nourishment: Observations of the Sand Engine pilot project". In: *Coastal Engineering* 111, pp. 23–38.

De Schipper, M. A., Sierd De Vries, J. Mil-Homens, A. Reniers, R. Ranasinghe and M. Stive (2015a). "Initial volume losses at nourished beaches and the effect of surfzone slope". In: World Scientific.

De Schipper, Matthieu A. and Sierd De Vries (2015b). *Monthly morphological measurements of Vlugtenburg beach (NL) - 2009-2012*. DOI: 10.4121/uuid:b798422a-69ec-41be-a394-740aad70df19. URL: https://doi.org/10.4121/uuid:b798422a-69ec-41be-a394-740aad70df19.

De Schipper, Matthieu A., Sierd De Vries, Roshanka W.M.R.J.B. Ranasinghe, Ad Reniers and Marcel J.F. Stive (2013). "Alongshore topographic variability at a nourished beach".

In: *Coastal Dynamics 2013: 7th International Conference on Coastal Dynamics, Arcachon, France, 24-28 June 2013*. Bordeaux University.

De Sonneville, Ben and A.J.F. Van der Spek (2012). "Sediment-and morphodynamics of shoreface nourishments along the North-Holland coast". In: *ICCE 2012: Proceedings of the 33rd International Conference on Coastal Engineering, Santander, Spain, 1-6 July 2012*. Coastal Engineering Research Council.

De Vries, Sierd, Max Radermacher, Mattiheu A. De Schipper and Marcel J.F. Stive (2015). "Tidal dynamics in the sand motor lagoon". In: *E-proceedings of the 36th IAHR World Congress, The Hague, the Netherlands, 28 June-3 July 2015*. IAHR.

De Zeeuw, Roeland C. (2011–2016). *Veldrapportage Monitoring Zandmotor morfologie, (Field report monitoring Sand Engine morphodynamics)*. Field reports accompanied by the surveys at the Sand Engine.

De Zeeuw, Roeland C., Matthieu A. De Schipper and Sierd de Vries (2016a). *NeMo morphology data survey path Delfland 2012-2016*. DOI: 10.4121/uuid:ac6a0962-91a8-4e20-a244-10e74a49a1d0. URL: https://doi.org/10.4121/uuid:ac6a0962-91a8-4e20-a244-10e74a49a1d0.

De Zeeuw, Roeland C., Matthieu A. De Schipper and Sierd de Vries (2016b). *Sand Motor Topographic Survey, actual surveyed path*. DOI: 10.4121/uuid:3836e5a5-4fdf-4122-84bd-a9bb679fb84c. URL: https://doi.org/10.4121/uuid:3836e5a5-4fdf-4122-84bd-a9bb679fb84c.

Dean, Robert G (1991). "Equilibrium beach profiles: characteristics and applications". In: *Journal of coastal research*, pp. 53–84.

Elko, Nicole A. and Ping Wang (2007). "Immediate profile and planform evolution of a beach nourishment project with hurricane influences". In: *Coastal Engineering* 54.1, pp. 49–66. ISSN: 0378-3839. DOI: http://dx.doi.org/10.1016/j.coastaleng.2006.08.001. URL: http://www.sciencedirect.com/science/article/pii/S037838390600113X.

Exner, Felix M. (1925). "Über die wechselwirkung zwischen wasser und geschiebe in flüssen". In: *Akad. der Wiss in Wien, Math-Naturwissenschafliche Klasse, Sitzungsberichte, Abt IIa* 134, pp. 165–203.

Grunnet, Nicholas M. and B.G. Ruessink (2005). "Morphodynamic response of nearshore bars to a shoreface nourishment". In: *Coastal Engineering* 52.2, pp. 119–137.

Hamm, L., M. Capobianco, H.H. Dette, A. Lechuga, R. Spanhoff and M.J.F. Stive (2002). "A summary of European experience with shore nourishment". In: *Coastal Engineering* 47.2. Shore Nourishment in Europe, pp. 237–264. ISSN: 0378-3839. DOI: http://dx.doi.org/10.1016/S0378-3839(02)00127-8. URL: http://www.sciencedirect.com/science/article/pii/S0378383902001278.

Hinton, C.L. and R.J. Nicholls (2007). "Shoreface morphodynamics along the Holland coast". In: *Geological Society, London, Special Publications* 274.1, pp. 93–101.

Hinton, Claire and Robert Nicholls (1998). "Spatial and temportal behavior of depth of closure along the holland coast". In: *Coastal Engineering Proceedings* 1.26. ISSN: 2156-1028. URL: https://icce-ojs-tamu.tdl.org/icce/index.php/icce/article/view/5812.

Hoekstra, P., K.T. Houwman, A. Kroon, B.G. Ruessink, J.A. Roelvink and R. Spanhoff (1996). "Morphological Development of the Terschelling Shoreface Nourishment in Response to Hydrodynamic and Sediment Transport Processes". In: *Coastal Engineering 1996, Proceedings of the 25th International Conference*. American Society of Civil Engineers. Chap. 224, pp. 2897–2910. DOI: 10.1061/9780784402429.224.

Holman, Robert A., David M. Lalejini, Kacey Edwards and Kay Veeramony (2014). "A parametric model for barred equilibrium beach profiles". In: *Coastal Engineering* 90, pp. 85–

94. ISSN: 0378-3839. DOI: http://dx.doi.org/10.1016/j.coastaleng.2014.03.005. URL: http://www.sciencedirect.com/science/article/pii/S0378383914000581.

Holman, Robert A., David M. Lalejini and Todd Holland (2016). "A parametric model for barred equilibrium beach profiles: Two-dimensional implementation". In: *Coastal Engineering* 117, pp. 166–175. ISSN: 0378-3839. DOI: http://dx.doi.org/10.1016/j.coastaleng.2016.07.010. URL: http://www.sciencedirect.com/science/article/pii/S0378383916301582.

Huisman, B.J.A., M.A. De Schipper and B.G. Ruessink (2016). "Sediment sorting at the Sand Motor at storm and annual time scales". In: *Marine Geology* 381, pp. 209–226. ISSN: 0025-3227. DOI: http://dx.doi.org/10.1016/j.margeo.2016.09.005. URL: http://www.sciencedirect.com/science/article/pii/S0025322716301918.

Huisman, B.J.A., E.E. Sirks, L. Van der Valk and D.J.R. Walstra (2014). "Time and spatial variability of sediment grading in the surfzone of a large scale nourishment". In: *Journal of Coastal Research* 70.sp1, pp. 127–132.

Kaji, A.O. (2013). "Assessment of the variables influencing sediment transport at the Sand Motor". MA thesis. Delft University of Technology.

Kamphuis, J. William (1991). "Alongshore sediment transport rate". In: *Journal of Waterway, Port, Coastal, and Ocean Engineering* 117.6, pp. 624–640.

Knoester, D. (1990). *De morfologie van de Hollandse kustzone (analyse van het Jarkusbestand 1964-1986)*. Tech. rep. Rijkswaterstaat, RIKZ (Dienst Getijdewateren).

Ludka, B. C., R. T. Guza, W. C. O'Reilly and M. L. Yates (2015). "Field evidence of beach profile evolution toward equilibrium". In: *Journal of Geophysical Research: Oceans* 120.11, pp. 7574–7597. ISSN: 2169-9291. DOI: 10.1002/2015JC010893. URL: http://dx.doi.org/10.1002/2015JC010893.

Luijendijk, Arjen P., Roshanka Ranasinghe, Matthieu A. De Schipper, Bas A. Huisman, Cilia M. Swinkels, Dirk J.R. Walstra and Marcel J.F. Stive (2017). "The initial morphological response of the Sand Engine: A process-based modelling study". In: *Coastal Engineering* 119, pp. 1–14. ISSN: 0378-3839. DOI: http://dx.doi.org/10.1016/j.coastaleng.2016.09.005. URL: http://www.sciencedirect.com/science/article/pii/S0378383916302563.

Man, W.Y. (2012). "Short-term changes in the Zandmotor morphology". MA thesis. University of Twente. URL: https://www.utwente.nl/ctw/wem/education/afstuderen/afstudeerverslagen/2012/Man.pdf.

Mil-Homens, João, Roshanka Ranasinghe, J.S.M. Van Thiel de Vries and M.J.F. Stive (2013). "Re-evaluation and improvement of three commonly used bulk longshore sediment transport formulas". In: *Coastal Engineering* 75, pp. 29–39. ISSN: 0378-3839. DOI: http://dx.doi.org/10.1016/j.coastaleng.2013.01.004. URL: http://www.sciencedirect.com/science/article/pii/S0378383913000112.

Minneboo, F.A.J. (1995). *Jaarlijkse Kustmetingen, richtlijnen voor de inwinning bewerking en opslag van gegevens van jaarlijkse kustmetingen (Annual coastal measurements, guidelines for collection, adjustment and storage of the data from annual coastal measurements)*. Tech. rep. Rijksinstituut voor Kust en Zee (RIKZ), Rijkswaterstaat.

Ojeda, E., B.G. Ruessink and J. Guillen (2008). "Morphodynamic response of a two-barred beach to a shoreface nourishment". In: *Coastal Engineering* 55.12, pp. 1185–1196. ISSN: 0378-3839. DOI: https://doi.org/10.1016/j.coastaleng.2008.05.006. URL: http://www.sciencedirect.com/science/article/pii/S0378383908000987.

Patterson, Dean (2013). "Shore-face profile response time-scale and its significance for shoreline evolution". In: *Proceedings of the 22nd NSW Coastal Conference 2013*.

Rijkswaterstaat (2016). *Annual cross-shore transect bathymetry measurements along the Dutch coast since 1965*.

Rijkswaterstaat and J. Van Houdt (2011). *Aerial photographs of the Sand Engine*. URL: https://beeldbank.rws.nl/MediaObject/Details/435144.

Ruessink, B.G., K.M. Wijnberg, R.A. Holman, Y. Kuriyama and I.M.J. Van Enckevort (2003). "Intersite comparison of interannual nearshore bar behavior". In: *Journal of Geophysical Research: Oceans* 108.C8.

Schwartz, Maurice (2006). *Encyclopedia of coastal science*. Springer Science & Business Media. ISBN: 978-1-4020-3880-8. DOI: 10.1007/1-4020-3880-1.

Shand, Roger D., Donald G. Bailey and Mike J. Shepherd (1999). "An inter-site comparison of net offshore bar migration characteristics and environmental conditions". In: *Journal of Coastal Research*, pp. 750–765.

Shand, Roger D., Donald G. Bailey and Mike J. Shepherd (2001). "Longshore realignment of shore-parallel sand-bars at Wanganui, New Zealand". In: *Marine Geology* 179.3 - 4, pp. 147–161. ISSN: 0025-3227. DOI: http://dx.doi.org/10.1016/S0025-3227(01)00223-7. URL: http://www.sciencedirect.com/science/article/pii/S0025322701002237.

Shand, Roger D., Mike J. Shepherd et al. (2003). "Associations between net offshore bar migration and backshore erosion". In: *Coasts & Ports 2003 Australasian Conference: Proceedings of the 16th Australasian Coastal and Ocean Engineering Conference, the 9th Australasian Port and Harbour Conference and the Annual New Zealand Coastal Society Conference*. Institution of Engineers, Australia, p. 205.

Slootjes, Nadine and Herman Van der Most (2016). *Achtergronden bij de normering van de primaire waterkeringen in Nederland*. Tech. rep. Ministerie van Infrastructuur en Milieu.

Southgate, Howard N. (2011). "Data-based yearly forecasting of beach volumes along the Dutch North Sea coast". In: *Coastal Engineering* 58.8, pp. 749–760. ISSN: 0378-3839. DOI: http://dx.doi.org/10.1016/j.coastaleng.2011.03.011. URL: http://www.sciencedirect.com/science/article/pii/S0378383911000469.

Stive, Marcel J.F., Matthieu A. de Schipper, Arjen P. Luijendijk, Stefan G.J. Aarninkhof, Carola van Gelder-Maas, Jaap S.M. van Thiel de Vries, Sierd de Vries, Martijn Henriquez, Sarah Marx and Roshanka Ranasinghe (2013). "A new alternative to saving our beaches from sea-level rise The sand engine". In: *Journal of Coastal Research* 29.5, pp. 1001–1008.

USACE (1984). *Shore Protection Manual*. Tech. rep. Washington: Department of the Army, U.S. Corps of Engineers.

Van de Rest, Pol (2004). "Morfodynamica en hydrodynamica van de Hollandse kust". MSc Thesis. TU Delft, Delft University of Technology. URL: http://resolver.tudelft.nl/uuid:e791dbed-9935-4c37-8307-8e9262665f78.

Van Koningsveld, M., G.J. De Boer, F. Baart, T. Damsma, C. Den Heijer, P. Van Geer and B. De Sonneville (2010). "OpenEarth-inter-company management of: data, models, tools & knowledge". In: *Proceedings WODCON XIX Conference. Beijing, China*.

Van Rijn, Leo C. (1995). "Dynamics of the closed coastal system of Holland". In: *Delft Hydraulics, report H* 2129.

Van Rijn, Leo C (1997). "Sediment transport and budget of the central coastal zone of Holland". In: *Coastal Engineering* 32.1, pp. 61–90.

Van Rijn, Leo C., J.S. Ribberink, A. Reniers and T. Zitman (1995). "Sand budget and coastline changes of the central Dutch Coast between Den Helder and Hoek van Holland". In: *Delft hydraulics, report H* 2129.

Van Son, S.T.J., R.C. Lindenbergh, M.A. De Schipper, S. De Vries and K. Duijnmayer (2009). "Using a personal watercraft for monitoring bathymetric changes at storm scale". In: *Hydro9 Conference, 10-12 November 2009, Cape Town, South Africa.*

Van Steijn, P.W. (2015). "Global Assessment on the Lifetime of Mega Nourishments". MA thesis. Delft University of Technology. URL: http://resolver.tudelft.nl/uuid:bbd754f4-b88b-4dd7-84c4-be8de1e466a1.

Verhagen, H.J. (1992). "Method for artificial beach nourishment". In: 23. DOI: 10.9753/icce.v23.%p. URL: https://journals.tdl.org/icce/index.php/icce/article/view/4868.

Verkeer & Waterstaat (1990). *Kustverdediging na 1990: Beleidskeuze voor de kustlijnzorg (Coastal defense after 1990: Policy for the coastline preservation).* Tech. rep. Ministerie van Verkeer en Waterstaat.

Wijnberg, Kathelijne M. (1995). "Morphologic behaviour of a barred coast over a period of decades". PhD thesis. Utrecht University.

Wijnberg, Kathelijne M. and Joost H.J. Terwindt (1995). "Extracting decadal morphological behaviour from high-resolution, long-term bathymetric surveys along the Holland coast using eigenfunction analysis". In: *Marine Geology* 126.1, pp. 301–330.

TU Delft Delft University of Technology

Hydraulic Engineering